Department of Chemical Engineering and Chemical Technology
Imperial College London

Application and Evaluation of Organic Solvent Nanofiltration in Pharmaceutical Processing

Elin M. Rundquist

A Thesis Submitted for the Degree of
DOCTOR OF PHILOSOPHY
Philosophiae Doctor (Ph.D.)

February 2013

Declaration of Originality

This is to certify that this thesis is the result of my own work, except as stated in the acknowledgement and references. Neither the thesis nor the work has previously been submitted to any institution for a degree.

Signature:

Name:

Elin Rundquist

Copyright Declaration

Abstract

Organic solvent nanofiltration (OSN) is a membrane based technique designed to separate molecules ranging between 200 – 1000 g mol^{-1}. OSN has been discussed as a promising alternative for applications in the pharmaceutical industry, and the central theme of this thesis is to investigate potential benefits and limitations to OSN implementation in pharmaceutical processing. This work successfully demonstrated that OSN can be used for common pharmaceutical processes including active pharmaceutical ingredient (API) purification (Chapters 3 and 4), solvent swapping (Chapter 5) and solvent recovery and recycle (Chapter 6). Benefits of OSN were demonstrated in significantly improved energy efficiency compared to distillation, as well as in enabling operation in situations where current unit operations are unsuitable (*e.g.* solvent swapping from a higher to a lower boiling point solvent). Some limitations of OSN were highlighted with regards to potentially significant yield losses, precipitation of solids during operation, as well as the large solvent requirement of OSN when operated in a diafiltration mode. The high solvent intensity was addressed in a combined process using OSN for separation, and a packed adsorbent column to enable solvent recovery and recycle from the permeate (Chapter 4). Limitations of OSN membranes should be further addressed through membrane development, primarily focusing on improving rejection.

The final section of this thesis discusses modelling of OSN membrane performance (Chapter 7). Limitations of currently available models were identified in lack of consistent predictions of performance for membrane-solvent-solute combinations not used for model development, as well as the often extensive experimental work required prior to model application. To facilitate OSN implementation in the pharmaceutical industry it is concluded that a simple model based on readily available data from membrane manufacturers is highly desirable.

Acknowledgements

Completion of this PhD thesis would not have been possible without the involvement of several people. Firstly I would like to express my sincere gratitude to my industrial supervisor Dr. Christopher Pink for his enthusiasm, commitment, patience and support which enabled me to keep my motivation and stay on this rewarding path. I would also like to thank my academic supervisor Prof. Andrew Livingston for his valuable input and advice, which has helped me grow and develop my research skills. Additionally, I would like to thank the members of Prof. Livingston's research group, especially Maria Fernanda Jimenez Solomon, as well as my colleagues at GlaxoSmithKline (GSK) for your contributions of both academic and industrial nature. Primarily, I would like to acknowledge Dr. Darren Oatley for supervising me during the first year of my PhD and Dr. Alastair Pert for extensive proof-reading of this thesis as well as for his constant encouragement and support. I would also like to thank the members of "lunch group" for much needed breaks from work and their somewhat alternative pep talks which have been a great help in keeping up my motivation.

I would further like to acknowledge the European Community's Seventh Framework Program Marie Curie Initiative (grant agreement: ITN 214226 NEMOPUR) for funding of this project and thank all the NEMOPUR collaboration partners for many enjoyable project meetings. Especially I would like to thank Emelie Fritz, for a rewarding scientific collaboration, and for her help in putting things in perspective in sharing the sometimes difficult burden of a PhD.

Finally, and most importantly, this work would not have been possible without the endless love, encouragement and support of my family. For this I am eternally grateful and give you my heartfelt thanks. I truly could not have done this without you.

Publications

Parts of this thesis have been published:

1. Rundquist, E., Pink, C., Vilminot, E., Livingston, A., Facilitating the use of counter-current chromatography in pharmaceutical purification through use of organic solvent nanofiltration, *Journal of Chromatography A*, 1229 (2012) 156-163.

2. Rundquist, E. M., Pink, C. J., Livingston, A. G., Organic Solvent Nanofiltration; a Potential Alternative to Distillation for Solvent Recovery from Crystallisation Mother Liquors, *Green Chemistry*, 14 (2012) 2197-2205.

3. Rundquist, E. M., Pink, C. J., Livingston, A. G., Impurity Removal through Combined Processing of Organic Solvent Nanofiltration (OSN) and Adsorbents: An Efficient Approach to Active Pharmaceutical Ingredient (API) Purification, *Organic Process Research & Development* (2013) *In preparation*.

Table of Contents

List of Figures

List of Tables

List of Abbreviations

ACS	American Chemical Society
AI	Acetamide imprinted
API	Active pharmaceutical ingredient
CCC	Counter-current chromatography
DCM	Dichloromethane
DMF	Dimethylformamide
DV	Diafiltration volume
EMA	European Medicines Agency
FDA	Food and Drug Administration
GC	Gas chromatography
GSK	GlaxoSmithKline
GTI	Genotoxic impurity
HPLC	High-performance liquid chromatography
IMS	Industrial methylated spirit
IPA	Iso-propyl alcohol
IPAc	Iso-propyl acetate
LC-MS	Liquid chromatography-mass spectrometry
LLE	Liquid-liquid extraction
MEK	Methyl ethyl ketone
MET	Membrane Extraction Technology
MF	Microfiltration
MiBK	Methyl isobutyl ketone
MIP	Molecularly imprinted polymer
MW	Molecular weight
MWCO	Molecular weight cut-off
NF	Nanofiltration
NIP	Non-imprinted polymer
OSN	Organic solvent nanofiltration
PAN	Polyacrylonitrile
PDMS	Polydimethylsiloxane
RO	Reverse osmosis
SDI	Solution-diffusion with imperfection
SEM	Scanning electron microscope
TEM	Transmission electron microscope
TFA	Trifluoroacetic acid
TFC	Thin film composite
THF	Tetrahydrofuran
UF	Ultrafiltration

Nomenclature

A	Membrane area (m^2)
a_0	Specific diffusivity value (m)
b_0	Specific permeability value (m)
Δc	Heat capacity (J mol^{-1} K^{-1})
C	Concentration (g L^{-1})
D	Diffusion coefficient (m^2 s^{-1})
E	Energy (J)
f	Membrane parameter (m s^{-1})
F	Flow (mol s^{-1} or L h^{-1})
ΔH_{vap}	Latent heat of vaporisation (J mol^{-1})
ΔH_c^o	Heat of combustion (J mol^{-1})
i	Van't Hoff coefficient (-)
J	Flux (L m^{-2} h^{-1} or m^3 m^{-2} s^{-1})
k	Mass-transfer coefficient (m s^{-1})
K_d	Partitioning coefficient (-)
m	Mass adsorbent (g)
R	Rejection (%)
R_{gas}	Ideal gas constant (J mol^{-1} K^{-1})
ΔT	Temperature difference (K)
T	Temperature (K)
t	Time (h)
V	Volume (L)
ΔP	Pressure difference (Pa or bar)
Q	Power (W)
x	Mass adsorbed solute (g)

Subscripts

1	NF sub-layer
2	UF sub-layer
b	Bulk
bp	Boiling point
d	Added DV
D	Pressure drop
f	Feed
fb	Feed-and-bleed re-circulation
i	Component i
m	Membrane-feed boundary layer
M	Molar
p	Permeate
r	Retentate
TM	Trans-membrane

Greek Letters

ϕ	Sorption value (gm gm^{-1})
α	Ratio dielectric constants (-)
β	Ratio surface tensions (-)
γ	Membrane surface tension (N m^{-1})
δ	Boundary layer thickness (m)
$\Delta\Pi$	Osmotic pressure (Pa or bar)
ε	Dielectric constant (-)
η	Pump efficiency (-)
λ	Solvent parameter (s m^{-2})
ρ	Density (g mL^{-1})
μ	Viscosity (Pa s)

Chapter 1: Introduction and Scope of Thesis

Membrane based techniques are well established in aqueous applications, and have been used extensively in waste-water treatment and desalination. Interest has long existed to extend application to organic solvents, however progress has been limited due to a lack of solvent-stable membranes. This problem has partly been rectified over the last decade through the development and commercialisation of membranes suitable for use in organic solvents. Organic solvent nanofiltration (OSN) is a pressure-driven technique which uses a membrane to separate an incoming feed stream into two streams referred to as the permeate (solvent and solutes able to pass the membrane) and the retentate (solvent and solutes unable to pass the membrane). Separation is based primarily on steric factors with OSN membranes designed to operate in a range between 200-1000 g mol^{-1}. Following recent membrane developments, OSN has become an emerging separation technique commonly discussed for application in the food, fine chemical, petrochemical and pharmaceutical industries. Application of OSN has successfully been demonstrated for a range of lab-scale, as well as some industrial, applications. These studies indicate a great potential for OSN, however applications have often been focused on model systems and limited work has been carried out looking at the more complex multi-solute systems often observed in industry. Additionally, OSN is commonly mentioned as offering benefits compared to unit operations currently in use with regards to improved energy- and mass efficiency, high process flexibility and capability of processing temperature sensitive material. Despite such advantages often being mentioned, to our knowledge almost no data has been presented comparing OSN to its more conventional counter-parts, and potential benefits of OSN application have hence not been fully investigated.

Therefore, the main focus of this thesis is to investigate potential benefits of OSN for processing in the pharmaceutical industry. Application of OSN is investigated for a range of industrially relevant case studies selected from current processes under development at GlaxoSmithKline (GSK). Case studies were selected to cover commonly used pharmaceutical processes including active pharmaceutical ingredient (API) purification (Chapter 3 and 4), solvent swapping (Chapter 5), and solvent recovery and recycle (Chapter 6). In addition to investigating if OSN can be used for the selected applications, process comparisons were carried out to evaluate potential benefits of OSN compared to competing unit operations. Process comparisons further aimed to investigate potential limitations of OSN implementation, as well as provide recommendations for how such limitations could be rectified.

A potential resistance to industrial implementation of OSN could be the current lack of predictive process performance tools. Modelling can be a useful tool for gaining improved understanding of transport through the membrane, as well as to facilitate lab-scale and industrial OSN application. Various models have been suggested for OSN, however current models struggle to provide accurate predictions of flux and rejection. In the final section of this thesis focus was placed on evaluating the use of modelling for prediction of OSN membrane performance (Chapter 7). Currently available OSN models were reviewed and potential limitations, primarily relating to the predictive power and the experimental work required, were evaluated. Additionally, this study aimed to provide recommendations providing a solid basis for future model developments more suited for industrial application.

Chapter 2: Background and Research Motivation

2.1 Introduction to Membrane Technology

A membrane can be defined as a physical barrier separating two phases by selectively restricting transport of various solutes. Membrane selectivity is based on differences in chemical and physical properties, and transport is made possible by the application of a driving force to at least one side of the membrane (Mulder, 1996a). During operation the membrane acts to separate an incoming feed stream into two components referred to as the permeate (solvent and solutes that are able to pass the membrane), and the retentate (solvent and solutes that are unable to pass the membrane) (Mulder, 1996a)(Baker, 2004a). A schematic representation of a membrane separation is given in Figure 2.1.

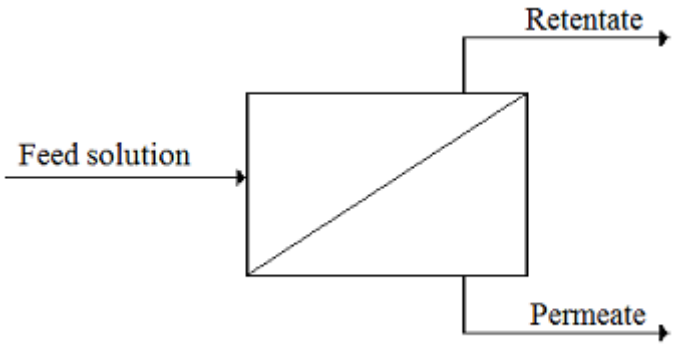

Figure 2.1. Schematic illustration of a membrane separation (adapted from Baker, 2004a)

A range of driving forces including differences in pressure, concentration, electrical potential and temperature are capable of driving a membrane process. For a given separation the main driving force can usually be controlled, however driving forces rarely occur alone and a combination of forces most commonly influences the separation (Mulder, 1996b). Effects from different driving forces will be discussed in more detail in Section 2.4.

Several membrane based separation techniques have been developed for industrial applications. For liquid-liquid separations, membrane processes include pressure-driven techniques; Microfiltration (MF); Ultrafiltration (UF); Nanofiltration (NF); and Reverse Osmosis (RO). For these techniques separation is based primarily on steric exclusion, with MF being used for separation of large molecules (0.1 – 10 μm, *e.g.* macromolecules, yeast and bacteria) ranging to RO which is used for separation of small molecules (0.1 – 1 nm, *e.g.* salts). In addition to molecular size, the charge and shape of the solutes, as well as interactions between the solute, the membrane and the solvent influence the separation and can potentially be used to fine-tune membrane performance (Section 2.2). The work presented in this report focusses on the application of NF in organic solvents. The properties of NF lie between UF and RO, with NF defined as retaining molecules between 0.5 – 5 nm corresponding to molecular weights between 200 – 1000 g mol^{-1} (Mulder, 1996d)(Koros *et al.*, 1996).

Membrane performance is commonly described in terms of two parameters, referred to as the solute rejection and the permeate flux. At thermodynamic equilibrium the solute rejection is defined as the percentage of a given solute that is unable to pass the membrane, and can be calculated according to Equation 2.1 where R_i is the rejection of species i, and C_i is the concentration in the feed (f) and the permeate (p) respectively (Mulder, 1996a).

$$R_i = \left(1 - \frac{C_{i,p}}{C_{i,f}}\right) \times 100\% \qquad \text{Equation 2.1}$$

The permeate flux is defined as the volume of solvent passing through the membrane per unit area and unit time. The flux is calculated according to Equation 2.2 where J is the flux, V is the volume, A is the membrane area and t is the permeate collection time. Flux is most commonly expressed in L m^{-2} h^{-1} but other units, such as m^3 m^{-2} s^{-1}, can also be used (Mulder, 1996a).

$$J = \frac{V_p}{At} \qquad \text{Equation 2.2}$$

An additional parameter used by membrane manufacturers to describe separation performance is the molecular weight cut-off (MWCO). MWCO is defined as the molecular weight for which 90% of a given solute is rejected by the membrane (See-Toh *et al.*, 2007a), and values are often supplied by manufacturers to provide an initial indication of the membrane operating range. However, the MWCO is highly dependent on the solvent-solute system used for the characterisation, and with varying methods employed by different manufacturers caution must be applied with regards to these values (See-Toh *et al.*, 2007a)(Luthra *et al.*, 2002)(Li *et al.*, 2009). In addition, as the MWCO is defined for a 90% rejection level, a further shift in molecular weight is required to reach a full rejection of 100%. If the membrane rejection curve is not sharp, the molecular weight required to reach full rejection might be significantly higher than the value indicated by the MWCO. This was illustrated by See-Toh *et al.* (2007a) during the development of a proposed standard method for membrane characterisation. Using a feed solution of polystyrene oligomers dissolved in toluene, the MWCO for membrane Starmem™122 was determined to be 220 g mol^{-1}. However, for the same membrane a rejection > 99.9% was first reached for a molecular weight of approximately 600 g mol^{-1}. Current shortcomings in membrane characterisation hinder direct membrane selection, making membrane screening an integral part of membrane process development.

2.2 Organic Solvent Nanofiltration (OSN)

Membrane separations have been in use since the middle of the 1800s, but it was not until the development of the asymmetric membrane (Section 2.3.1) in the 1960s that NF/RO started to gain more widespread recognition as a valuable separation technique (Loeb and Sourirajan, 1962). To date multiple applications of NF/RO have been reported for aqueous systems (Raman *et al.*, 1994)(Wenten *et al.*, 2002), and there has been a long-standing interest in extending applications to operation in organic solvents. OSN was initially attempted by Sourirajan (1964) in the 1960s, however industrial progress has since been slow due to a lack of commercially available membranes with sufficient solvent stability. This problem has been partially rectified over the last few decades through the development and release of new OSN membranes to market (Section 2.3.3), while a range of lab-scale and industrial applications have been presented in the literature (Section 2.6) (Vandezande *et al.*, 2008).

The principle of NF operation is similar in aqueous and organic solvent systems. However, for polymeric membranes the solvent used can interact with the membrane, resulting in compaction, solvation and differential swelling. Solvent interactions influence membrane characteristics, and are likely to affect both the rejection and the overall membrane permeability (Mulder *et al.*, 2005). Studies indicate that for a range of hydrophilic NF membranes the rejection of similar size solutes decreased during operation in organic solvents compared to aqueous solutions (Yang *et al.*, 2001)(van der Bruggen *et al.*, 2002a). Similar observations were made by Geens *et al.* (2005a) where the rejection of raffinose for a range of hydrophilic membranes was observed to decrease with decreasing water content in water-solvent mixtures. However, for hydrophobic membranes the opposite trend was observed with the rejection of raffinose increasing from 34% in water to 65% in methanol, and 41% in

ethanol. Increased rejection in organic solvents compared to aqueous solutions was also observed for various neutral solutes during operation of hydrophobic membrane MPF-50 (Zhao and Yuan, 2006a). Conversely, the same study showed that for hydrophobic Starmem™ membranes the rejection of neutral molecules decreased in organic solvents compared to water, indicating that while some trends can be observed for hydrophilic and hydrophobic membranes, the full explanation for solvent-solute-membrane interactions is complex.

Variations in rejection for given solutes have been observed when using the same membrane in a range of organic solvents, confirming that the solvent has a significant impact on membrane performance (Yang *et al.*, 2001)(Bhanushali *et al.*, 2002)(Geens *et al.*, 2005b)(Zhao and Yuan, 2006a). Suggested explanations for the changing rejection in various solvents include:

- Solvent-membrane interactions (*e.g.* hydration/solvation of the polymer) resulting in membrane swelling and/or increased movement of the polymer chains. Such interactions alter the effective membrane structure resulting in changes to the solute rejection (van der Bruggen *et al.*, 2002a)(Geens *et al.*, 2005a)(Geens *et al.*, 2005b)(Zhao and Yuan, 2006a).
- Solvent-solute interactions (*e.g.* hydration/solvation of the solute) resulting in an increased effective molecular size, and alterations to the shape of the solute molecule. (Yang *et al.*, 2001)(Geens *et al.*, 2005a)(Geens *et al.*, 2005b).

The type of solvent and solvent properties has also been shown to influence the membrane flux. For a range of hydrophilic membranes the flux was observed to decrease with decreasing solvent polarity, while the opposite behaviour was observed for hydrophobic membranes

(Bhanushali *et al.*, 2001)(Van der Bruggen *et al.*, 2002a). The solvent polarity is related to the surface tension and is believed to be one of the major factors influencing the solvent flux. Nevertheless, literature suggests that solvent polarity alone is not sufficient to explain the significant variations in flux observed for various solvents, and additional factors such as solvent viscosity, steric influence and dielectric effects are also believed to be of importance (Machado *et al.*, 1999)(Bhanushali *et al.*, 2001)(Geens *et al.*, 2006a).

2.3 Membrane Material and Types

An ideal membrane for OSN application should have a high permeability as well as high selectivity. Additionally, sufficient chemical, mechanical and thermal resistance is required to maintain membrane performance throughout the separation process. OSN membranes made from both polymeric and inorganic/ceramic materials are currently commercially available. The vast majority of OSN membranes used in industrial applications are however polymeric, as polymeric membranes are relatively cheap to manufacture and can be made in a range of MWCOs while maintaining sufficient fluxes and mechanical robustness (Baker, 2000a).

2.3.1 Polymeric Membranes

During early development of polymeric membranes, cellulose acetate was widely used throughout the industry. Membranes showed high water permeability combined with high salt rejection, and were ideal for use in desalination. However, cellulose acetate has poor chemical and mechanical stability and has gradually been replaced with more advanced polymers including polysulphone, polyethersulphone, polydimethylsiloxane (PDMS), polyacrylonitrile (PAN), polyamide and polyimide (Mulder, 1996d)(Vandezande *et al.*, 2008).

Based on the membrane structure and the separation mechanism used, polymeric membranes can be divided into nonporous (or dense) and porous membranes (Nunes and Peinemann, 2006). Nonporous/dense membranes are made up of tightly packed polymer chains and solvent and solutes are transported through the membrane using a solution-diffusion mechanism. Transport is made possible through free-volume elements that appear and disappear at approximately the same time-scale as the transport of permeate through the membrane. Selectivity is based on solubility and diffusivity of the solute, while the overall resistance to mass-transfer is related to the membrane thickness. To ensure sufficient mechanical stability, a minimum membrane thickness is required, commonly resulting in nonporous membranes having a low overall flux (Mulder, 1996c)(Nunes and Peinemann, 2006).

Porous membranes are similarly comprised of packed polymer chains, however the structure contains clearly defined pores, which are fixed in space. Porous membranes can be divided into symmetric and asymmetric structures, with symmetric membranes being uniform throughout and asymmetric membranes differing in both structure and material in different parts of the membrane (Baker, 2004a)(Baker, 2004b)(Nunes and Peinemann, 2006). Asymmetric membranes are commonly composed of a thin dense top layer, performing the separation while minimising the resistance to solvent flux. The top layer is further attached to a porous support layer, helping the membrane to maintain sufficient mechanical strength. This is highly desirable for all membrane applications, and many commercially available membranes have asymmetric structures (Baker, 2004b).

Asymmetric membranes can be sub-divided into integrally skinned asymmetric membranes and thin film composites (TFCs) (Figure 2.2). Integrally skinned asymmetric membranes are

prepared via phase inversion, generating a membrane in which the free volume decreases towards the membrane surface. Integrally skinned membranes are composed of the same material throughout and separation is achieved through a thin, denser top layer (Vandezande *et al.*, 2008). TFCs are made via dip-coating or interfacial polymerization, differing from integrally skinned membranes in that the support and top-layer can be of different chemical composition. TFCs can offer benefits as each layer can be optimized individually to obtain the desired selectivity and permeability, as well as high chemical, mechanical and thermal resistance. However, TFCs are potentially more sensitive to membrane failure resulting from differential material swelling or chemical incompatibility of the two layers (Petersen, 1993)(Vankelecom and Gevers, 2005).

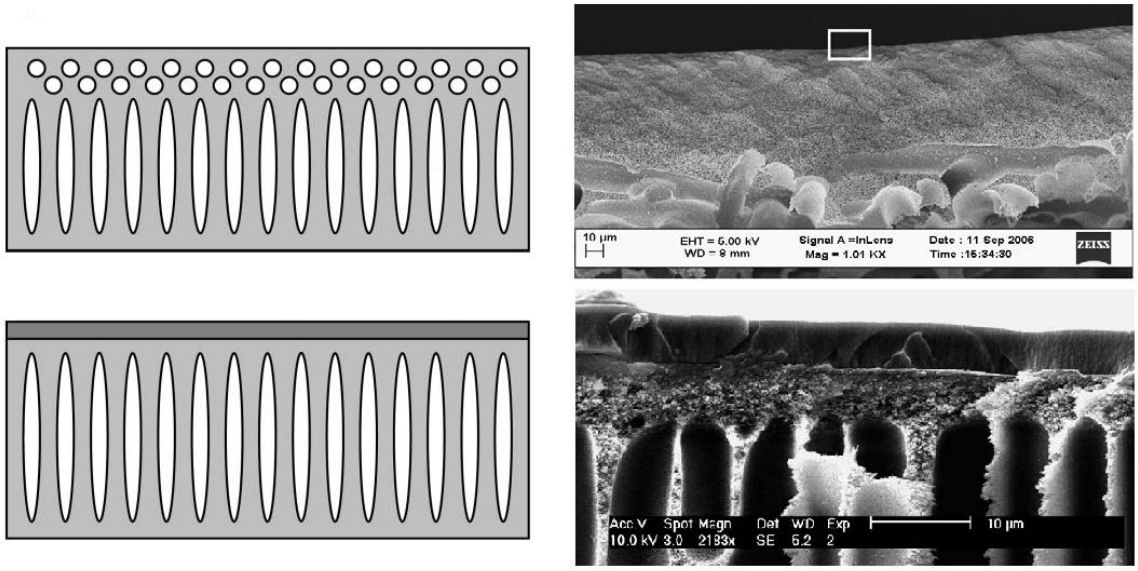

Figure 2.2. Schematic representations (*left*) and scanning electron microscope (SEM) images (*right*) of a polyimide integrally skinned asymmetric membrane (*top*) and a PDMS TFC membrane on a polyimide support (*bottom*) (Gevers *et al.*, 2006)(See-Toh *et al.*, 2007b)(Vandezande *et al.*, 2008)

2.3.2 Ceramic Membranes

Ceramic membranes are made from inorganic materials including alumina, silica, titanium and zirconium oxides. Membranes are generally prepared via sol-gel synthesis, generating an asymmetric structure with a denser top layer which is used for separation (Mulder, 1996b)(Tsuru, 2008). Ceramic membranes are only marginally influenced by system parameters such as solvent, temperature and pressure, while membranes commonly have a long life span with high chemical and thermal stability. Ceramic membranes have successfully been produced in the NF range, however they tend to be brittle, making large-scale synthesis and module construction difficult and relatively expensive (Tsuru *et al.*, 2003)(Tsuru, 2008).

2.3.3 Commercially Available OSN Membranes

A range of OSN membranes are commercially available enabling application in a number of solvents. However, as OSN is a relatively young technique, the range of available membranes is still limited, with further membrane development being an important area of OSN research. A summary of commercially available OSN flat sheet membranes is given in Table 2.1 along with basic membrane characteristics.

Table 2.1. Commercially available OSN membranes and their properties

Manufacturer/ distributer	Membrane	MWCO (g mol^{-1})	Material	Membrane Type	Reference
Evonik MET	Starmem™122	220[a]	Polyimide	Integrally skinned asymmetric	Evonik MET, 2011a
	Starmem™240	400[a]	Polyimide	Integrally skinned asymmetric	Nair *et al.*, 2002
Evonik MET	Duramem™150	150[b]	Polyimide	Integrally skinned asymmetric	Evonik MET, 2011b
	Duramem™200	200[b]	Polyimide	Integrally skinned asymmetric	
	Duramem™300	300[b]	Polyimide	Integrally skinned asymmetric	
	Duramem™500	500[b]	Polyimide	Integrally skinned asymmetric	
	Duramem™900	900[b]	Polyimide	Integrally skinned asymmetric	
Evonik MET	Puramem™280	280[c]	Polyimide	Integrally skinned asymmetric	Evonik MET, 2011c
	Puramem™S380	600[c]	Polyimide	TFC	Evonik MET, 2011d
Borsig GmbH	GMT-oNF-1	~330[d]	Silicon polymer	TFC	Borsig, 2011a
	GMT-oNF-2	~320[e]	Silicon polymer	TFC	Borsig, 2011b
SolSep BV.	SolSep 010206	~300[f]	-	-	Cuperus, 2005 SolSep, 2008
	SolSep 030705F	~500[g]	-	-	
	SolSep 010306	~1000[h]	-	-	
	SolSep 030306F	~1000[h]	-	-	
Koch Membranes	SelRO®MFP-44	250[i]	-	TFC	Yang *et al.*, 2001 Van der Bruggen *et al.*, 2002b
Inopor	SiO_2 (1.0 nm)	600[j]	SiO_2	Ceramic	Inopor, 2012 Kühnert, 2012
	TiO_2 (1.0 nm)	750[j]	TiO_2	Ceramic	
	TiO_2 (0.9 nm)	450[j]	TiO_2	Ceramic	

[a]Based on rejection of n-alkanes in toluene.
[b]Based on rejection of styrene oligomers in acetone.
[c]Based on rejection of styrene oligomers in toluene.
[d]Based on 88% rejection of Methyl Orange in 2-propanol.
[e]Based on 93% rejection of Methyl Orange in 2-propanol.
[f]Based on 95% rejection of 300 g mol^{-1} molecule in unspecified solvent.
[g]Based on 95+% rejection of colorant in ethanol.
[h]Based on rejection of oily molecule in acetone.
[i]Based on rejection of glucose in water.
[j]Based on rejection of polyethylene glycols in water.

The Starmem™ membranes were originally developed as a trade-mark of W. R. Grace for use in the oil and gas industry. Starmem™ was later sold to Honeywell UOP, with UK distribution handled by Evonik Membrane Extraction Technology (MET). All Starmem™ membranes are polyimide based and stable for use in a range of solvents, including alkanes, aromatics, ethers and esters (Evonik MET, 2011a). Originally four membrane types were commercially available, with MWCOs of 200 g mol^{-1} (Starmem™120), 220 g mol^{-1} (Starmem™122), 280 g mol^{-1} (Starmem™228) and 400 g mol^{-1} (Starmem™240). Membranes with cut-offs of 200 and 280 g mol^{-1} were later discontinued and currently only Starmem™122 and 240 are available. Starmem™ membranes are made through immersion precipitation which is a phase inversion technique where a controlled transformation from the liquid to the solid state is achieved by immersion of the membrane casting solution in a non-solvent bath (Mulder, 1996c). Immersion precipitation result in an integrally skinned asymmetric membrane having a dense top layer. Membranes are not cross-linked, but are treated with a conditioning agent to improve membrane stability and flexibility in a dry state, as well as to facilitate handling (White *et al.,* 1993)(White and Nitsch, 2000)(White, 2001). The Starmem™ series is stable up to 60 bar pressure and temperatures of 50 ^{o}C, with membranes available as flat sheets or spiral-wound modules.

The Duramem™ series has been developed by Evonik MET, and is sometimes referred to as the second generation of OSN membranes. All Duramem™ membranes are made from modified polyimide, with MWCOs of 150, 200, 300, 500 and 900 g mol^{-1} currently available. Similar to Starmem™, the Duramem™ series is formed via immersion precipitation to generate asymmetric membranes. Membranes are treated with a chemical cross-linker to improve the overall stability, and a conditioning agent to facilitate membrane dry handling. Membranes are stable for use in a range of solvents, including alcohols, aromatics, ethers,

ketones and polar aprotic solvents, while functioning at temperatures up to 50 ^{o}C and maximum pressures of 20 (Duramem™ 500 and 900) or 60 bar (Duramem™150, 200 and 300) respectively (Evonik Met, 2011b)(Livingston and See-Toh, 2007)(See-Toh *et al.*, 2008).

The Puramem™ series has also been developed by Evonik MET. Puramem™ membranes are polyimide based and reported stable for operation at temperatures up to 50 ^{o}C, and maximum pressures between 20-60 bar depending on the MWCO. Solvent stability is assured in toluene, heptane, ethyl acetate, methyl ethyl ketone (MEK) and methyl isobutyl ketone (MiBK), whereas use in most polar and polar aprotic solvents is not recommended. Puramem™S380 has been reported to be a TFC, however as the Puramem™ series have only recently been released to market limited information is available about these membranes in literature (Evonik MET, 2011c)(Livingston *et al.*, 2011).

The most recent addition to the commercially available OSN membranes is GMT-oNF 1 and 2 which have been developed by Borsig GmbH. These membranes are TFCs consisting of a non-porous top layer and a micro-porous support layer, both made of a silicon-based polymer. GMT-oNF 1 and 2 are reported as stable for operation in solvents including alcohols, aromatics, alkanes, ethers and ketones. Membranes can be operated at temperatures up to 60 ^{o}C and maximum pressures of 35 bar, however allowable working conditions may vary depending on the application (Borsig, 2011a)(Borsig, 2011b)(Borsig GmbH, 2012).

Over the years a range of SolSep membranes have been made available for gas and liquid separations, with the current commercial range including four NF membranes ranging in MWCO between 300-1000 g mol^{-1}. Membranes are stable for operation at temperatures up to 150 ^{o}C and maximum pressures of 20-40 bar, and are chemically stable in a range of solvents

including alcohols, aromatics, ketones, esters, polar aprotic and some chlorinated solvents (Cuperus, 2005)(SolSep BV., 2008). Most available SolSep membranes have not been studied extensively in literature, however SEM images have been reported for SolSep 010206 indicating that the membranes have a TFC structure (Székely *et al.*, 2011).

The SelRo® series was released by Koch Membranes in the 1990s and were the first commercially available OSN membranes. The initial series contained three membranes; MPF-44 (MWCO 250 g mol^{-1}), MPF-60 (MWCO 400 g mol^{-1}) and MPF-50 (MWCO 700 g mol^{-1}). However, production of MPF-50 and -60 was later discontinued and currently only MPF-44 remains on the market. MPF-44 is a hydrophilic TFC membrane consisting of a cross-linked PDMS top layer attached to a PAN support (Linder, 1991)(Linder, 1993). MPF-44 is available as flat sheet and spiral-wound (MPS-44) modules and stability is claimed in alcohols, aromatics, ketones, aqueous mixtures and chlorinated solvents (van der Bruggen *et al.*, 2002b). However, testing by Van der Bruggen *et al.* (2002b) indicates that MPF-44 is only semi-stable, with membranes showing variable performance and visible damage after longer exposure to organic solvents (methylene chloride, acetone, hexane, ethyl acetate and ethanol).

The Inopor series includes three different NF membranes as well as a number of membranes operating in the UF and MF range. Membranes are ceramic with an asymmetric structure, and can be manufactured into mono-channel and multi-channel tubes of variable dimensions (Inopor, 2012). Ceramic membranes indicate a great potential for application in organic solvents due to their high stability and lack of swelling. The Inopor NF membranes only became commercially available in the late 00's, resulting in limited data presented in literature to date.

2.4 Membrane Parameters and Performance

NF separations are influenced by a range of factors, making prediction of membrane performance difficult. Selectivity is believed to be primarily dependent on steric factors though additional parameters such as pressure, temperature, charge and concentration have been observed to influence membrane performance, and can be used to fine-tune the separation. Additionally, factors such as concentration polarisation and membrane pre-conditioning are important to consider, and for OSN an additional level of complexity is added from interactions between the membrane, the solute and the solvent which can result in significantly changed performance for the same membrane during operation in different solvents.

2.4.1 Pressure

Pressure is the main driving force used for NF, and operation is commonly carried out at pressures ranging between 5-60 bar. However, a distinction must be made between the applied and the effective pressure, with the effective pressure being defined as the difference between the applied and the osmotic pressure. Effective pressure can be calculated according to Equation 2.3 where ΔP is the pressure difference and $\Delta \Pi$ is the osmotic pressure difference.

$$\Delta P_{Effective} = \Delta P_{Applied} - \Delta\Pi \qquad \text{Equation 2.3}$$

The osmotic pressure is caused by a difference in solute concentration on either side of the membrane. For a dilute system the osmotic pressure is assumed to be negligible, making the applied pressure equal to the effective pressure. However, for more concentrated systems the osmotic pressure should be included in all calculations. For low concentrations (< 0.2 M) the osmotic pressure can be calculated using the Van't Hoff equation (Equation 2.4), where *i* is

the Van't Hoff coefficient (1 for non-electrolytes), R_{gas} is the ideal gas constant, T is the temperature and C is the concentration of species i. For higher concentrations the Van't Hoff equation is however no longer valid and the osmotic pressure must be evaluated experimentally (Mulder, 1996d)(Whu *et al.*, 2000).

$$\Delta\Pi = iR_{gas}T\Delta C_i \qquad \text{Equation 2.4}$$

Several authors have studied the effect of pressure on membrane performance, with data showing a significant impact on both flux and rejection. A linear increase in flux was observed by both Whu *et al.* (2000) and Scarpello *et al.* (2002) for an increase in pressure from 0-30 bar using MPF-60 in methanol, Starmem™240 in ethyl acetate and Starmem™122 in both ethyl acetate and tetrahydrofuran (THF). Increasing the pressure raised the overall driving force of the system, and the observed increase in flux is in accordance with the expected behaviour.

For a range of alcohols, a non-linear increase in flux was however observed for MPF-50 operated at pressures between 0-30 bar (Machado *et al.,* 1999). During high pressure operation polymeric membranes are believed to become compacted, resulting in a less permeable membrane structure. Increased compaction will result in a gradual levelling of the flux towards a plateau value. Depending on the compaction occurring in a given solvent, the plateau is reached at different pressures and the flux increase can appear linear or non-linear depending on the pressure interval studied (Whu *et al.*, 2000)(Yang *et al.*, 2001)(Sheth *et al.*, 2003). The theory of membrane compaction is supported by an observed decrease in flux occurring during the initial stages of membrane operation. Compaction is believed to be partially reversible, which is supported by the observation that when a polymeric membrane is

allowed to rest (no applied pressure) before starting a second filtration, the pure solvent flux is generally found to be higher during the initial stage of the second filtration compared to the final flux observed during the first filtration (Whu *et al.*, 2000)(Sheth *et al.*, 2003).

Solute rejection has also been reported to increase at higher pressures. Whu *et al.* (2000) observed a change in rejection from 45.0% to 86.9% for Safranin O, and from 82.6% to 93.8% for Brilliant Blue R when the pressure was increased from 15 to 30 bar (Table 2.2). A similar trend was observed by Scarpello *et al.* (2002) where the rejection of Jacobsen catalyst dissolved in ethyl acetate was observed to increase from 98.9% to 99.5% for Starmem™122, and 93.5% to 95.5% for Starmem™240 during operation at 10 and 30 bar respectively (Table 2.2). This increase in rejection at increased pressure is again believed to be a result of membrane compaction resulting in a decreased size of pores or free-volume elements. A high solute rejection is often desirable to increase the overall product yield, and varying rejections with pressure could provide a useful way of optimising membrane performance.

Table 2.2. Summary of solute rejections measured at different pressure levels for various membrane-solvent-solute systems

Solute – Solvent	Membrane	P_1[a] (bar)	R_1[b] (%)	P_2[a] (bar)	R_2[b] (%)	Reference
Safranin O – methanol	MPF-60	15	45.0	30	86.9	Whu *et al.*, 2000
Brilliant Blue – methanol	MPF-60	15	82.6	30	93.8	Whu *et al.*, 2000
Jacobsen catalyst – ethyl acetate	Starmem™122	10	98.9	30	99.5	Scarpello *et al.,* 2002
Jacobsen catalyst – ethyl acetate	Starmem™240	10	93.5	30	95.5	Scarpello *et al.*, 2002

[a]Low (P_1) and high (P_2) operating pressures selected for testing

[b]Measured rejections during operation at low (R_1) and high (R_2) operating pressures selected for testing

2.4.2 Temperature

Machado *et al.* (1999) observed an increase in the flux of acetone through MPF-50 and MPF-60 when increasing the temperature from 0-40 ^{o}C. A similar trend was observed by Scarpello *et al.* (2002), where the flux was observed to increase during operation of Starmem™122 in THF and ethyl acetate, as the temperature was varied from 20-40 ^{o}C (Table 2.3). Scarpello *et al.* (2002) also observed that changes in temperature affected the rejection, which was observed to decrease with increasing temperature, for Starmem™122 using systems of Wilkinson catalyst dissolved in THF and Jacobsen catalysts dissolved in ethyl acetate respectively. Conversely, for Wilkinson catalyst dissolved in ethyl acetate, Starmem™122 showed no change in rejection with temperature, indicating that temperature effects are system specific. Changes in membrane performance with temperature have been attributed to: reduced solvent viscosity; increasing diffusion coefficients of the solvent and solutes; and a potential increase in the polymer chain mobility increasing the free volume in the membrane (Mulder, 1996b)(Machado *et al.*, 1999)(Scarpello *et al.*, 2002). No conclusive evidence has yet been provided for the suggested explanations, and as temperature effects on membrane performance seem highly system dependent, no definite conclusions regarding trends can be made.

Table 2.3. Summary of fluxes measured during operation at different temperatures for various membrane-solvent systems

Solvent	Membrane	T_1[a] (^{o}C)	J_1[b] (L m^{-2} h^{-1})	T_2[a] (^{o}C)	J_2[b] (L m^{-2} h^{-1})	Reference
Acetone	MPF-60	0	~70	40	~140	Machado *et al.*, 1999
Acetone	MPF-50	0	~250	40	~680	Machado *et al.*, 1999
THF	Starmem™122	20	~70	40	~150	Scarpello *et al.*, 2002
Ethyl acetate	Starmem™122	20	~100	40	~175	Scarpello *et al.*, 2002

[a]Low (T_1) and high (T_2) operating temperatures selected for testing

[b]Measured fluxes during operation at low (J_1) and high (J_2) operating temperatures selected for testing

2.4.3 Charge

For NF operation in aqueous systems, electrostatic interactions and the charge of solute molecules is widely considered to be an important influence on membrane separation performance (Donnan, 1995)(Yaroshchuk, 1998)(Van der Bruggen *et al.*, 1999)(Nghiem and Schäfer, 2005). For applications in organic solvents, charge effects are generally believed to be of less importance due to systems typically being uncharged (Mulder, 2005). However, during operation in methanol Yang *et al.* (2001) observed a significantly lower rejection for the uncharged solute Solvent Blue, compared to charged solutes Orange II and Safranin O, despite all solutes having the same molecular weight (350 g mol^{-1}). Variations in membrane performance could be a result of charge effects, however additional factors such as solvation, molecule shape, pH and charge delocalisation could be also be of importance. Compared to Orange II and Safranin O Solvent Blue has straight structure, which could potentially allow the molecules to pass more easily through the membrane resulting in a lower rejection (Figure 2.3).

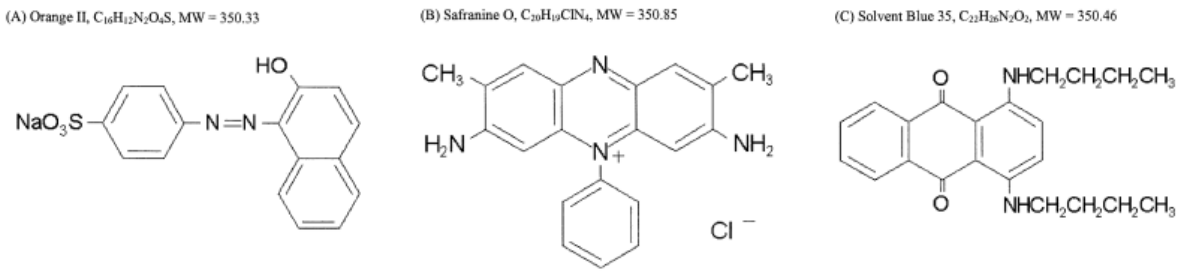

Figure 2.3. Molecular structures of Orange II, Safranin O and Solvent Blue (Yang *et al.*, 2001)

Charge effects on membrane rejection can be explained by looking at interactions between the solute and the membrane. For any given membrane system solutes are driven towards the

permeate side in an attempt to minimise the concentration difference and reduce the osmotic pressure. Most polymeric membranes carry a slight charge resulting from the polymer side-chains. When a charged molecule encounters a charged membrane, co-ions will be repelled, resulting in a high rejection of such solutes. To maintain the overall charge neutrality of the system, an equal amount of counter-ions must also be retained by the membrane resulting in a high rejection for all charged solutes. The retained solutes will strive to minimise the system charge effect and solutes will become arranged with the counter-ions forming an electrical double-layer at the interface between the membrane and the feed solution. If the ion concentration is sufficiently high (> 0.1 M) the double-layer will achieve full coverage, resulting in the counter-ions completely screening the membrane charge, rendering rejection to be dependent primarily on steric factors. For a lower ion concentration, the counter-ions present are not sufficient to balance the full membrane charge, and only a partial screening effect will be achieved. For a charged solute-membrane system the rejection is hence likely to be concentration dependent, with the rejection increasing for a decrease in concentration (Donnan, 1995)(Yaroshchuk, 1998)(Bowen and Welfoot, 2002)(Oatley, 2003)(Waite, 2005).

2.4.4 Concentration

Several authors have observed that solute concentration has an effect on both solute rejection and permeate flux. For an increase in concentration the flux is generally observed to decrease. It has been suggested that decreasing flux is a result of increased osmotic pressure lowering the effective pressure in the system. However, the solute concentrations used for testing have generally been low and hence the osmotic pressure is not sufficient to account for the significant changes in flux observed. More likely the decreasing flux is the result of a combination of factors, including increased osmotic pressure, concentration polarisation and

pore blocking (Section 2.4.5) (Whu *et al.*, 2000)(Scarpello *et al.*, 2002)(Peeva *et al.*, 2004)(Silva and Livingston, 2006a).

Solute concentration has further been observed to influence the solute rejection. Whu *et al.* (2000) observed an increase in rejection from 67.6% to 93.5% for Safranin O and from 94.8% to 99.7% for Brilliant Blue R for an increase in concentration from 0.01% to 1.0% (by weight) during operation of MPF-44 in methanol, with similar trends being observed for equivalent solutions using MPF-50 and MPF-60 (Table 2.4). Scarpello *et al.* (2002) also observed an increase in rejection from 97.1% to 99.5% for Wilkinson catalyst when changing the concentration from 0.785 mM to 5 mM during operation of Starmem™122 in THF (Table 2.4). Opposing trends for solute rejection were however observed by Peeva *et al.* (2004), with decreasing rejection of docosane for a change in concentration from 0.33 M to 0.67 M during operation of Starmem™122 in toluene (Table 2.4). Similar observations were made by Silva and Livingston (2006a), where the rejection of dimethyl methyl-succinate in methanol was observed to decrease from 30% to 18% for Starmem™122 in the concentration interval 5-35% (by weight) (Table 2.4). Silva and Livingston (2006a) also observed a constant rejection for dimethyl methyl-succinate in methanol during operation of MPF-50 in an equivalent concentration interval. Possible explanations for rejection variations with concentration include concentration polarisation, pore blocking and fouling, highlighting the importance of the hydrodynamic conditions at the feed side of the membrane (Whu *et al.*, 2000)(Scarpello *et al.*, 2002)(Peeva *et al.*, 2004).

Table 2.4. Summary of rejections measured during operation at different concentrations for various membrane-solute-solvent systems

Solute –Solvent	Membrane	C_1[a]	R_1[b] (%)	C_2[a]	R_2[b] (%)	Reference
Safranin O – methanol	MPF-44	0.01[c]	67.6	1.0[c]	93.5	Whu *et al.*, 2000
Brilliant Blue R – methanol	MPF-44	0.01[c]	94.8	1.0[c]	99.7	Whu *et al.*, 2000
Wilkinson catalyst – THF	Starmem™122	0.785[d]	97.1	5[d]	99.5	Scarpello *et al.*, 2002
Docosane – toluene	Starmem™122	0.33[e]	~95	0.67[e]	~90	Peeva *et al.*, 2004
Dimethyl methyl-succinate – methanol	Starmem™122	5[c]	30	35[c]	18	Silva and Livingston , 2006a

[a]Low (C_1) and high (C_2) feed concentrations selected for testing

[b]Measured rejections during operation at low (R_1) and high (R_2) feed concentrations selected for testing

[c]% (by weight), [d]mM, [e]M

2.4.5 Concentration Polarisation and Fouling

During operation some solutes are retained by the membrane, causing accumulation and formation of a boundary layer with a higher concentration close to the membrane surface. This phenomenon is referred to as concentration polarisation, and can have a significant effect on membrane performance, as the increased concentration acts as an additional resistance against solute and solvent mass-transfer. During membrane operation, solutes are brought to the boundary layer by convective transport and removed through diffusive flow back to the bulk solution (Figure 2.4). The convective and diffusive flows are assumed to be in equilibrium, and the ratio of concentrations between the feed and the boundary layer (C_m) can be calculated as a function of the flux (J), the solute mass-transfer coefficient (k) and the concentration in the bulk (C_b) and the permeate (C_p) as detailed in Equation 2.5, where D is the diffusion coefficient of solute i and δ is the boundary layer thickness. (Mulder, 1996f)(Schäfer *et al.,* 2005).

$$J = k \ln\left(\frac{C_m - C_p}{C_b - C_p}\right) \text{ with } k = \frac{D_i}{\delta} \qquad \text{Equation 2.5}$$

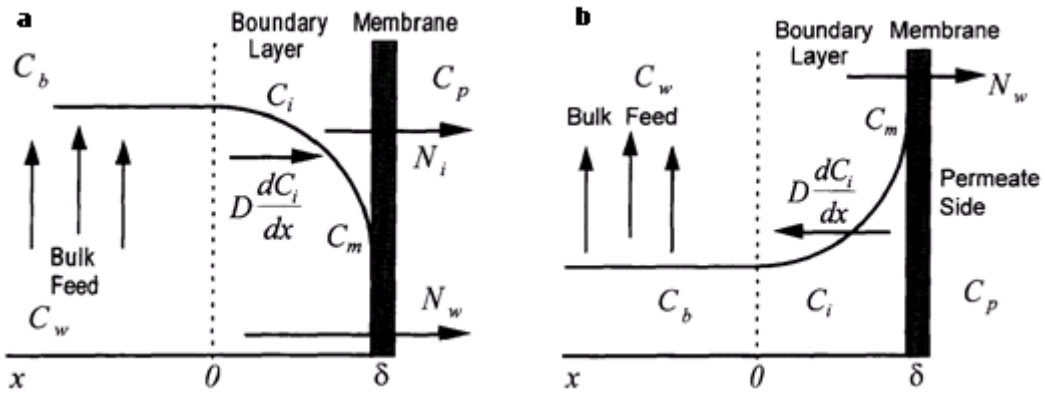

Figure 2.4. Concentration profile of (a) permeating and (b) retained component at steady state conditions where *C* is the concentration of the solvent (*w*) or species *i* in the in the bulk (*b*), permeate (*p*) or membrane boundary layer (*m*) and *N* is the flux of the solvent (*w*) and species *i* respectively (Bhattacharya and Hwang, 1997)

Concentration polarisation commonly results in a decreased flux, which is attributed to a significant increase in osmotic pressure resulting from the elevated concentration observed immediately adjacent to the membrane surface. Increased osmotic pressure further influences the separation performance, resulting in a decreased driving force for highly permeable components and an increased driving force for less permeable components (Bhattacharya and Hwang, 1997).

Concentration polarisation results from poor hydrodynamic conditions in the equipment used for filtration. The process is reversible and can be rectified by improving mass-transfer in the system through increased stirring, permeate pulsing, use of cross-flow operation and/or inclusion of baffles or spacers. If the concentration polarisation is not rectified, the build-up in solute concentration may cause precipitation and crystallisation on the membrane surface, potentially causing membrane damage (Schäfer *et al.*, 2005). Deposition of solids at the

membrane surface or in pores is referred to as membrane fouling, and can be the result of a number of mechanisms, including adsorption, gel layer formation, cake formation and pore blocking. Adsorption is an interaction between a membrane and a solute, resulting in a solid layer forming on the membrane surface. Adsorption is generally considered to be the first step in fouling and results in an alteration of the membrane's surface characteristics. Gel layer formation results from the precipitation and deposition of organic material on the membrane surface, and is commonly a result of concentration polarisation causing the concentration of a specific solute to exceed the solubility limit. Cake formation and pore blocking refers to a build-up of solid particles on the membrane surface or inside the pores. Where the solute radii are smaller than the pore, the solute can enter and deposit on the pore walls, gradually decreasing the pore radius until it is fully blocked. Where the solute radii are similar in size to the pore radius, immediate blockage can occur, while solute radii larger than the pore will result in cake formation on the membrane surface. Initially, pore blocking and cake formation is a result of membrane-solute interactions, but solute-solute interactions become increasingly more important as the solute layer is built-up (Koros *et al.*, 1996)(Bhattacharya and Hwang, 1997)(Peeva *et al.*, 2004)(Schäfer *et al.,* 2005).

Both concentration polarisation and fouling are problematic for industrial applications as they result in increased energy costs, reduced membrane life-time and additional costs associated with maintenance and cleaning (Schäfer *et al.,* 2005). Concentration polarisation and fouling has been studied extensively in aqueous systems, but to date only limited work has been carried out looking at effects in OSN. Some studies of concentration polarisation in OSN have nevertheless been presented in literature, with initial data indicating good agreement in estimating and correlating concentration polarisation and membrane transport performance in

dead-end, cross-flow and spiral-wound systems (Peeva *et al.*, 2004)(Stamatialis *et al.*, 2006)(Silva and Livingston, 2006a)(Silva and Livingston, 2006b)(Silva *et al.*, 2010).

2.4.6 Pre-conditioning

OSN data is dependent on the membrane-solvent-solute system used for testing, where varying membrane performance is commonly observed for the same membrane type during operation in different solvents. Additionally, inconsistent membrane performance has been observed during operation in the same solvent when comparing data reported by different authors for a given membrane type. Several authors have suggested that observed variations could be a result of varying protocols for washing and pre-conditioning prior to membrane operation (Gibbins *et al.*, 2002)(Bhanushali and Bhattacharyya, 2003)(Zhao and Yuan, 2006b).

Many commercial membranes are supplied in a preservative liquid (*e.g.* MPF-44) or have been treated with a preservative to facilitate dry handling of the membrane sheets (*e.g.* the Duramem™, Starmem™ and Puramem™ series). Hence, membrane discs should first be washed by soaking the membrane in the operating solvent prior to fitting, or by flushing the membrane disc via permeation of the operating solvent at the selected operating pressure. The latter method is recommended by manufacturer Evonik MET, who advise washing each membrane with a minimum of 40 L solvent per m^2 membrane area (Bhanushali and Bhattacharyya, 2003)(Zhao and Yuan, 2006b)(Evonik MET, 2011a-c).

Following initial pressurisation, a reduction in flux is commonly observed. This is believed to be a result of membrane compaction occurring as polymer chains are rearranged under the

applied pressure. After permeation of a sufficient amount of solvent, a steady-state is reached and stable flux and rejection data can be obtained. The required time to reach steady-state is highly dependent on the solvent-membrane system used for operation, and for each test sufficient pre-conditioning time to reach maximum membrane compaction must be allowed before samples are collected. Additionally, compaction effects are partially reversible, so if the system has been depressurised or altered (*e.g.* change of solvent), a new pre-conditioning is required before the membrane can be considered to operate at steady-state and reliable measurements can be made (Mulder, 1996f)(Gibbins *et al.*, 2002)(Vankelecom *et al.,* 2004)(Zhao and Yuan, 2006b).

2.5 Membrane Equipment, Scale-up and Mode of Operation

Initial feasibility of OSN membrane performance can be studied in lab-scale filtrations using flat sheet membranes. Lab-scale studies are designed to maintain a low material and volume requirement, enabling use of equipment with a limited membrane surface area. Limiting the membrane area could be advantageous during membrane development to facilitate selection of a consistent membrane disc and minimise the membrane area used, as well as to limit the feed requirement for an initial membrane application test. Utilisation of a small membrane area will however limit the processing time, and for operation on a larger scale a significant increase of the membrane area is required. During scale-up of OSN operations, use of flat sheet membranes becomes less practical and membranes are scaled into modules to facilitate handling, minimise the equipment footprint and provide effective fluid management (Vandezande *et al.*, 2008). OSN equipment used for lab-scale operation is discussed in Section 2.5.1, followed by Section 2.5.2, which describes scale-up of membrane operations.

2.5.1 Lab-scale Equipment

The most basic type of OSN lab-scale equipment is a dead-end filtration cell (Figure 2.5), consisting of a feed tank with a flat sheet membrane fitted onto a porous support plate at the bottom of the tank. The membrane is sealed using an o-ring of suitable material, while mixing in the system is provided by a magnetic stirrer fitted just above the membrane surface. During operation the dead-end cell is attached to a high pressure source supplying the driving force for the operation. For lab-scale operations pressure is most commonly supplied through gas pressure (*e. g.* nitrogen), though back-pressure through pumps can also be used. The dead-end filtration cell is simple to operate and has a relatively small membrane area, making it ideal for initial feasibility studies. However, disadvantages include the fixed membrane area and the limited mass-transfer achieved using the magnetic stirrer, potentially leading to concentration polarisation and observation of misleading rejection and flux values (Mulder, 1996g)(Fane, 2005).

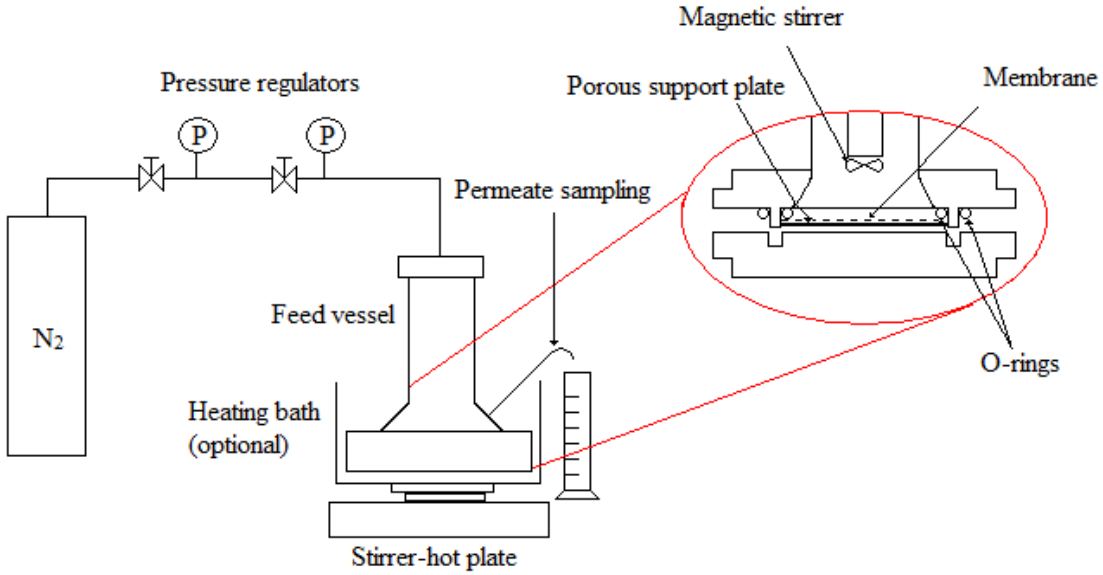

Figure 2.5. Schematic of OSN dead-end filtration kit and cross-section of equipment

Scale-up of OSN operation is relatively simple, as the volumetric flow rate of permeate is directly proportional to the membrane area. A larger volume of feed solution can thus be processed within a fixed time-frame by simply adjusting the membrane area. For lab-scale operation the membrane area can be increased through use of a cross-flow filtration system (Figure 2.6), where multiple membrane-containing cells are separated from the feed tank and connected in series. Similar to the dead-end cell, the cross-flow system is operated using flat sheet membranes and pressurisation is achieved through a gas source. Mixing in the system is improved by inclusion of a gear pump re-circulating the feed solution, causing a tangential flow over the membrane surface. The cross-flow set-up improves the hydrodynamic conditions close to the membrane surface, and is generally believed to provide a more representative measure of large-scale membrane performance (Silva and Livingston, 2006b). The ability to fit multiple membranes into the cross-flow system provides a convenient way to increase the membrane area for lab-scale operation. Additionally, different membrane types can be fitted into the individual filtration cells, allowing simultaneous screening of multiple membranes while maintaining near identical conditions (Mulder, 1996g)(Fane, 2005).

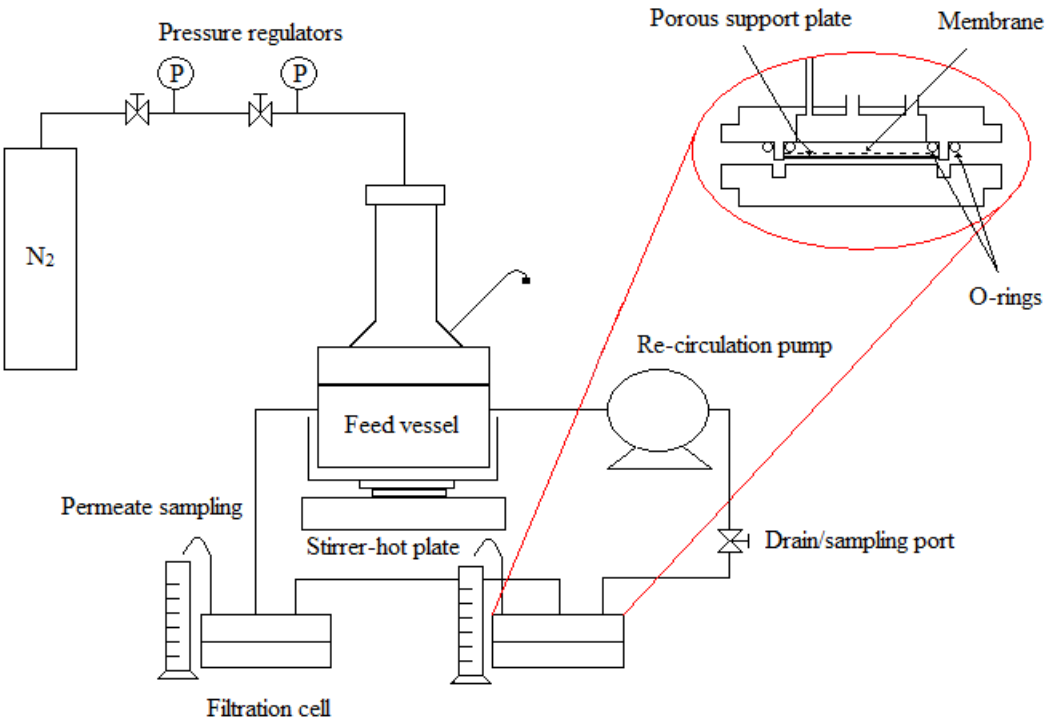

Figure 2.6. Schematic of OSN cross-flow filtration kit and cross-section of filtration cell

2.5.2 Membrane Modules and Scale-up Considerations

For OSN operation on an industrial scale, several square metres of membrane area are commonly required to enable processing of large volumes within a reasonable time-frame. Flat sheet membranes are therefore no longer suitable for use due to the difficulty in handling large sheets of membranes and the resulting large equipment footprint. For large scale operation membranes are instead packed into modules, which are designed to support the membrane and providing effective fluid management, while maintaining a low ratio between the equipment size and the membrane area (Mulder, 1996g)(Fane, 2005).

For flat sheet membranes the predominant module design used for industrial NF application is the spiral wound module (Figure 2.7). The spiral wound module uses flat sheet membranes, which are glued together along three sides to form a leaf-like structure. The un-sealed edge of

the membrane leaves are attached to a permeate collection tube and the membrane is wound around the tube, and covered by a protective outer casing. The membrane sheets are separated by permeate spacers placed inside the leaf-structure with the individual leaves separated by feed channel spacers. The spacers provide support for the membranes as well as create flow-paths through the module to facilitate fluid management. Design of the spacers also influences mass-transfer, packing density and pressure drop occurring over the module. During operation the feed solution flows tangentially to the membrane surface in a cross-flow regime, with solvent and smaller solutes passing through the membrane, flowing inwards to the permeate collection tube. Spiral wound modules can be made into different sizes by varying the module diameter, while multiple modules can be connected in series or parallel during operation to obtain the desired membrane area (Mulder, 1996g)(Gould *et al.*, 2001)(Fane 2005).

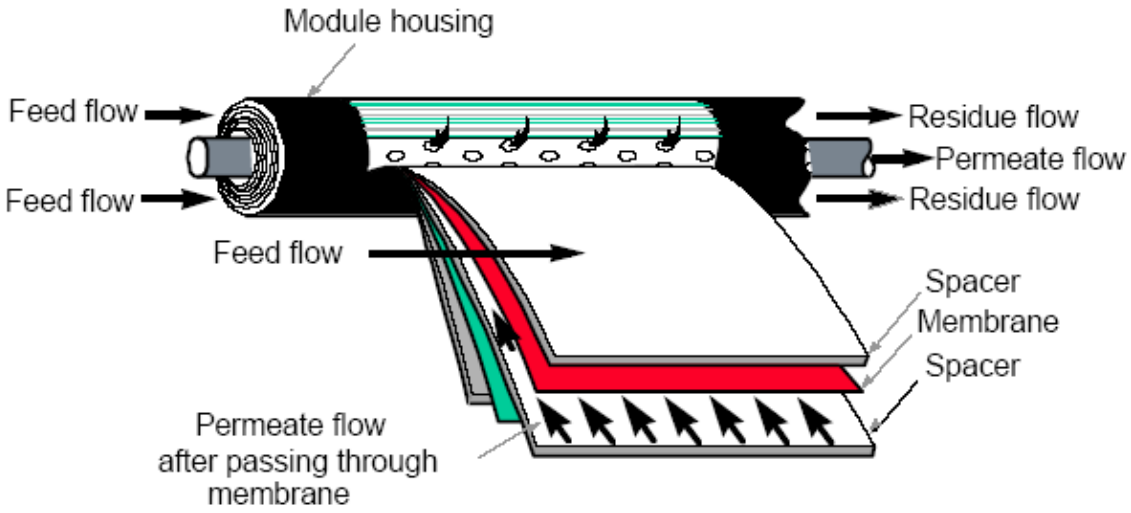

Figure 2.7. Schematic of a spiral wound membrane module (Oatley, 2003)

For industrial OSN operation the use of gas cylinders to pressurise the system is not practical, and the required back-pressure is more commonly supplied by a pump (Figure 2.8). Depending on the volume to be processed and the potential for concentration polarisation in the system, the back-pressure pump may be sufficient to supply both the pressure and the required mixing through re-circulation of the feed solution. However, for more concentrated systems, a second pump can be included in a re-circulation loop over the membrane module. The re-circulation loop is placed before the back-pressure valve and the flow in the loop is 5-10 times higher than the feed flow. Inclusion of a re-circulation loop thus enables a high cross-flow velocity over the membrane surface without having to re-circulate the full feed volume through the back-pressure valve, hence minimising the overall energy consumption. Operation of membrane modules in this dual pump configuration is referred to as a feed-and-bleed system (Figure 2.8) (Mulder, 1996g)(Baker, 2004c).

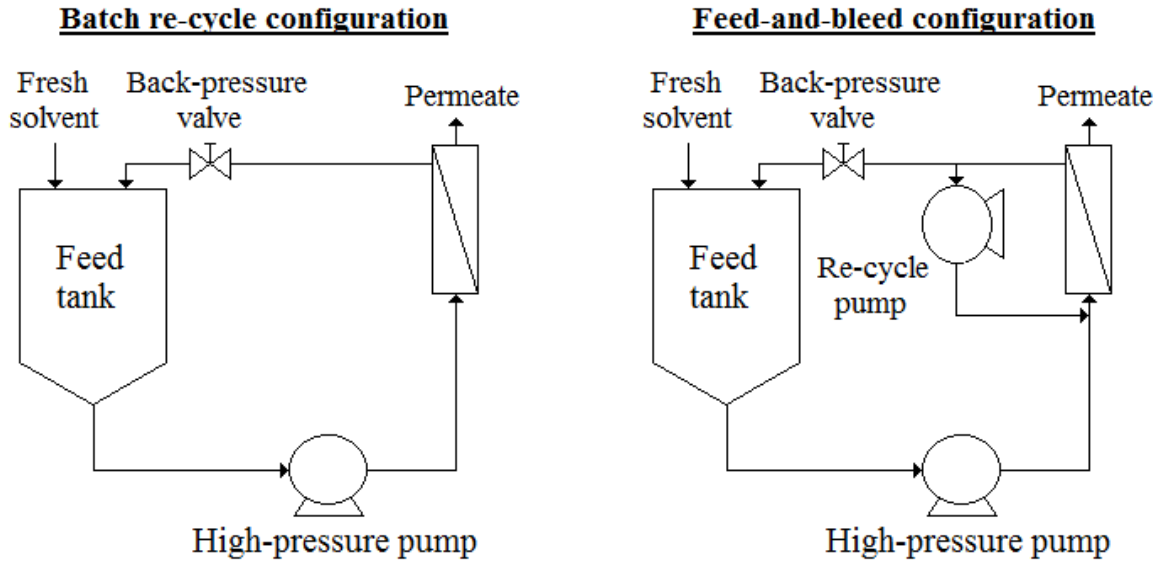

Figure 2.8. Schematic representation of a batch re-circulation OSN industrial system (*left*) and a feed-and-bleed system (*right*)

2.5.3 Modes of Operation

For process development and scale-up of membrane operations, equipment selection is only the first step, with additional factors such as system assembly and mode of operation being important further considerations. The system assembly is designed to fit the requirements of the application while also considering process economics. The most suitable mode of operation is selected based on process requirements, such as mass- and energy efficiency and required product purity. Common operating regimes include batch (*e.g.* single pass), continuous and semi-continuous (*e.g.* diafiltration) (Fane, 2005)(White, 2006).

Diafiltration can be operated in a continuous or dis-continuous (put-and-take) mode. During continuous constant volume diafiltration fresh solvent is added to the system at a rate equal to the permeation. During operation, smaller molecules are washed out through the membrane while larger molecules are retained, resulting in a gradual purification of the retentate. Diafiltration can be operated both with the desired component retained and impurities passing, or with the desired component passing while larger impurities are retained. Processing can be continued until the selected target level is reached, however to keep losses to a minimum, and prevent contamination of the permeate, the retained component should ideally have a high rejection (close to 100%) while the solutes to be washed out should have a low rejection (close to 0%). Put-and-take diafiltration is based on a similar operating regime, but operation is carried out in cycles where the smaller solutes are initially removed during a concentration of the retentate, prior to addition of fresh solvent to the original volume level. Retentate concentration and solvent additions are repeated in cycles until the desired target level is reached, with put-and-take operation often requiring a lower overall solvent addition compared to continuous operation. Though diafiltrations can enable separation of solutes, a

gradual solvent addition is required, and operation can be highly solvent intensive (Mulder, 1996g)(Fane, 2005)(Livingston and Nasso, 2009).

2.6 Lab-scale and Industrial Applications of OSN

As previously stated NF is an established technique for aqueous applications and has been used extensively for water purification, waste-water treatment, desalination and various applications in the food and dairy industries. Extending NF applications to organic solvents has long been an area of interest, with some of the main applications discussed including:

- Product purification/impurity removal
- Concentration of process solutions
- Recovery and recycling of valuable reagents (*e. g.* catalysts)
- Recovery and recycling of processing solvents
- Solvent swaps

Membrane technology offers potential advantages with regards to low capital investment and operating costs, as well as simple equipment construction, operation and scale-up. Additionally, as OSN is a non-thermal technique, operation is generally energy-efficient and can be used in the processing of heat sensitive material. Finally, OSN can enable solvent swaps between any miscible solvents, including the difficult case of going from high to low boiling point solvents. Advantages of OSN can include economic and environmental benefits, highlighting the technique as a promising alternative to the unit operations currently in use in various chemical industries. OSN has been investigated for applications within the food, fine chemical, petrochemical and pharmaceutical industries, and a selection of studies carried out to date is summarised in Table 2.5 and Table 2.6.

Table 2.5. Overview of OSN applications in the food and fine chemical industries

Industry	Membrane	Solvent	Application	Reference
Food	MPF	Hexane	Solvent recovery and de-acidification of vegetable oils	Raman *et al.*, 1996
	Cellulose acetate, polyamide, polyimide	Various alcohols, acetone, butyl acetate, hexane, water	Concentration and separation of amino acids	Reddy *et al.*, 1996
	DS7, polyamide	Hexane	De-gumming of crude vegetable oil	Lin *et al.*, 1997
	Polyamide, cellulose acetate	Acetone, ethanol, 2-propanol, hexane	De-acidification of vegetable oil	Zwijnenberg *et al.*, 1999
	DS7, MPF	Hexane, methyl esters	Recovery of carotenoids from red palm oil	Darnoko and Cheryan, 2006
	Starmem™, Duramem™	Hexane, ethyl acetate	Refining of rice brand oil	Sereewatthanawut *et al.*, 2011
Fine Chemical	MPF	Methanol	Catalyst recovery and recycle	de Smet *et al.*, 2001
	Starmem™	Toluene	Recovery and reuse of homogeneous phase transfer catalyst	Luthra *et al.*, 2002
	Starmem™, MPF	THF, water, acetonitrile	Recovery and recycle of homogeneous Heck catalyst	Nair *et al.*, 2002
	Starmem™, MPF	Ethyl acetate, THF, DCM[a]	Separation of homogeneous organometallic catalysts	Scarpello *et al.*, 2002
	Starmem™	Toluene, THF, water acetone, ethyl acetate	Recovery and recycle of homogeneous catalyst	Livingston *et al.*, 2003
	PDMS-PAN TFC	Toluene, cyclohexane	Homogeneous catalyst separation	Datta *et al.*, 2003
	Silicon based	Diethyl ether	Recovery and recycle of homogeneous Co-Jacobsen catalyst	Aerts *et al.*, 2004
	Starmem™	Methanol, toluene, ethyl acetate	Separation of products and ionic liquids	Han *et al.*, 2005
	Starmem™	Ethyl acetate	Recovery and reuse of ionic liquids and palladium catalyst	Wong *et al.*, 2006
	Starmem™	Ethyl acetate	Palladium removal from post-reaction solutions	Pink *et al.*, 2008
	Starmem™	Methanol	Recovery and reuse of Ru-BINAP homogeneous catalyst	Nair *et al*, 2009
	Starmem™	Dodecene, octane	Separation and recovery of homogeneous catalyst	Priske *et al.*, 2010
	Duramem™	MEK	Product recovery from ionic liquids	Van Doorslaer *et al.*, 2010

[a]Dichloromethane

Table 2.6. Overview of OSN applications in the petrochemical and pharmaceutical industries

Industry	Membrane	Solvent	Application	Reference
Petrochemical	Polyimide	MEK, toluene	Solvent recovery from lube oil filtrate (MAX-DEWAX®)	White and Nitsch, 2000
	Polyimide	MEK, toluene	Solvent recovery from lube oil filtrate	Kong *et al.*, 2006
	Polyimide	Toluene	Aromatic enrichment in refinery streams	White and Wildemuth, 2006
	Starmem™, SolSep	Biodiesel, methanol	Biodiesel synthesis and separation	Othman *et al.*, 2010
Pharmaceutical	MPF	Ethyl acetate, methanol	Diafiltration based solvent exchange	Sheth *et al.*, 2003
	Starmem™	Toluene, methanol, ethyl acetate	Diafiltration based solvent exchange	Livingston *et al.*, 2003
	Starmem™	Multiple	Solvent exchange and recycle of resolving agents	Ferreira *et al.*, 2006
	Starmem™	Toluene, methanol	Continuous solvent exchange	Lin and Livingston, 2007
	Starmem™	Toluene, hexane	Enantiomer separation	Ghazali *et al.*, 2006
	Starmem™	Toluene, methanol	Removal of APIs from solvents	Geens *et al.*, 2007
	Duramem™	DMF[a], THF	API purification	Sereewatthanawut *et al.*, 2010
	SolSep, GMT	MEK, THF	API purification	Székely *et al.*, 2011
	SolSep, GMT	MEK, THF, DCM	API purification	Székely *et al.*, 2012a
	Polyimide	Butyl acetate	Concentration of antibiotic extract	Shi *et al.*, 2006
	Inopor ZrO_2	DMF[a]	Membrane enhanced peptide synthesis	So *et al.*, 2010

[a]Dimethylformamide

2.7 Research Motivation and Objectives of the Present Work

With the recent development and commercialisation of membranes with increased solvent stability, OSN has been identified as a promising alternative to traditional unit operations. Multiple studies have demonstrated the capability of OSN for applications in the food, fine chemical, petrochemical and pharmaceutical industries. Studies have increased the understanding of currently available OSN membranes. However, much of the data presented is limited to model systems demonstrating separation for molecules having a large difference in molecular weight (300 g mol^{-1} and upwards) (Luthra *et al.*, 2002)(Wong *et al.*, 2006)(Sereewatthanawut *et al.*, 2010). Examples of OSN application in concentrated multi-component systems, which are of interest for industrial application, remain virtually un-addressed. Additionally, to date there is limited published data which compares OSN performance against unit operations currently in use. Lack of comparative data makes it difficult to evaluate the true gain of OSN applications, which in combination with the chemical and pharmaceutical industries often being hesitant to switch from conventional, established techniques, has restricted industrial implementation of OSN to date.

The objective of this thesis is to evaluate the potential for OSN application in the pharmaceutical industry. The work is intended to identify potential benefits to membrane technology compared to traditional separation techniques, with regards to operability, sustainability and cost. The work further aims to identify and address potential limitations of OSN. The overall objective can be divided into three sections relating to; i) investigating OSN in industrial applications, ii) provide process comparisons, and iii) evaluate potential benefits from application of transport models for prediction of membrane performance.

Objective 1: Investigate application of OSN in pharmaceutical processes including API purification, solvent swapping and solvent recovery

This section aims to investigate OSN application in a range of unit operations including API purification, solvent swapping, and solvent recovery and recycling. Applications tested were selected from industrially relevant processes from GSK, with focus placed on situations where traditional techniques are insufficient or unsuitable. This study investigates OSN both as a stand-alone technique and in combination with additional unit operations (*e.g.* chromatography and adsorbents), with the aim of providing data for process comparisons (Objective 2).

Objective 2: Provide process comparisons for OSN and unit operations currently in use

This section aims to highlight benefits and limitations of OSN, and to provide a basis for evaluating OSN against more conventional options. OSN data obtained in Objective 1 is used to carry out the process comparisons commonly missing in literature.

Objective 3: Evaluate the use of modelling for prediction of OSN performance

Modelling of membrane performance can be a useful tool for membrane selection and process optimisation. Several models predicting membrane performance are available in literature and though good estimations have been demonstrated for dilute aqueous systems, current models lack the generality to predict membrane performance across a wide range of solvent-solute systems. Additionally, available models are commonly based on physical properties of the membrane which can be time-consuming and difficult to measure, and hence are often assumed. In this section current OSN transport models and characterisation experiments needed for application will be reviewed. This section aims to evaluate the potential for use of modelling in facilitating industrial OSN application.

Chapter 3: API Purification through OSN Diafiltration

3.1 Introduction

Regulators of the pharmaceutical industry, such as the European Medicines Agency (EMA) and the Food and Drug Administration (FDA), are continually evolving their rules and regulations to ensure patient safety, with key focus being placed on quality (FDA, 2009)(FDA, 2011). Manufacturing high purity drug products is a challenging responsibility faced by the pharmaceutical industry, with the increasing demand for higher purity products often testing the limitations of conventional separation techniques. Consequently, scientists are increasingly looking to less established methods in order to exploit potential advantages in separation efficiency.

API purification is commonly highlighted as a potential area for OSN application, and some studies have been performed demonstrating OSN capability for separation (Sereewatthanawut *et al.*, 2010)(Székely, 2011). This section will discuss work carried out to ascertain whether OSN can be used for separation of an intermediate size API (~330 g mol^{-1}) from a smaller impurity (~110 g mol^{-1}) in a mixture of THF and water. Additionally, this work focused on evaluating whether OSN could offer benefits over liquid-liquid extraction (LLE) currently used for separation, while identifying potential benefits and limitations to OSN application. Furthermore, with regard to contemporary work on membrane stability in THF (Székely, 2011), an evaluation of membrane stability was included to ensure accuracy and consistency of collected data.

The work in this chapter was carried out in collaboration with M. F. Jimenez Solomon (Imperial College London).

3.2 Materials and Methods

3.2.1 Feed Solution and Membrane Selection

The feed solution was based on a model system for an API and impurity separation. The system was comprised of a mixture of THF and water (75:25) containing 12.5 g L^{-1} API (~330 g mol^{-1}) and 4.3 g L^{-1} impurity (~110 g mol^{-1}). High-performance liquid chromatography (HPLC) grade THF (Sigma Aldrich) and de-ionised water was used for all processing.

Based on manufacturer recommendations and membrane MWCO, commercially available Duramem™200 (Evonik MET Ltd.) was selected for study. Additionally, two developmental membranes from Imperial College London were included for screening (Table 3.1). All testing was carried out using duplicate discs of each membrane type.

Table 3.1. Summary of developmental membranes from Imperial College London selected for testing in API and impurity separation

Membrane	Supplier	Membrane Type	Membrane Material
H	H. Siddique	Integrally skinned asymmetric	Polyimide
M	M. F. Jimenez Solomon	TFC	Polyamide/polyimide[a]

[a]Jimenez Solomon *et al.*, 2012

3.2.2 Membrane Screening

Membrane screening was carried out in a cross-flow system set up at Imperial College London. The cross-flow system was made up of 6 cross-flow cells, each holding an individual membrane area of 1.4×10^{-3} m^2. Filtration cells were connected in series and attached to a feed tank with a volume capacity of 3.0 L. Mixing in the system was provided via re-circulation of the feed solution using a diaphragm pump, which was also used for pressurisation through a

back-pressure regulator attached after the cross-flow cells. System pressure and temperature was monitored throughout operation.

Prior to starting the experiment, all membrane discs were washed and pre-conditioned by re-circulating 2.5 L of pure THF for 4.5 hours at 30 bar pressure and ambient temperature (~30 ^{o}C). After 4.5 hours re-circulation, a stable flux was reached indicating that maximum membrane compaction had been achieved. After pre-conditioning the system was de-pressurised and drained, before adding 2.5 L of feed solution. The system was then re-pressurised to 30 bar and the feed solution re-circulated through the membranes for 96 hours without de-pressurisation. Permeate samples were collected after 96 hours, while feed and retentate samples were collected at the start and finish of the experiment respectively. Flux was measured every 8-15 hours, through collection of permeate over a fixed time period (2 minutes for membrane M and 4 minutes for Duramem™200 and membrane H).

Membrane screening was carried out to investigate membrane performance and facilitate selection of a suitable membrane for the desired API and impurity separation. API purification is achieved through diafiltration, with the API retained and the smaller impurity gradually being washed out through the membrane. To keep API losses to a minimum, the ideal membrane should fully retain the API while allowing the impurity to pass through unhindered. Additionally, a high flux is desirable, to limit the required membrane area and processing time.

3.2.3 Membrane Stability Testing

A membrane stability test was performed as a continuation of the membrane screening. The system was run for an additional 72 hours with pressure cycles, implemented by de-pressurising the system and leaving the membranes to rest for 0.5 h before re-pressurisation. During the fourth day of operation four one-hour pressure cycles were carried out, with this cycle time being increased on the fifth and sixth days to enable monitoring of compaction, whereby three two-hour cycles were instead performed. Permeate samples were collected at the end of the stability test and the flux was monitored before and after each pressure cycle.

3.2.4 Diafiltration Predictions

Due to limited material availability no diafiltration experiments were carried out. To provide a basis for comparison between the membranes tested and the LLE currently in use, a theoretical comparison was instead performed. Diafiltration performance was predicted based on mass-balance calculations (Equation 3.1), with C being the concentration of solute i in the retentate (r) and feed (f) respectively, V_f the feed volume, J the flux, A the membrane area, R the rejection and t the operating time.

$$C_{i,r} = \frac{C_{i,f}V_f - JA\Delta t\left(1 - \frac{R_i}{100}\right)C_{i,f}}{V_f} \qquad \text{Equation 3.1}$$

If the rejection of a given solute is not 100%, the concentration in the feed tank will change gradually throughout the diafiltration. The retentate concentration can therefore not be calculated in a single step, and mass-balances were carried out as integrations based on a feed volume of 2.5 L and one hour time intervals.

3.2.5 Analysis

API and impurity concentrations were monitored using an Agilent 1100 Series HPLC system. Samples were analysed using an 8 minute gradient method, with eluents passing from 100% 0.05% (by volume) trifluoroacetic acid (TFA) in water to a mixture of 5% water and 95% acetonitrile containing 0.05% (by volume) TFA. Flow rate was set to 1.0×10^{-3} L min^{-1} through a Phenomenex Luna C18 column (50 × 2.0 mm, 3.0 μm) held at 40 ^{o}C. Components were detected using a diode array detector set to a fixed wavelength of 220 nm.

3.3 Results and Discussion

3.3.1 Membrane Screening

Screening data indicated that all membranes tested had a high API rejection close to the ideal value of 100% (Table 3.2). The highest rejection was observed for membrane H, with an average value of 99.4% and an impurity rejection of 46.3%. Despite the impurity rejection measured deviating from the ideal value of 0%, API purification through diafiltration is still possible. However, the higher impurity rejection will result in the impurity passing less readily through the membrane, giving an extended separation run-time in turn requiring higher solvent addition. Impurity rejections around 40% were also observed for membrane M (37.4%) and Duramem™200 (45.7%), with API rejections of 99.1% and 98.2% respectively. Similarities in the API and impurity rejections for all membranes tested complicate direct membrane selection, and all three membranes were selected for further study of diafiltration performance.

Table 3.2. Summary of performance data from membrane screening using a feed solution of 12.5 g L^{-1} API and 4.3 g L^{-1} impurity dissolved in a mixture of THF and water (75:25) (test was operated in cross-flow at 30 bar pressure and ambient temperature)

Membrane	R_{API}[a] (%)	$R_{Impurity}$[a] (%)	Flux (L m^{-2} h^{-1})
Duramem™200	98.2 ± 0.1	45.7 ± 0.0	11 ± 0
Membrane H	99.4 ± 0.8	46.3 ± 5.2	16 ± 2
Membrane M	99.1 ± 1.3	37.4 ± 1.6	32 ± 5

[a]Based on average data from two membrane discs

3.3.2 Diafiltration Predictions

Diafiltration performance was calculated (Equation 3.1) using the average data for API and impurity rejections measured during the membrane screening. The impurity target was set to 5% (by mass) in the retentate solution, and for all membranes tested calculations show a gradually decreasing impurity concentration in the retentate, until the target level is reached after passage of 4.8, 5.5 and 5.6 diafiltration volumes (DV) for membrane M, Duramem™200 and membrane H respectively (Figure 3.1). Each DV is equal to one feed volume and is used to provide a time independent measure of the solvent consumption. The API rejection was high for all membranes tested, resulting in the concentration remaining close to the original value throughout operation. Important to note is that as the API rejections were not 100% some API passed through the membrane resulting in gradual losses totalling 3.3% (membrane H), 4.2% (membrane M) and 9.4% (Duramem™200).

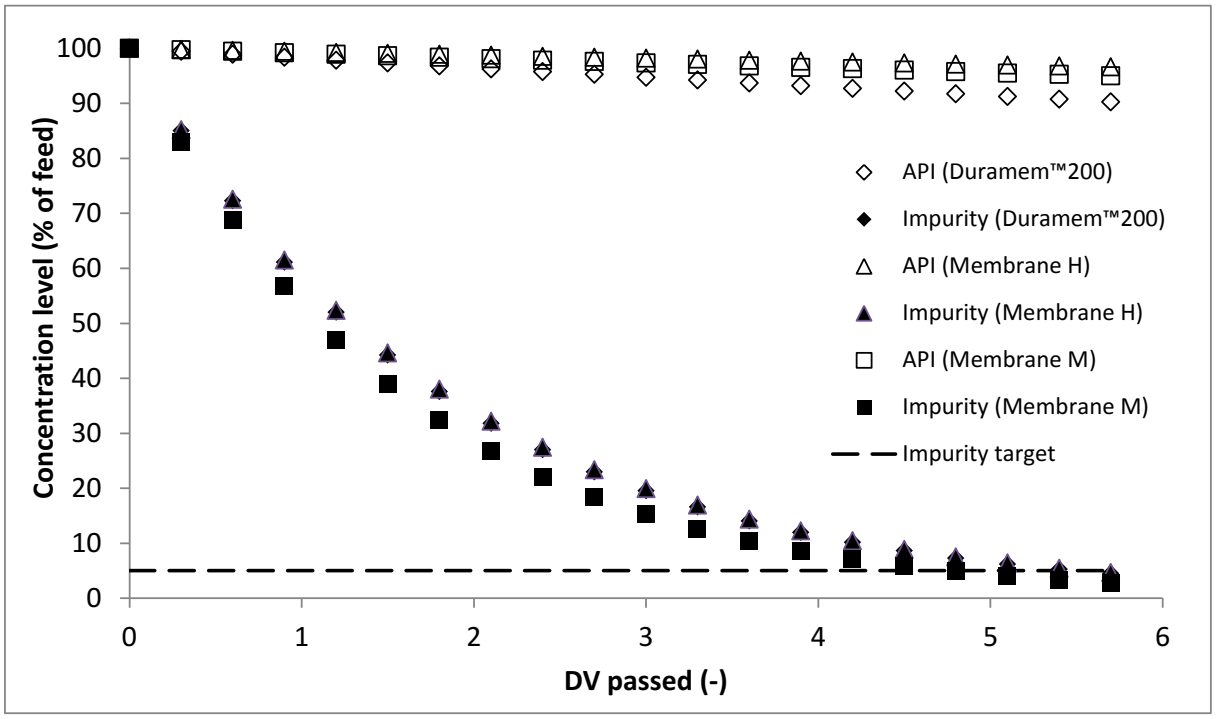

Figure 3.1. Summary of calculated diafiltration performance for Duramem™200, membrane H and membrane M based on membrane screening data (trends were calculated from mass-balance predictions based on membrane screening data in Table 3.2)

3.3.3 Process Comparison

The unit operation currently in use for API purification is a three stage LLE. In order to reach the set impurity target of 5% (by mass), the LLE requires an overall addition of 0.009 L solvent per gram purified API, resulting in an API loss of 5%. Process comparison (Table 3.3) indicates that when a membrane with a high API rejection (> 99%) is used for diafiltration, the overall API loss is lower for OSN compared to the LLE. However, diafiltration prediction demonstrates that even for a small reduction in the API rejection to 98.2% (Duramem™200), the API loss is significant (9.4%), despite a seemingly high rejection.

Diafiltration predictions further indicate that OSN requires between 0.4 L and 0.5 L of solvent per gram purified API to reach the desired impurity target (Table 3.3). Data also demonstrate that despite Duramem™200 having a lower impurity rejection compared to membrane H, the overall solvent consumed per gram purified API is higher as a result of the larger API loss. For this specific separation the process comparison indicates that all diafiltrations require significantly more solvent compared to the LLE in order to reach equivalent impurity levels, indicating diafiltration to be a solvent intensive method. For all membranes tested the impurity rejection is approximately 40%, resulting in prolonged processing times required to reach the impurity target. However, even assuming a theoretical impurity rejection of the ideal value of 0%, passage of 3.0 DV is still required for membrane M, resulting in an API loss of 2.6% and a solvent usage of 0.243 L per gram purified API. If a membrane with a high rejection is used, OSN may offer sufficient benefits with regards to improved API yield to make operation financially viable despite the high solvent consumption. However to date, discussion of the high solvent intensity for OSN has been limited, and this issue needs to be addressed in order to facilitate industrial OSN application.

Table 3.3. Process comparison based on solvent consumption and API losses for LLE and diafiltration operation using Duramem™200, membrane H and membrane M respectively

Purification technique	**Impurity level (%)**	**API yield loss (%)**	**Solvent consumption (L g^{-1} API)**
LLE	5	5.0	0.009
OSN (Duramem™200)	5	9.4	0.487
OSN (membrane H)	5	3.3	0.460
OSN (membrane M)	5	4.2	0.397

As significant API losses were observed during OSN operations, theoretical API yields were calculated for rejections between 90-100% to evaluate the influence of membrane rejection performance (Figure 3.2). Diafiltration calculations were based on performance data for membrane M and demonstrate that even for a high rejection of 99%, the API loss totals 4.7% for passage of 4.8 DV, increasing to 21.4% for a rejection of 95%. Predicted data indicate that relying on rejection values alone can provide false confidence in the separation, and potential losses in a membrane system should always be calculated. This is especially important for high value compounds where yield losses can have a significant negative impact on the process economics. If near 100% rejection can be achieved, required investment cost for OSN equipment could more easily be justified, increasing the likelihood of OSN being used in API purification. Ergo, achieving high rejection is crucial to OSN application, highlighting improved rejection as an important area of research for membrane development.

Theoretical prediction of diafiltration, based on performance of membrane M, demonstrates that for a rejection of 90% (the selected definition for MWCO) passage of 4.8 DV result in an API loss of almost 40%. Calculation of significant API losses occurring for a 90% rejection indicates that for systems where prolonged diafiltration is required, the defined rejection used to determine MWCO might be set too low to provide a realistic indication of membrane performance. A more valuable tool to facilitate membrane selection could instead be the MWCO curve between 90-100% for a range of solvents commonly used in the pharmaceutical industry.

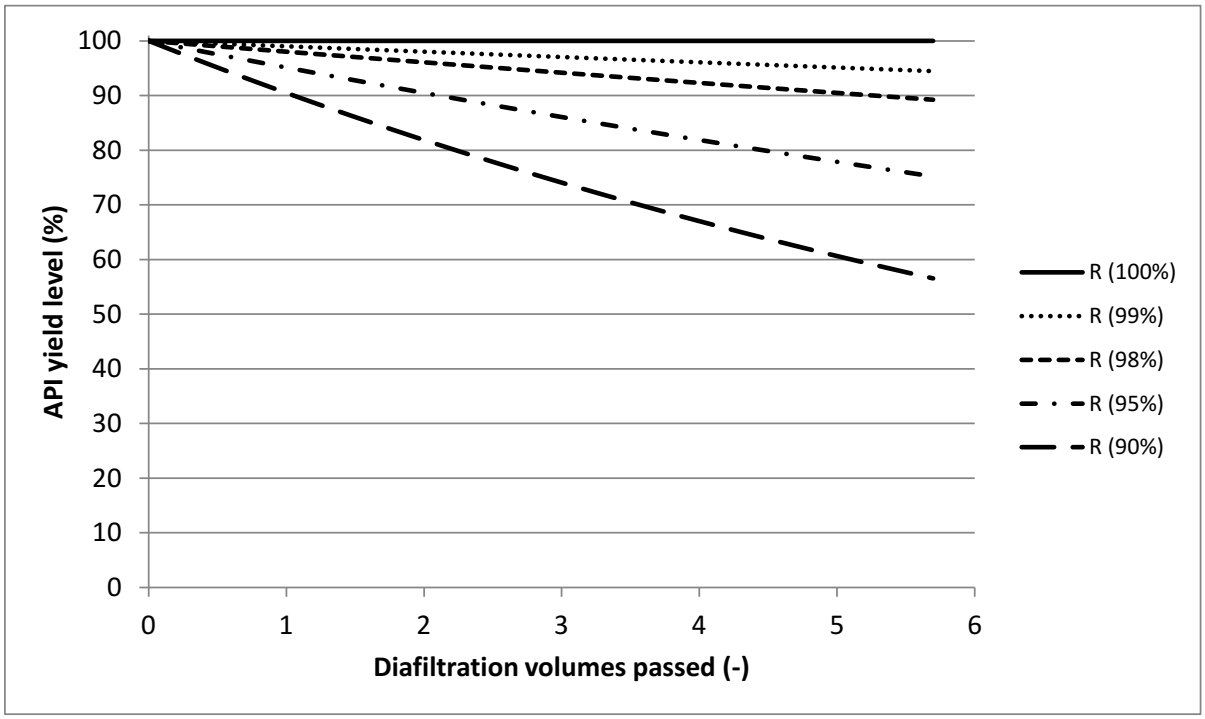

Figure 3.2. Changes in API yield levels during diafiltration for theoretical rejection levels between 90% and 100% (based on mass-balance predictions and theoretical performance data for membrane M)

3.3.4 Membrane Stability

Flux measurements can be used to give an indication of membrane performance and stability throughout operation. Flux data obtained for Duramem™200, membrane H and membrane M indicate that after an initial compaction all membranes reached steady state at 5, 6 and 25 L m^{-2} h^{-1} respectively (Figure 3.3). Data for membrane H deviate from Duramem™200 and membrane M in that an increase in flux was observed following the initial pressurisation. Upon contact with the process solvent swelling of the membrane polymer is expected. Such swelling potentially causes the membrane structure to re-arrange slightly following initial pressurisation. Membrane re-arrangement is likely to occur for all the membranes tested.

However, as membrane H has a very tight structure, such re-arrangement potentially results in the membrane becoming more permeable, hence explaining the increase in observed flux.

To investigate membrane stability pressure cycles were started after 96 hours of operation. During the pressure cycles the OSN system was depressurised and the membrane left to rest for 0.5-2.0 h prior to re-pressurisation. Flux was monitored throughout operation and although a minor reversible compaction effect was observed during the initial cycle, all membranes tested returned to and remained close to steady state throughout operation.

In addition to the flux, rejection values were measured after the stability test, and data was compared to rejections calculated for the membrane screening (Table 3.4). This demonstrated that for all membranes tested, the rejection of both the API and the impurity increased or remained close to a constant value after completion of the stability test. Consistent rejection data in combination with only minor flux variations observed during pressure cycles indicate that the membranes tested have a high stability in the mixture of THF and water, and membrane performance can be considered reliable.

Table 3.4. Summary of membrane performance data before and after membrane stability test using feed solution of 12.5 g L^{-1} API and 4.3 g L^{-1} impurity dissolved in a mixture of THF and water (75:25) (test was operated in cross-flow at 30 bar pressure and ambient temperature)

Membrane	Prior to pressure cycles		Post pressure cycles	
	R_{API} (%)	$R_{Impurity}$ (%)	R_{API} (%)	$R_{Impurity}$ (%)
Duramem™200	98.2 ± 0.1	45.7 ± 0.0	98.3 ± 0.4	45.5 ± 0.2
Membrane H	99.4 ± 0.8	46.3 ± 5.2	100.0 ± 0.0	52.0 ± 4.1
Membrane M	99.1 ± 1.3	37.4 ± 1.6	99.3 ± 1.1	39.8 ± 1.7

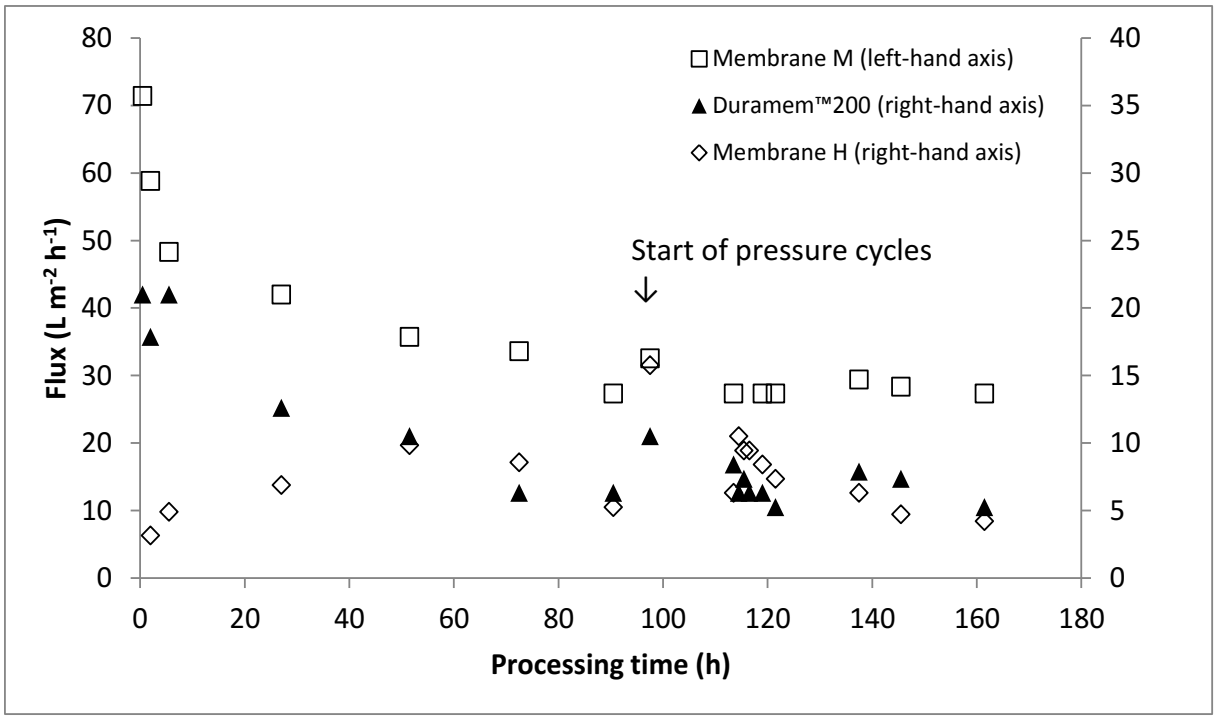

Figure 3.3. Flux data for Duramem™200, membrane H and membrane M during membrane screening and stability testing through pressure cycles where the membranes were depressurised and left to rest for 0.5-2.0 h before the system was re-pressurised (test was operated in cross-flow at 30 bar pressure and ambient temperature)

Upon removal from the cross-flow system, all membrane discs were visually inspected for potential damage. For both Duramem™200 and membrane M, formation of circular ridges was observed on the discs, whereas no visual damage could be observed on membrane H (Figure 3.4). Ridge formation is believed to be a result of differential swelling between the membrane and the backing material. For operation in the THF-water mixture, the swelling of the membrane is lower compared to the backing material, causing the membrane to curl upward. Upon pressurisation, the disc is forced down toward the support plate and is believed to become compacted to fit into the available cell area, causing ridges to form. Ridge formation is likely to result in a weakened point in the membrane and could be the first indication of mechanical stability issues for the selected membrane-solvent combination.

Consistent flux and rejection data throughout the test indicate sufficient stability of the membranes tested, however ridge formation could influence the long-term stability, and membrane performance should be continuously monitored.

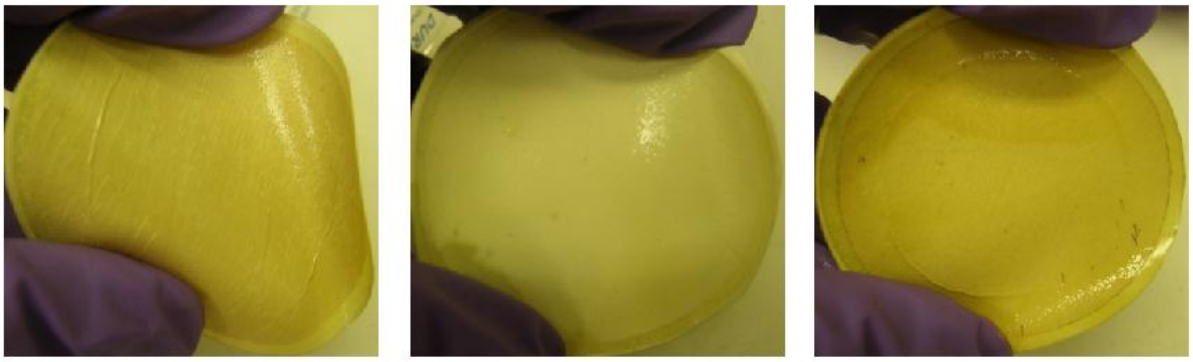

Figure 3.4. Duramem™200, membrane H and membrane M (*left to right*) upon removal from the cross-flow system after membrane screening and stability testing

3.4 Conclusion

For the API and impurity separation studied in this chapter, membrane screening and diafiltration predictions demonstrate that OSN can be successfully used for API purification. Process comparison with LLE further demonstrates that for a membrane with a high rejection, OSN can offer benefits with regards to improved API yield. Important to note is that for membranes with less than 100% rejection, OSN processing will result in gradual API losses, which can add up to significant values even for a seemingly high rejection (> 98%). Hence, availability of OSN membranes capable of 100% rejection for molecules is crucial for industrial application of OSN, highlighting membrane development as an important area of research. Process comparison further demonstrated that OSN is a solvent intensive technique, using 40-50 times more solvent per gram purified API compared to the LLE used for the API purification discussed. High solvent intensity of diafiltrations is likely to stifle industrial application and should be addressed to facilitate a more wide-spread use of OSN.

Chapter 4: API Purification through Combined Processing Utilising OSN Diafiltration and Adsorbents

4.1 Introduction

Over the last decade increased focus has been placed on extended control of impurities of unusually high toxicity. One such example is genotoxic impurities (GTIs) which are compound capable of causing damage to the DNA (Robinson, 2012). In 2007 the EMA introduced revised guidelines further limiting the allowed level of GTIs present in APIs (EMA, 2007). To comply with the stricter regulations pharmaceutical companies have employed various approaches, to limit the formation of GTIs as well as to demonstrate that compounds are not harmful when present at low levels (FDA, 2008)(Robinson, 2012)(Raman *et al.*, 2011). Limiting GTI formation can be achieved through process re-design including changes to the reaction conditions, reagents or synthetic route, as well as alterations to work-up stages and processing (Raman *et al*., 2011).

Various techniques for GTI removal have been investigated in literature, including more established unit operations such as solvent exchange/washes and re-crystallisation (Schülé *et al.*, 2010); preparative chromatography (Reddy *et al.*, 2009) and reactive resins (Lee *et al.*, 2010); as well as emerging separation techniques, such as molecularly imprinted polymers (MIPs); (Székely *et al.*, 2012a)(Székely *et al.*, 2012b) and OSN (Székely *et al.*, 2011)(Székely *et al.*, 2012a). Székely *et al*. (2011) demonstrated high flexibility of OSN in removing various size GTIs from API containing solutions. However, testing demonstrated that even for separations having close to the ideal separation performance (API rejection of 99.3% and GTI rejection of 2.2%), a significant solvent addition of 5 DV was required to reach the desired

target of 99.5% GTI removal. To facilitate industrial application of OSN, addressing this significant solvent usage is hence highly desirable.

In this chapter the potential of reducing the solvent burden of OSN for GTI removal from an API containing solution, was investigated through use of a combined OSN and adsorbent approach. The application selected for study investigates the removal of potential GTI acetamide (59 g mol^{-1}) from a model system containing GTI and API (~450 g mol^{-1}) dissolved in ethyl acetate. Adsorbents have previously been used for colour and odour removal, treatment of industrial effluents, and separation and recovery of solutes (Coulson *et al.*, 2002a)(LeVan and Carta, 2008). When using adsorbents in product containing streams, both high selectivity and loading capacity for the component to be removed are desirable. Hence extensive screening and optimisation work are required prior to adsorbent application.

Adsorbents and OSN were initially studied as stand-alone techniques to bench-mark performance for GTI removal (Figure 4.1 a and b). A combined approach, aimed at overcoming individual technique limitations, was then investigated and compared to the performance of the stand-alone techniques (Figure 4.1 c). For combined processing, a membrane was used to separate the GTI from the API, while adsorbents were used to remove GTI from the permeate solution, allowing solvent to be recycled back into the diafiltration. As the separation was achieved by the membrane, high selectivity of the adsorbent was not required, minimising the screening work commonly required for adsorbent applications. Combined processing with solvent recycling further addressed the high solvent usages commonly observed for OSN diafiltration.

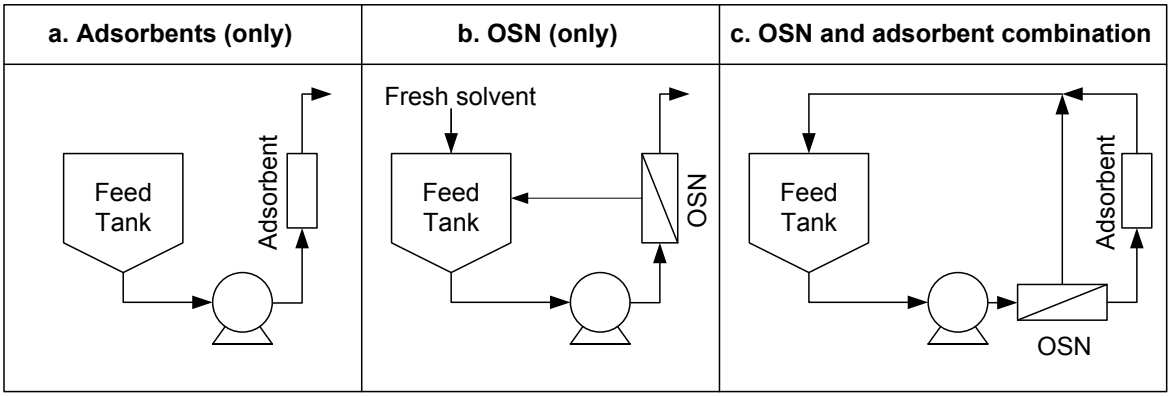

Figure 4.1. Schematic process diagrams of adsorbent, OSN and combined approach investigated for acetamide (potential GTI) removal

4.2 Materials and Methods

4.2.1 Feed Solution

Experiments were carried out using solutions of potential GTI acetamide (59 g mol^{-1}) and API (~450 g mol^{-1}) dissolved in ethyl acetate. Concentrations were based on previous OSN testing for GTI removal (Székely *et al.*, 2011), although altered to account for solubility and system loading capacities (Table 4.1). HPLC grade ethyl acetate (Sigma Aldrich) was used for all processing.

Table 4.1. Reference table of GTI and API concentrations used for testing in this chapter

Experiment	GTI concentration (g L^{-1})	API concentration (g L^{-1})
Membrane screening	1.0	1.0
Adsorbent screening and isotherm	0.5	-
Adsorbent selectivity	0.5	5.0
MIP screening	0.05	-
MIP isotherms	0.025, 0.05 and 0.10	-
MIP selectivity	0.05	0.1
Breakthrough test	0.5	-
API purification with adsorbents	0.5	5.0
Diafiltration	0.5	5.0

4.2.2 Adsorbent Screening

Adsorbents selected for testing included activated carbons, amberlite, Celite®, zeolite molecular sieves, Isolute and Evolute polymers, and various MIPs (Table 4.2). Adsorbents included for screening can be divided into the three groups: powder adsorbents, zeolites and MIPs. The powder adsorbents include activated carbon, ion-exchange resins and various polymers, and range significantly in their properties. Several powder adsorbents were selected for study to investigate potential advantages and limitations of the different types. Powder adsorbents such as activated carbon, are commonly inexpensive and could offer benefits from a financial perspective. However potential limitations, including poor selectivity, result in significant screening and optimisation work being required prior to application in mixed solute systems. Zeolites - also referred to as molecular sieves - are made up of silica and alumina arranged into cage structures, selectively allowing transport of molecules below approximately 1 nm (Coulson *et al.*, 2002a). Smaller molecules are hence able to pass into the structure while larger molecules (*e.g.* APIs) are retained, resulting in zeolites having a high selectivity for small molecules. Finally, MIPs are polymerised in the presence of a template molecule, resulting in the generation of a highly selective polymer containing specific binding sites suited for binding of the template molecule only (Vasapollo *et al*, 2011). Both zeolites and MIPs were selected for study due to their potentially high selectivity, which highlight methods as interesting for study in API purification, particularly for process streams having a large difference in size between the API and impurities present.

During screening, 20 mg of each adsorbent – including two non-adsorbent control samples – were added to individual test tubes containing 20 mL of feed solution. The solutions were left stirring for 24 h with periodic sampling to monitor progress towards equilibrium.

Table 4.2. Summary of adsorbent types included for screening

Adsorbent type	Types	Supplier
Activated carbon	S53, S54 and S55	CUNO
Ion-exchange resin	Amberlite	Fisher Scientific
Silicon oxide	Celite® 545	Sigma Aldrich
Molecular sieves (zeolites)	3A, 4A, 5A and 10A	GeeJay Chemicals Ltd.
Isolute	SP65, T, ENV+, 101 and 102	Biotage
Evolute	ABN	Biotage
MIP	ExploraSep plate type A and U	Biotage
MIP	Acetamide imprinted (AI)[a]	E. Fritz (TU Dortmund)

[a]Currently under development at TU Dortmund

MIPs were pre-packed into columns containing 40 mg of polymer. For each MIP tested, the corresponding non-imprinted polymer (NIP) was included to enable evaluation of potential imprinting effects. During operation, MIP-NIP columns were attached to a vacuum manifold (VacMaster 96) and the manufacturer recommended protocol was used for testing (Table 4.3).

Table 4.3. Summary of protocol and solutions used for operation of MIP-NIP columns

Process	Solution	Volume (mL)	Equilibration (min)
Pre-conditioning	Methanol/acetic acid/water 60:30:10 Methanol Application solvent (ethyl acetate)	2×1	1
Sample loading[a]	Feed solution	1×1	5
Washing	Acetonitrile 0.5% acetic acid in acetonitrile 3% acetic acid in acetonitrile 5% formic acid in acetonitrile	1×1	5
Regeneration	Methanol/acetic acid/water 60:30:10 Methanol	2×1	1

[a]Eluent collected as sample and used to evaluate degree of GTI binding to column

4.2.3 Adsorbent Isotherm and Selectivity Testing

For CUNO 55S and zeolite 10A, isotherm testing was carried out through addition of 20, 40, 60, 80 and 100 mg of adsorbent to test tubes containing 20 mL of feed solution. Solutions were left stirring for 24 h before sampling, to ensure that equilibrium was reached. A similar protocol was used for selectivity testing through use of a mixed-solute solution and only one test tube containing a 20 mg adsorbent addition.

As MIPs and NIPs are delivered in pre-packed columns, the amount of adsorbent cannot be varied during isotherm testing. The concentration in the feed solution was instead altered and binding tests were repeated at concentrations of 0.025, 0.050 and 0.100 g L^{-1}. MIP-NIP isotherm and selectivity testing was carried out according to the protocol in Table 4.3, using single- and mixed-solute solutions respectively.

4.2.4 GTI Removal Using Adsorbents Only

For CUNO 55S a stainless steel housing holding a packed adsorbent disc of 47 mm diameter (mass = 2.95 ± 0.03 g) was used for testing. During operation, an HPLC pump was connected to the housing and feed solution was passed through the CUNO disc at a flow rate equivalent to the flux observed during combined diafiltration (0.8×10^{-3} L min^{-1}). The eluting solvent was collected in fractions, with the test continued through addition of feed solution until 100% breakthrough of all solutes had been reached. An equivalent protocol was applied for zeolite 10A, substituting the CUNO disc with a stainless steel HPLC column (4.6 × 50 mm) packed with zeolite 10A powder (mass = 0.60 ± 0.03 g). Additionally, the flow rate was adjusted to a value of 1.8×10^{-3} L min^{-1}.

4.2.5 Membrane Screening

Based on manufacturer recommendations, OSN membranes Duramem™150, Duramem™200, Puramem™280 (Evonik MET), SolSep 010206 (SolSep BV.) and GMT-oNF-2 (Borsig GmbH) were selected for testing. Membrane screenings were carried out in a stainless steel cross-flow system (Evonik MET, Figure 2.6), connecting either two or three filtration cells (individual area of 5.4×10^{-3} m^2) in series. Membranes were washed by permeation of 0.2 L fresh ethyl acetate at 10 bar (SolSep 010206 and GMT-oNF-2) or 30 bar (Duramem™150, Duramem™200 and Puramem™280) pressure and ambient temperature (25-30 ^{o}C). The feed solution was then added to the system and the membranes pre-conditioned through permeate re-circulation at 10 bar (SolSep 010206 and GMT-oNF-2) or 30 bar (Duramem™150, Duramme™200 and Puramem™280) for 2 hours before permeate samples were collected. The pressure was further increased to 20 bar (SolSep 010206 and GMT-oNF-2) or 60 bar (Duramem™150, Duramem™200 and Puramem™280), and pre-conditioning was repeated for an additional 2 hours prior to collection of a second set of permeate samples. Feed and retentate samples were collected at the start and finish of the experiment, and flux was measured every 30 minutes throughout testing.

4.2.6 GTI Removal Using OSN Only and in Combination with Adsorbents

Diafiltrations were carried out using Duramem™200 operated in a dead-end filtration system (Evonik MET, Figure 2.5). For OSN only, an HPLC pump was connected to the filtration vessel and fresh solvent was added to the system throughout the diafiltration. For combined OSN and adsorbent processing, a second HPLC pump was connected to the permeate outlet, pumping the permeate through the respective adsorbent housings and back into the filtration vessel (Figure 4.2). Diafiltrations were operated at 30 bar and ambient temperature (25-30

^{o}C), using an initial feed volume of 0.11 L. Samples of the feed and retentate were collected at the start and finish of each diafiltration, and permeate samples were collected at the start of operation and after each DV passed. For combined processing, additional samples of the solvent eluting from the adsorbent housing were collected at the start of operation, and after each DV passed. The flux was monitored after each DV, and the HPLC flow rate adjusted to maintain a constant volume in the feed vessel throughout diafiltration.

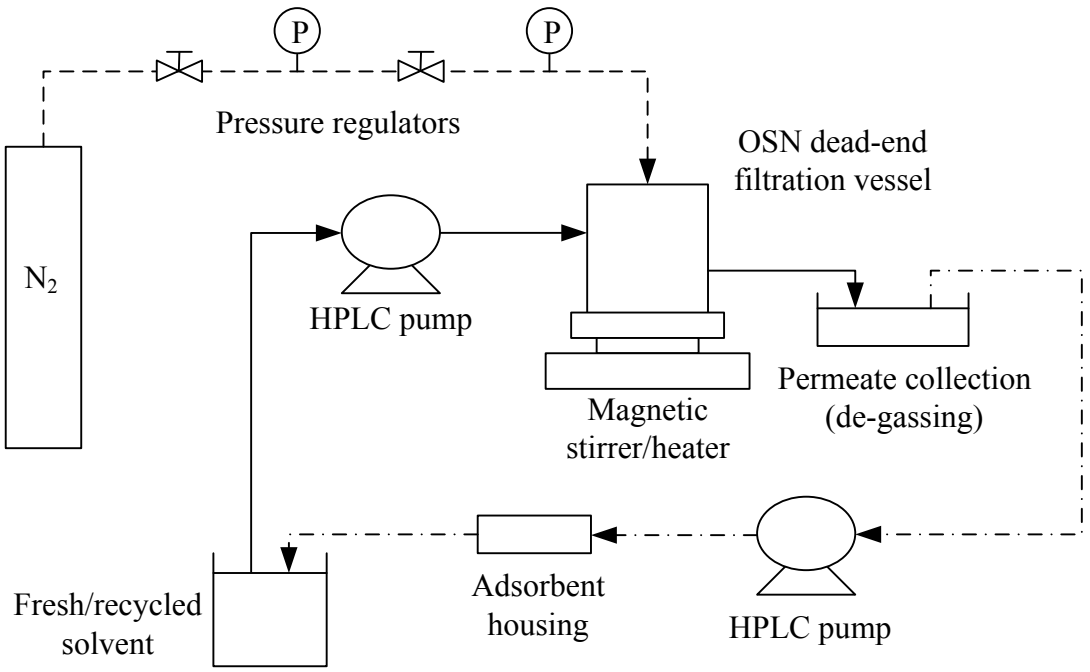

Figure 4.2. Schematic of equipment set-up used for diafiltration in combination with adsorbents for solvent recycle

4.2.7 Analysis

API concentrations were monitored by HPLC as detailed in Section 3.2.5 (fixed wavelength of 268 nm). GTI concentrations were measured using liquid chromatography-mass spectrometry (LC-MS), comprising a Hewlett Packard 1100 Series HPLC system coupled to a Waters micromass ZQ system for mass spectrometry analysis. HPLC used a 10 minute

gradient method (Table 4.4) with a Phenomax Luna C18 column (50×2.1 mm, 3.5 µm) held at 40 ^{o}C for separation. A mass-spectrometer was set to detection in ES+ ionization mode with single ion monitoring at m/z = 60.

Table 4.4. Summary of HPLC 10 minute gradient method used for GTI analysis

Time (min)	Eluent A[a] (%)	Eluent B[b] (%)	Flow (mL min^{-1})
Start (t = 0)	100	0	0.3
8.0	5	95	1
8.6	0	100	1
End (t = 10.0)	0	100	0

[a]0.05% (by volume) TFA in water
[b]0.05% (by volume) TFA in acetonitrile

4.3 Results and Discussion

4.3.1 Adsorbent Screening, Isotherm and Selectivity Testing

GTI adsorption was observed for all adsorbents tested. The highest values in each group were observed for CUNO 55S and zeolite 10A at 50 mg and 70 mg (GTI) per gram (adsorbent) respectively (Figure 4.3). For the MIPs tested, the highest GTI adsorption was observed for MIP A.10 (ExploraSep plate A) at 0.5 mg (GTI) per gram (adsorbent). However, the GTI adsorption was similar for the MIP and the NIP, indicating that adsorption was not selective as a result of the imprinting (Figure 4.4). The GTI binding capacity of MIP A.10 was approximately 100 times lower compared to CUNO 55S and zeolite 10A, and any benefits from further study of MIP A.10 were considered limited. The highest GTI adsorption resulting from the imprinting was observed for the AI MIP, at 0.4 mg (GTI) per gram (adsorbent), and the AI MIP was selected for isotherm and selectivity study (Figure 4.4).

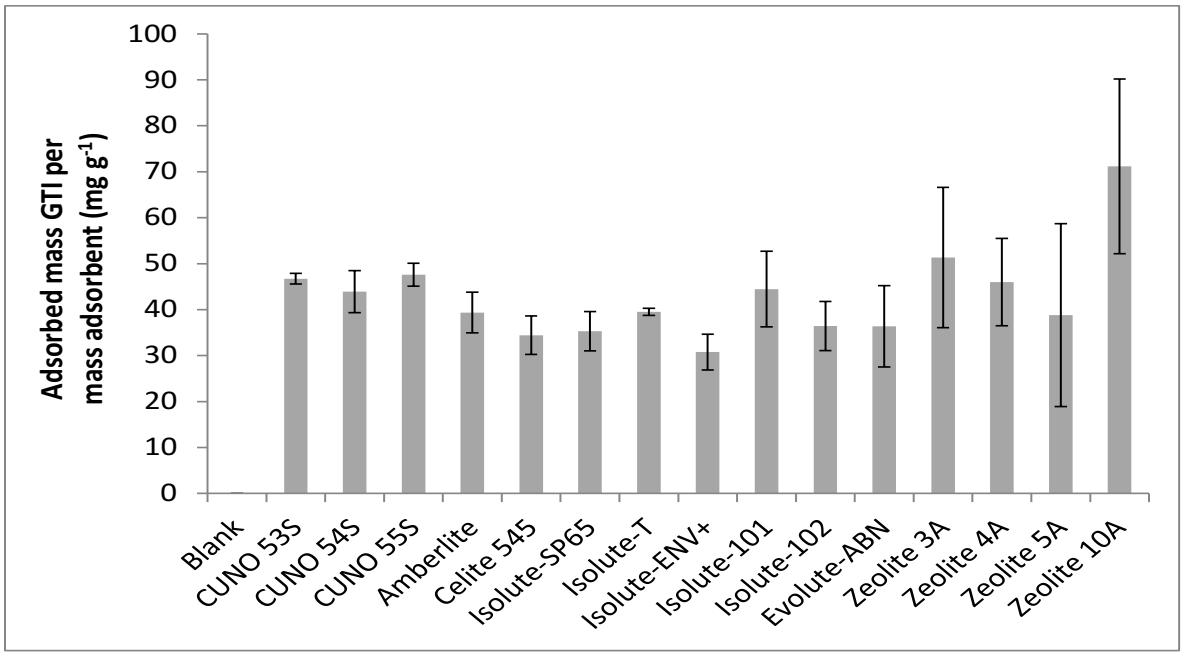

Figure 4.3. Summary of GTI loadings calculated from 24 h batch adsorbent screening test operated in test tubes containing 1 g L^{-1} adsorbent powder or zeolite bead and feed solution of 0.5 g L^{-1} GTI in ethyl acetate (equivalent to a loading of 0.5 g GTI per g adsorbent)

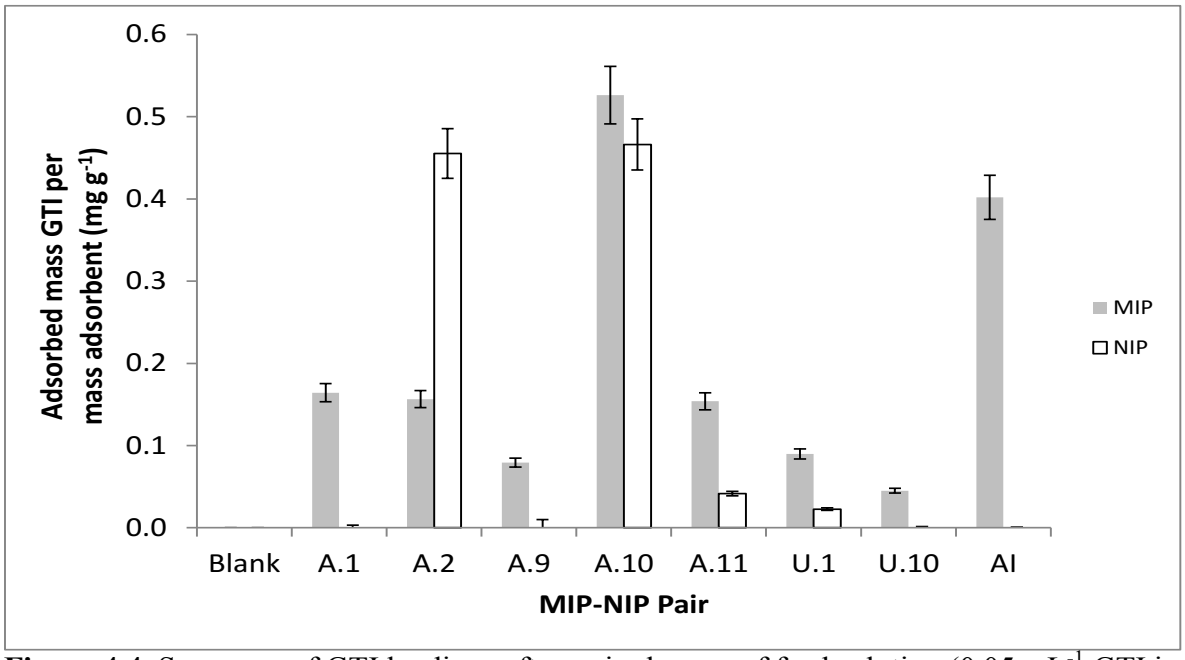

Figure 4.4. Summary of GTI loadings after a single pass of feed solution (0.05 g L^{-1} GTI in ethyl acetate) through packed columns containing 40 mg MIP or NIP polymer (equivalent to a loading of 1.25 mg GTI per g adsorbent)

Adsorbent screening data demonstrates that the loading capacities measured were similar for all powder adsorbents tested (Figure 4.3). The feed solution used for the screening test was made up of acetamide dissolved in ethyl acetate. Comparison of the molecular structures demonstrated significant similarities between acetamide and ethyl acetate respectively (Figure 4.5), which could potentially result in competitive binding within the selected system. For any given solvent-solute-adsorbent combination the loading capacity of each component is dependent on an equilibrium forming between the molecules present in the surrounding solution and the adsorbent matrix respectively. As more solvent (ethyl acetate) compared to solute (acetamide) is present in the system, the equilibrium loading capacity of ethyl acetate is likely to be favoured. This potentially results in decreased acetamide adsorption and could explain the similar loading capacities observed. For the MIP-NIP systems a lower feed concentration was used for testing to avoid overloading of the columns. For these systems the relative ratio of ethyl acetate to acetamide is hence even higher, potentially explaining why even lower acetamide adsorption was observed.

Figure 4.5. Molecular structures of potential GTI acetamide (*left*) and ethyl acetate (*right*)

Isotherm and selectivity testing was carried out for the adsorbents displaying the highest GTI binding in each class tested (CUNO 55S, zeolite 10A and the AI MIP). For CUNO 55S and zeolite 10A, loading capacities were measured using the feed concentration of the diafiltration, whereas for the lower loading capacity AI MIP, the feed concentration was reduced to avoid overloading the column. Data from the respective isotherm tests were fitted to Freundlich isotherms as described in Equation 4.1 where x is the mass adsorbed solute (g),

m is the mass adsorbent (g), *C* is the concentration of solutes in solution when equilibrium has been reached with the solutes adsorbed (g L^{-1}) and *K* and *n* are constants (Coulson *et al.*, 2002a). For a solute-adsorbent combination following a Freundlich isotherm a logarithmic plot of log(*C*) versus log(*x/m*) will result in a straight line with a slope 1/*n* and a y-intercept of *K*.

$$\frac{x}{m} = KC^{\frac{1}{n}} \qquad \text{Equation 4.1}$$

For solute-adsorbent combinations where Freundlich isotherm behaviour is observed, the adsorption capacity is dependent on an equilibrium forming between the solutes present in the passing solution and the adsorbent matrix respectively. For a reduced feed concentration, the equilibrium will be shifted, resulting in a decreased adsorption. Isotherm testing demonstrated that data for CUNO55S, zeolite 10A and the AI MIP were consistent with Freundlich isotherms in the concentration intervals tested (Figure 4.6). The measure loading capacities were calculated to range between 39 mg to 63 mg (GTI) per gram (adsorbent) for CUNO 55S, and 50 mg to 63 mg (GTI) per gram (adsorbent) for zeolite 10A. Similar to the screening, the loading capacity for the AI MIP was significantly lower at 0.2 mg to 0.4 mg (GTI) per gram (adsorbent). As a higher feed concentration was used for testing of CUNO 55S and zeolite 10A compared to the AI MIP, a direct comparison of the measured loading capacities cannot be made. However, testing of the AI MIP at equivalent concentration resulted in a significant overloading of the column and reliable data could not be obtained. Column overloading occurred despite a similar mass of the AI MIP being used for testing (40 mg AI MIP *cf.* 20-100 mg CUNO 55S and zeolite 10A), and though a direct comparison was not possible, the observed behaviour strongly indicate that the loading capacity of the AI MIP is significantly lower compared to CUNO 55S and zeolite 10A.

CUNO 55S and zeolite 10A displayed similar loading capacities, indicating both adsorbents as promising for GTI removal. A sharper gradient was observed for CUNO 55S which could potentially indicating adsorbent as a more suitable alternative for use in more concentrated systems (Figure 4.6).

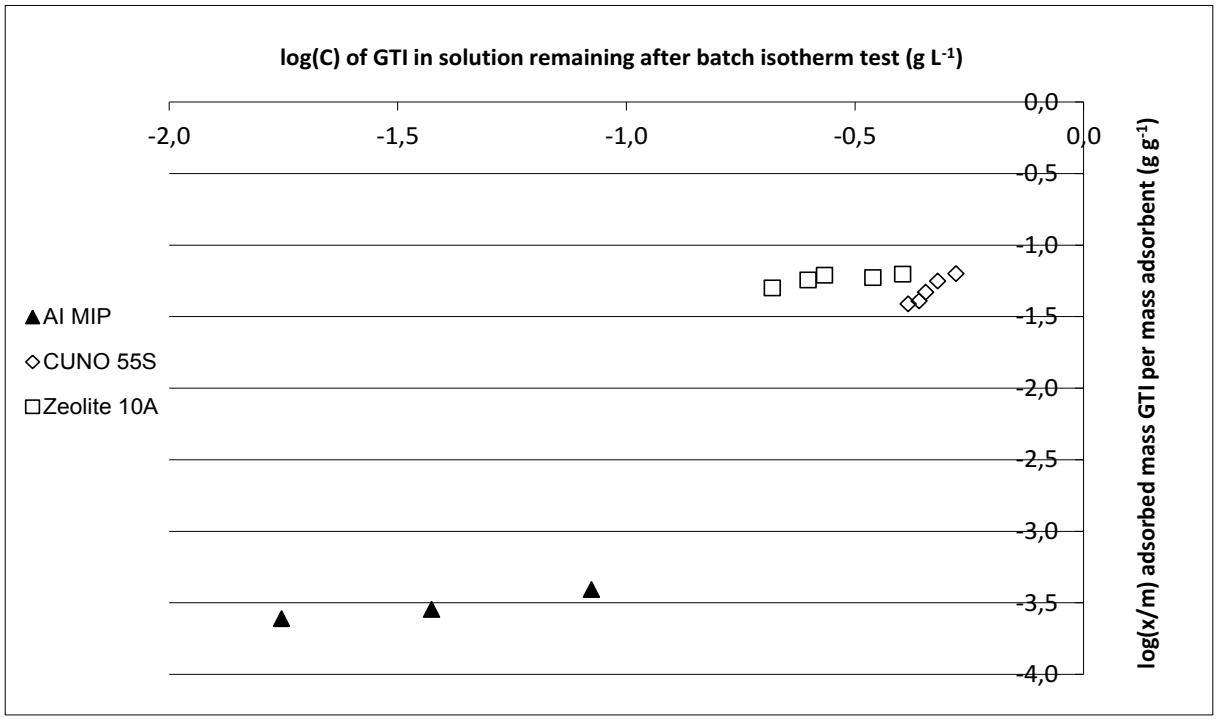

Figure 4.6. Freundlich isotherms for the AI MIP based on a single-pass of feed solutions through packed MIP columns (loadings of 0.63, 1.25 and 2.50 mg GTI per g adsorbent), and CUNO 55S and zeolite 10A in batch loading tests of GTI and adsorbents dissolved in ethyl acetate (loadings of 0.10, 0.13, 0.17, 0.25 and 0.50 g GTI per g adsorbent) (batch loading test was carried out in test tubes containing the selected adsorbent and the feed solution with samples collected after 24 h when equilibrium was assumed reached)

For adsorbent application in mixed-solute solutions, sufficient selectivity and high loading capacity are required to minimise product losses during processing. Selectivity testing for CUNO 55S and zeolite 10A were carried out using the desired feed concentration of the

diafiltration, while for the AI MIP concentrations were lowered to avoid overloading the column. Zeolite 10A and the AI MIP both demonstrated high selectivity, removing 20-30% of the added GTI while keeping API losses to less than 1% (Figure 4.7). Binding capacities were calculated as 0 mg (API) and 0.4 mg (GTI) per gram (adsorbent) for the AI MIP, and 45 mg (API) and 90 mg (GTI) per gram (adsorbent) for zeolite 10A. Though some API adsorption was observed for zeolite 10A, it is important to note that a high concentration of API (5 g L^{-1}) was used during testing, hence shifting the equilibrium towards a higher API adsorption. The percentage adsorption of API still remained low and, depending on the relative API to GTI concentrations, use of zeolite 10A in API containing solutions might still be possible while maintaining low yield losses. The high selectivity observed for zeolite 10A could be a result of the smaller GTI molecules being able to pass into the cage-like zeolite structure, hence accessing more binding sites compared to the larger API molecules, which are restricted to binding sites available on the zeolite surface. Zeolite 10A demonstrated a higher GTI adsorption compared to the AI MIP which in combination with zeolites being readily available for industrial use, highlight zeolite 10A as the more suitable candidate for study in direct API purification

For CUNO 55S, 6% API and 4% GTI was adsorbed, which is equivalent to adsorption capacities of 260 mg (API) and 35 mg (GTI) per gram (adsorbent) (Figure 4.7). For CUNO 55S, all binding sites are equally available to the solutes present in the feed solution, and no selective binding of various solutes based on steric hindrance is expected. The observed adsorption is hence likely to be highly dependent on the respective concentrations of the solutes present, and the resulting shift in adsorption equilibrium between solutes in solution and adsorbed to the active carbon molecules. As the API and GTI concentrations used during selectivity testing were different (5.0 g L^{-1} API *cf.* 0.5 g L^{-1} GTI), a direct comparison

between the API and GTI adsorption capacity for CUNO 55S cannot be made. However, the observed API adsorption was significant, indicating that though CUNO 55S could be suitable for use in single-solute GTI systems, use for API purification in the mixed-solute solution studied in this chapter is not recommended.

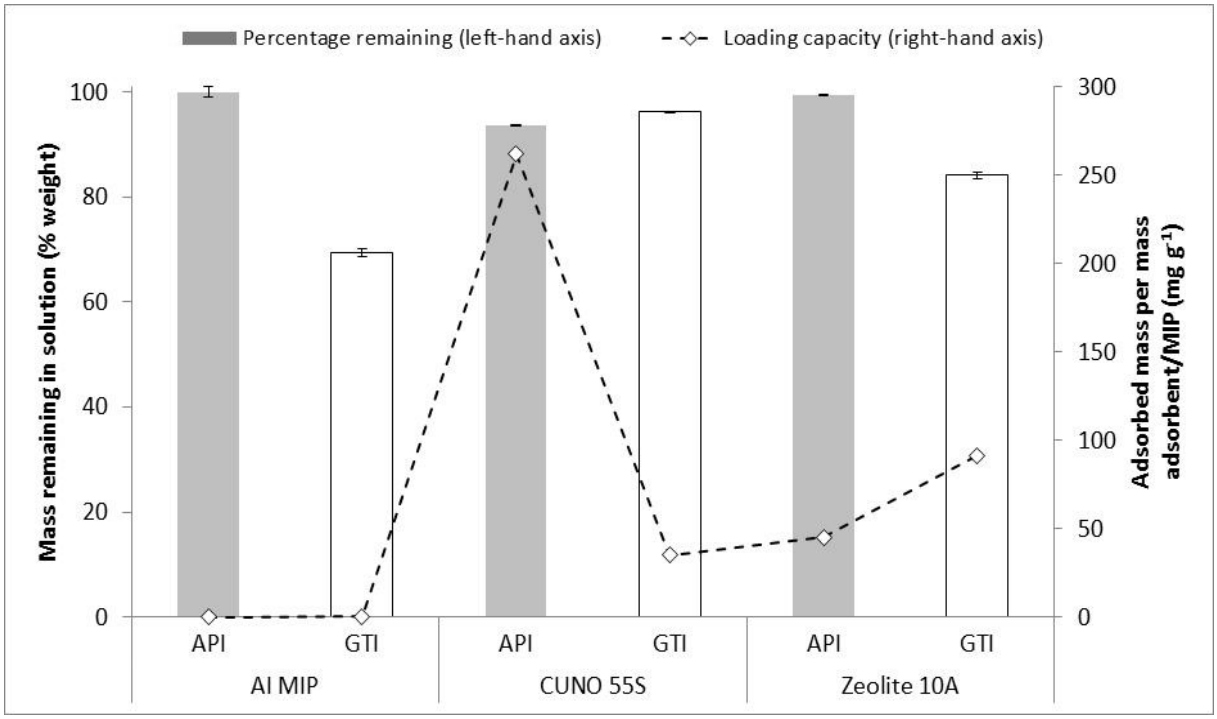

Figure 4.7. Summary of selectivity test for the AI MIP, CUNO 55S and zeolite 10A illustrating the percentage GTI remaining in solution (*white*) relative to the corresponding API yield loss (*grey*) at equilibrium. Calculated GTI and API loading capacities (*dashed line*) is further included (batch loading tests for CUNO 55S and Zeolite 10A were carried out in test tubes containing the adsorbents and feed solution containing API and GTI dissolved in ethyl acetate with samples collected after 24 h whereas MIP-NIP loading tests were carried out as a single-pass of the feed solution through the respective packed columns)

4.3.2 GTI Removal Using Adsorbents Only (Figure 4.1 a)

Industrial application of adsorbents for solute removal can be carried out by a single-pass of the process liquor through a packed adsorbent bed. The adsorbent mass is selected to match the desired solute binding, and the flow rate through the packed bed is set to ensure sufficient equilibration time between the adsorbent and the solutes. Single-pass breakthrough tests were carried out for CUNO 55S and zeolite 10A in mixed-solute solutions to investigate purification capability and adsorption capacities.

During the CUNO breakthrough test, both GTI and API were observed to break through the disc from the start of the test, followed by a gradual increase in concentration until full breakthrough was reached after 0.3 L of feed solution had passed (Figure 4.8). Loading capacities were calculated as 15 mg (GTI) and 110 mg (API) per gram (adsorbent), which is approximately half of the values observed during the selectivity test. The lower adsorption could potentially be attributable to the reduced contact area between the adsorbent and solutes when using a packed bed compared to powder adsorbents. After passage of one DV of feed solution (0.11 L) the concentration in the eluted solvent was 0.25 g L^{-1} GTI, with 63% of the added API adsorbed in the CUNO disc. Due to poor selectivity and early GTI breakthrough, CUNO 55S was deemed unsuitable for GTI removal in the system studied. Nevertheless, CUNO 55S could still be of interest for single-solute solutions of GTI in the suggested permeate recycle system (Section 4.3.4).

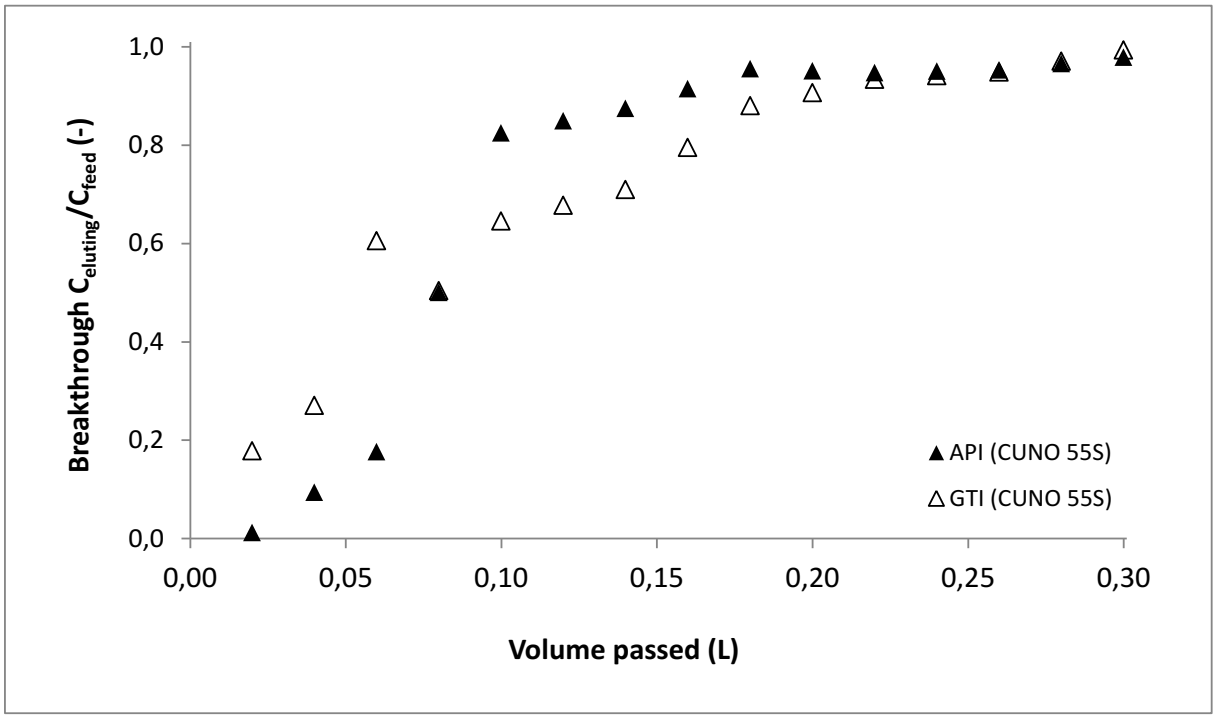

Figure 4.8. Breakthrough of GTI and API through a CUNO 55S disc using a feed flow rate of 0.8 L min^{-1} for a mixed-solute solution of 0.5 g L^{-1} GTI and 5.0 g L^{-1} API dissolved in ethyl acetate

For the zeolite 10A breakthrough test, the API was observed to pass through the column from the start of the test with full breakthrough reached after only 0.01 L of feed solution had passed. Conversely, breakthrough of the GTI was not observed until 0.12 L of feed solution had passed, followed by a gradual increase in concentration until full breakthrough was reached after passage of 0.24 L (Figure 4.9). Loading capacities were calculated as 135 mg (GTI) and 20 mg (API) per gram (adsorbent), indicating a significant increase in adsorption for the GTI (135 mg *cf.* 90 mg per gram adsorbent) as well as a significant decrease in the loading capacity of the API (20 mg *cf.* 45 mg per gram adsorbent) compared to the selectivity test. Increased GTI adsorption could potentially be a result of increased access to binding sites resulting from using zeolite 10A in a powder rather than bead form, as well as decreased competitive binding occurring due to the reduced API adsorption. The lower API adsorption

could in turn be a result of the contact time between the API and adsorbent being insufficient, resulting in equilibrium not being reached during operation in a single-pass system. If a lower flow rate was used, a higher API adsorption, close to the value previously observed, would then be expected. Single-pass purification of one DV feed solution resulted in an eluent containing 0.0006 g L^{-1} GTI while the API loss was limited to 3%, indicating that zeolite 10A is a suitable alternative for direct application in the API purification studied in this chapter.

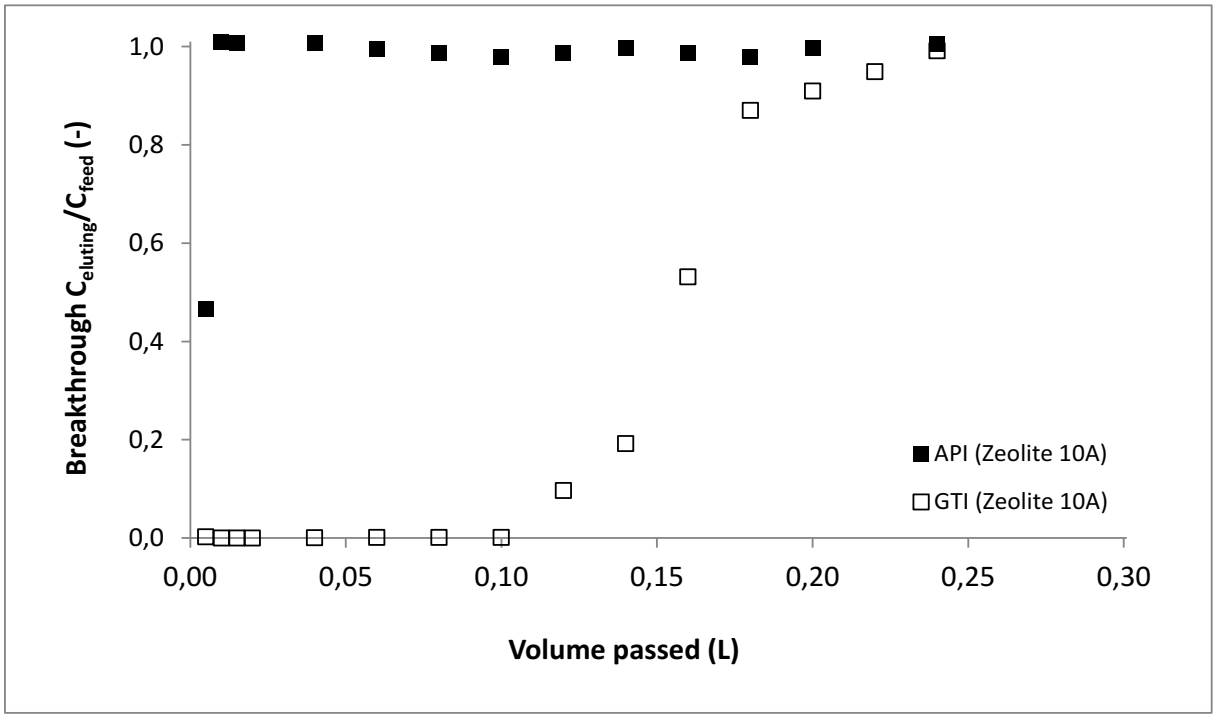

Figure 4.9. Breakthrough of GTI and API through a packed zeolite 10A column using a feed flow rate of 1.8 L min^{-1} for a mixed-solute solution of 0.5 g L^{-1} GTI and 5.0 g L^{-1} API dissolved in ethyl acetate

4.3.3 GTI Removal Using OSN Only (Figure 4.1 b)

The ideal membrane for the separation studied in this chapter, should have a high API rejection while keeping the GTI rejection to a minimum. Various OSN membranes were

selected for testing, and a performance optimisation was carried out, repeating the screening at both intermediate and maximum pressure for each membrane. The membrane screening demonstrated that all membranes tested have low GTI rejections (0-6.6%) combined with API rejections above 90%. The most suitable rejection performance was observed for Duramem™150 operated at 60 bar, with an API rejection of 99.5% and a GTI rejection of 0.9%. However, Duramem™150 displayed a low flux (6 L m^{-2} h^{-1}) resulting in long processing times and requirements for a large membrane area. To enable lab-scale processing within a reasonable time-frame, Duramem™200 was instead selected for all diafiltrations. Duramem™200 operated at 30 bar demonstrated respective API and GTI rejections of 98.6% and 0.0%, combined with a flux of 34 L m^{-2} h^{-1}. For operation at a higher pressure a minor increase in the GTI rejection (0.9% *cf.* 0.0%) and flux (36 L m^{-2} h^{-1} *cf.* 34 L m^{-2} h^{-1}) was observed while the API rejection remained constant (Table 4.5). No benefits were hence observed to motivate operation at a higher pressure, and Duramem™200 operated at 30 bar was selected for processing.

Table 4.5. Summary of membrane performance data obtained from screening operated in cross-flow system (Evonik MET) using a mixed-solute solution of 1.0 g L^{-1} API and 1.0 g L^{-1} GTI dissolved in ethyl acetate (test operated at 10, 20, 30 or 60 bar and ambient temperature)

Membrane	Pressure (bar)	R_{API} (%)	R_{GTI} (%)	Flux (L m^{-2} h^{-1})
SolSep 010206	10	91.5	2.2	14
SolSep 010206	20	93.4	2.0	24
GMT-oNF-2	10	91.6	6.6	23
GMT-oNF-2	20	91.4	2.6	43
DuraMem™150	30	99.0	0.0	4
DuraMem™150	60	99.5	0.9	6
DuraMem™200	30	98.6	0.0	34
DuraMem™200	60	98.6	0.9	36
PuraMem™280	30	95.8	1.8	139
PuraMem™280	60	94.2	1.0	187

Diafiltrations were carried out using OSN both as a stand-alone technique and in combination with adsorbents (CUNO 55S or zeolite 10A) for solvent recycle. For use of OSN only operation was carried out in a single-pass with fresh solvent gradually being added to the system at a rate equal to the permeation. The flux was measured to a stable value of 22 L m^{-2} h^{-1} which was lower compared to the membrane screening. This decreased flux was most likely a result of the higher API concentration used during the diafiltration (5.0 g L^{-1} *cf.* 1.0 g L^{-1}). The GTI rejection remained low (0.6%) throughout operation, resulting in a gradually decreasing concentration until only 0.6% (by weight) of the added GTI remained in the retentate after passage of 5 DV (Figure 4.10, Section 4.3.4). The API rejection averaged 97.5% throughout operation, resulting in an API loss of 17.7% for passage of 5 DV. Diafiltration data showed that in order to reach a GTI level of 0.6% (by weight) OSN required a 0.15 L addition of ethyl acetate per gram purified API. High API losses, as well as significant solvent consumption, again highlight the importance of improved rejections and decreased solvent usage as major areas of concerns for OSN application.

4.3.4 GTI Removal Using Adsorbents and OSN in Combination (Figure 4.1 c)

For combined operation of CUNO 55S and diafiltration, the average rejection of the GTI and API were measured to 0.4% and 97.1%, with a flux of 12 L m^{-2} h^{-1}. Rejections were consistent with OSN only, whereas the flux was significantly lower compared to values previously observed (12 L m^{-2} h^{-1} *cf.* 22 L m^{-2} h^{-1}). During the combined diafiltration, the initial permeate was used to flood the CUNO 55S housing (hold-up volume 55 mL), resulting in a gradual concentration of the retentate prior to the start of the solvent recycle. The decrease in flux was therefore believed to be a result of increased concentration effects.

Throughout the diafiltration, the GTI level gradually decreased until saturation of the CUNO disc was reached after passage of 4 DV, at which point 18% (by weight) GTI remained in the retentate. For passage of 4 DV, the API loss totalled 12.9% (Figure 4.10), and loading capacities were calculated as 15 mg (GTI) and 60 mg (API) per gram (adsorbent). Observed GTI adsorption was consistent with the breakthrough test, whereas the API loading capacity was significantly lower compared to values previously observed (110 mg API per gram adsorbent). During the diafiltration, the majority of the API was retained by the membrane, resulting in the concentration in the permeate passing through the CUNO 55S disc being significantly lower during the solvent recycle compared to the breakthrough test (~0.2 g L^{-1} *cf.* 5.0 g L^{-1}). As previously mentioned the measured adsorption capacity is dependent on an equilibrium forming between the solutes in the passing solution and solutes adsorbed (Section 4.3.1). The decreased API loading capacity observed is hence consistent with expected performance, based on the lower API concentration present in the solvent recycle loop. Despite the reduced loading capacity, significant API adsorption was however still observed and the majority of the API passing the membrane was adsorbed.

For the zeolite 10A diafiltration, average rejections equalled 0.8% for the GTI and 97.9% for the API respectively, in combination with a flux of 21 L m^{-2} h^{-1}. The hold-up volume for the zeolite 10A housing was low compared to CUNO 55S (15 mL *cf.* 55 mL), and only minor concentration of the retentate was expected. Flux and rejection data for the zeolite 10A diafiltration were consistent with OSN only, demonstrating reproducible membrane performance. Similar to the CUNO 55S diafiltration, zeolite 10A demonstrated a decrease in the GTI level for passage of 4 DV, at which point saturation was reached, with 17.0% (by weight) of the added GTI remaining in the retentate. Loading capacities were calculated as 130 mg (GTI) and 7 mg (API) per gram (adsorbent). The GTI loading capacity was consistent

with the breakthrough test, whereas a small decrease, attributed to decreased concentration, was observed for the API. Due to the low loading capacity, the API passed through the column and was re-circulated to the feed vessel. Re-circulation of the API minimised the overall losses, which totalled only 0.9% for passage of 4 DV (Figure 4.10).

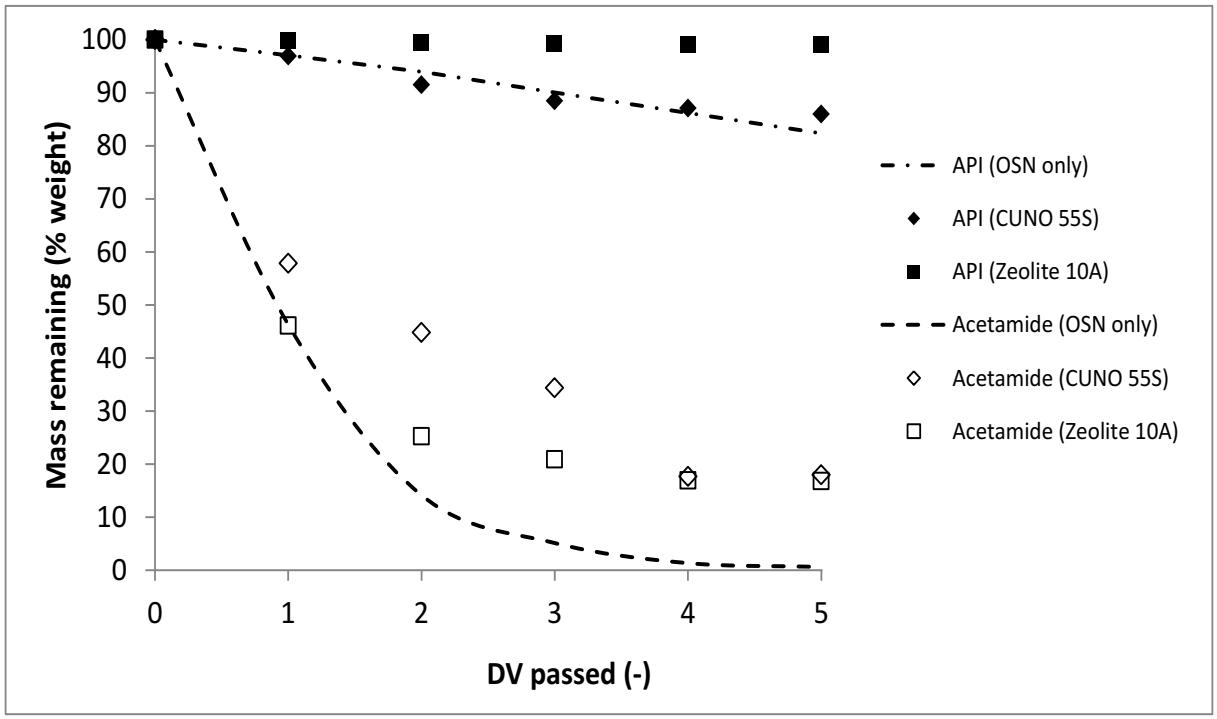

Figure 4.10. GTI and API levels obtained during single-pass diafiltration using OSN only, as well as for OSN in combination with CUNO 55S and zeolite 10A for solvent recycle (test was operated in dead-end using Duramem™200 at 30 bar and ambient temperature with the flow rate through the respective adsorbent housings adjusted to match the permeate flux)

4.3.5 Process Comparison of Investigated GTI Removal Techniques

API purification through adsorbents only was investigated for CUNO 55S and zeolite 10A. For CUNO 55S, significant breakthrough of both the GTI and API was observed throughout testing. A GTI to API ratio of 1.8×10^{-2} could be reached with no solvent addition however

API losses were high, reducing the yield to 37% (Table 4.6). Conversely, for zeolite 10A immediate breakthrough of the API was observed, while the GTI was adsorbed in the column. Using zeolite 10A, a GTI to API ratio of 1.4×10^{-3} could be reached in a single-pass while maintaining the API yield at 97% (Table 4.6). Adsorbent data demonstrated that when a selective adsorbent is used, API purification is possible while maintaining API losses to a minimum. However, when using a lower selectivity adsorbent, yield losses can be significant and despite the advantage of no solvent being used during adsorbent purification, direct application in mixed-solute solutions is not recommended.

For use of OSN only, achieving a GTI to API ratio equivalent to a single-pass of zeolite 10A (1.4×10^{-3}) requires the diafiltration to be run for 4.5 DV, resulting in an API yield of 89% and a solvent consumption of 1.4 L per gram purified API (Table 4.6). OSN data highlight the significant solvent consumption and API losses occurring during prolonged OSN processing, even when a membrane close to the ideal separation performance is used.

The high solvent intensity of OSN was addressed through combined OSN and adsorbent processing. Combining OSN and CUNO 55S, a GTI to API ratio of 2.5×10^{-2} was reached with no solvent addition, resulting in an API yield of 87%. Corresponding data for OSN and zeolite 10A indicated that a GTI to API ratio of 2.2×10^{-2} could be reached, while achieving a high API yield of 99% (Table 4.6). Using OSN only, a GTI to API ratio equivalent to combined zeolite 10A processing (2.2×10^{-2}), required 0.4 L solvent per gram purified API, resulting in an API yield of 95% (Table 4.6). Ergo, combining OSN and zeolite 10A offers significant benefits with regards to both improved yield and reduced solvent usage, indicating combined processing as a promising alternative for API purification. Combining OSN and CUNO 55S also minimised the solvent consumption, however the API yield loss was higher

compared to stand-alone OSN for an equivalent GTI target (Table 4.6). Using equivalent feed concentrations, similar API losses are expected for OSN only and in combination with CUNO 55S. However, the hold-up volume of the CUNO housing (55 mL) results in an increased feed concentration for the combined process compared to OSN only. The rejection is based on a ratio between the permeate and feed concentrations (Equation 2.1), and an increase in the feed concentration must be accompanied by an increase in the permeate concentration to maintain constant rejection. If equivalent concentrations were used, similar yield levels would be expected for OSN only and in combination with CUNO 55S.

Table 4.6. Key results for process evaluation comparing GTI removal, API yield levels and solvent consumption using adsorbents and OSN alone and in combination

Technique	GTI/API ratio (-)	API yield (%)	Fresh solvent required (L g^{-1} API)
Adsorbent only (CUNO 55S)	1.8×10^{-2}	37	-
Adsorbent only (zeolite 10A)	1.4×10^{-3}	97	-
OSN only (GTI/API ratio equal to zeolite 10A only)	1.4×10^{-3}	89	1.4
OSN and adsorbents (CUNO 55S)	2.5×10^{-2}	87	-
OSN and adsorbents (zeolite 10A)	2.2×10^{-2}	99	-
OSN only (GTI/API ratio equal to combined zeolite 10A processing)	2.2×10^{-2}	95	0.4

4.4 Conclusion

Successful GTI removal through OSN has been demonstrated. However, limitations of diafiltration were highlighted with regards to the large solvent requirement and potentially significant API losses occurring throughout processing. The high solvent requirement was addressed by combining OSN with adsorbent processing, and solvent recovery and recycling of the permeate was demonstrated.

Provided that a membrane with a high selectivity and API rejection (> 99%) is used, introduction of low cost, non-selective adsorbents could offer significant benefits in reducing the solvent requirements for diafiltrations. Additionally, as the membrane is responsible for the separation, adsorbent selectivity becomes less important, and the extensive screening work required for identification of suitable adsorbents can be minimised. This study further demonstrated that for direct API purification using adsorbents, a high selectivity is essential to avoid API losses. For the separation discussed, promising removal performance of the small GTI impurity was observed for zeolite 10A, potentially indicating zeolites as a viable alternative for application in a wider range of API purifications.

Chapter 5: Combined use of Counter-Current Chromatography (CCC) and OSN Diafiltration

5.1 Introduction

Promising performance for API purification using OSN has been demonstrated in Chapter 3 and 4. However, OSN selectivity is based primarily on steric factors, and despite on-going research in membrane development the ability to fractionate similar sized solutes using OSN remains poor. This is reflected in literature where applications of commercially available OSN membranes have commonly been limited to separations of solutes having a large difference in molecular weight, ranging from 300 g mol^{-1} and upwards (Luthra *et al.*, 2002)(Ghazali *et al.*, 2006)(Wong *et al.*, 2006)(Pink *et al.*, 2008)(Sereewatthanawut *et al.*, 2010). For fractionation of multi-component solute mixtures other techniques must hence be used, with successful options including various chromatographic techniques. One such alternative is counter-current chromatography (CCC) which has demonstrated a promising performance on a lab-scale. In this chapter a combination of OSN and CCC is investigated, demonstrating that through combined use additional benefits to both OSN and CCC can be provided.

CCC is a liquid-liquid chromatography technique enabling separation based on differential solubility of solutes between two immiscible phases. During operation a liquid stationary phase is placed in the CCC column, which is generally made up of a length of tubing wound around a bobbin. The column is rotated around its own axis, as well as a central axis, causing the stationary phase to be held in place by centrifugal forces. Liquid mobile phase is then pumped through the stationary phase and the rotational movement generate a series of mixing and settling zones throughout the length of the column (Figure 5.1). When a sample is injected the mixing and settling zones facilitate distribution of the solutes present between the

stationary and mobile phases respectively. Solute distribution is dependent on the solutes respective affinities for either phase, and determines the degree of separation in the column. Solutes having a high affinity for the mobile phase will pass through the column more easily and will hence elute early. Conversely, solutes having a high affinity for the stationary phase will be retained in the column causing them to elute later (Ito, 2005)(Guzlek *et al.*, 2010).

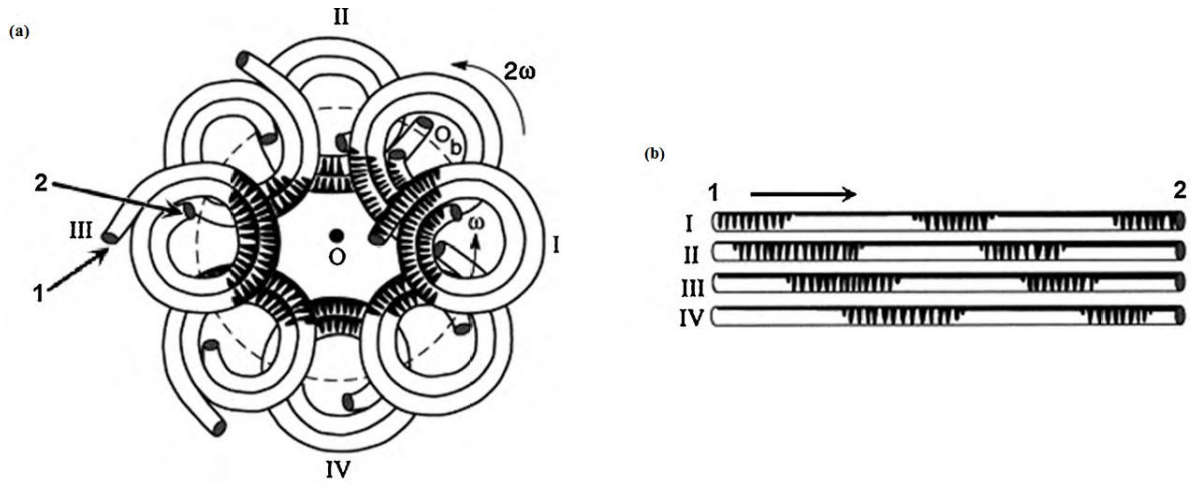

Figure 5.1. (a) Schematic illustration of mixing and settling zones inside a wound tubing CCC column where *1* and *2* represent the column inlet and outlet respectively, *O* is the central axis and O_b is the orbital axis for the column rotation (b) Schematic of the movement of mixing and settling zones through the column during CCC operation (Ito, 2005)

Selection of a suitable solvent system is a key factor in achieving efficient CCC separation. In theory any biphasic solvent mixture could be used, provided that the target molecule and related impurities are fully soluble in either phase. However, it is desirable that the selected phases have a sufficient difference in density to enable satisfactory retention of the stationary phase in the column. Additionally, the time required to partition the solvent phases after mixing of the mobile and stationary phases should be low, to facilitate the presence of defined mixing and settling zones throughout the CCC column. Based on this the most important

criteria used for solvent selection are polarity, density, viscosity and solubility. The most commonly used solvent systems for CCC operation are HEMWat systems, which are composed of heptane, ethyl acetate, methanol and water in various ratios corresponding to different overall polarities (Ito, 2005).

Solvent selection is enabled through study of the partitioning coefficient (K_d) of the target compound, and related impurities, in a range of solvent combinations. K_d describes the solute distribution between the immiscible phases, and is calculated as the ratio between the solute present in the stationary and mobile phase respectively. For the target compound K_d should be close to 1 which is equivalent to solute elution after passage of one column volume of mobile phase. Additionally, the separation factor, defined as the ratio between the K_d values of the target compound and related impurities, should ideally be above 1.5 to enable sufficient separation of solutes. Solvent selection is generally started through identification of a combination of solvents (*e.g.* HEMWat) that has been used for previous CCC separation of molecules with similar properties to the current target molecule. A combination of solvents corresponding to a system of medium polarity is then selected as the starting point, and K_d values are measured. If the K_d value of the target compound is below 1 the solute will elute closer to the solvent front. This could potentially result in less efficient resolution of peaks and a less polar solvent system should be tested. Conversely, if the K_d value is above 1 the product will have a high retention in the column resulting in potential broadening of the sample peak, as well as a longer operating time prior to elution. A more polar solvent system should then be investigated for use (Ito, 2005).

To avoid solvent contamination of the column, CCC applications begin with a solvent swap transferring the solute matrix from the process solvent into the selected stationary or mobile

phase composition (Ito, 2005)(Du *et al.*, 2003). Solvent swaps can be carried out using thermal techniques (*e.g.* evaporation) and though capable of sample generation, application is limited to swaps going from a lower to a higher boiling point solvent, and processing can be time-consuming, energy-intensive and potentially cause product degradation. On a larger scale, thermal operation becomes even less viable due to equipment limitations. In addition to the required solvent swap, further limitations of CCC include the high solvent usage required for separation, and solvent recovery of the mobile phase would be desirable to make its application more financially viable. Both solvent swap and solvent recovery steps are commonly overlooked when discussing CCC applications, but such considerations are critical to consider if CCC is to be used at anything other than a lab-scale.

In this chapter a combined approach of OSN and CCC was used to recover pure API (~650 g mol^{-1}) from a crystallisation mother liquor (82.0% methanol, 15.9% MiBK and 2.1% toluene) containing API and various impurities of different sizes and properties. OSN was used to perform the initial solvent swap from the process liquor into the mobile phase, prior to CCC application for recovery of the API. The solvent burden of CCC was further addressed through a second OSN stage for recovery and recycle of mobile phase (Figure 5.2). As OSN is a non-thermal technique, benefits of combined processing is envisaged by facilitating the application of CCC at large scale and improving process mass- and energy efficiency.

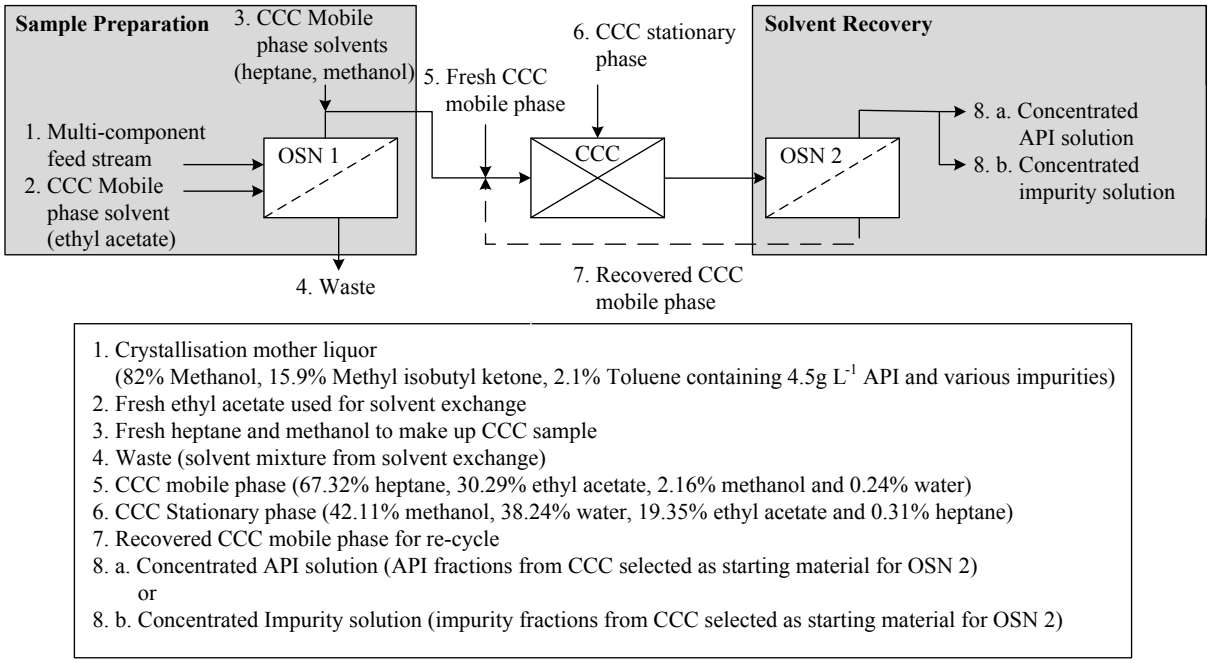

Figure 5.2. Process diagram detailing combined application of OSN and CCC for recovery of API from multi-solute crystallisation mother liquor

5.2 Materials and Methods

5.2.1 Feed Solution

The initial feed solution for combined OSN and CCC processing was selected as a crystallisation mother liquor, made up of 82.0% methanol, 15.9% MiBK and 2.1% toluene containing 4.5 g L^{-1} API (~650 g mol^{-1}) and 27 impurities of various sizes.

5.2.2 Membrane Pre-conditioning

All membrane discs were washed by permeation of 0.2 L pure solvent at 30 bar pressure and ambient temperature (25-30 ^{o}C). The washing solvent was selected based on the solvents used for operation, with pure ethyl acetate used for the membrane solvent swap and a mixture of 30:70% ethyl acetate and heptane used for the membrane solvent recovery. After washing, the

filtration system was depressurised and the content changed for the feed solution. The system was re-pressurised and the feed re-circulated through each membrane, at the desired operating pressure, for a minimum of 1 hour or until a stable flux was reached.

5.2.3 Membrane Screening

Based on listed solvent stability and MWCO values, Duramem™150, Duramem™200, Starmem™122, Starmem™240 and Puramem™280 were selected for testing. Screening was carried out in a cross-flow system (Evonik MET, Figure 2.6) connecting either two or three filtration cells (individual area 5.4×10^{-3} m^2) in series. Three separate tests were carried out investigating membrane performance at 30 bar pressure in the CCC mobile phase (screening solution I), pure ethyl acetate (screening solution II) and the crystallisation mother liquor (screening solution III) respectively. Permeate samples were collected at the end of the pre-conditioning phase, and the feed and retentate was sampled at the start and finish of each test. The flux was monitored every 30 minutes throughout operation.

5.2.4 OSN Solvent Swap

The solvent swap was carried out in a dead-end filtration system (Evonik MET), using Starmem™122 operated at 30 bar and ambient temperature (25-30 ^{o}C). A 0.4 L mixture of 50:50% ethyl acetate and crystallisation mother liquor was initially added to the system and the solution was concentrated down to 0.2 L (starting volume). The solvent swap was then carried out through gradual addition of ethyl acetate in a discontinuous put-and-take diafiltration. Put-and-take diafiltration was selected for operation as this method generally requires less solvent compared to continuous, constant volume diafiltration (Section 2.5.3). For each cycle the feed solution was concentrated through removal of 70% of the original

solvent, before the system was de-pressurised and the concentrate mixed with pure ethyl acetate to the original volume level (0.2 L). Concentration and solvent addition cycles were continued until the desired solvent composition was reached. To ensure maximum concentration in the CCC sample, no solvent addition was made after the final concentration cycle.

Prior to each concentration, the membrane used was pre-conditioned through permeate re-circulation. The flux was measured every 30 minutes during the pre-conditioning and for every 0.05 L permeate passed during the solvent swap cycles. Permeate samples were collected at the start and finish of each concentration, in addition to samples of the combined permeate. To minimise API losses, feed and retentate samples were only collected at the start and finish of the full solvent swap. At all intermediate stages rejection values were calculated based on mass-balance concentrations obtained from Equation 5.1, where C is the concentration of component i in the feed (f), permeate (p), added DV (d) and retentate (r) respectively. Equation 5.1 was further used to predict the solvent composition in the retentate throughout the solvent swap, assuming a 0% solvent rejection.

$$C_{i,r} = \frac{V_f C_{i,f} - V_p C_{i,p} + V_d C_{i,d}}{V_r} \qquad \text{Equation 5.1}$$

To monitor membrane stability, the same membrane disc was used for the full solvent swap, with the membrane exposed to nine pressure cycles and over-night storage during two subsequent nights.

5.2.5 OSN Solvent Recovery of Mobile Phase

OSN recovery of CCC mobile phase was carried out in a dead-end filtration system (Evonik MET) using Starmem™240 operated at 30 bar pressure and ambient temperature (25-30 ^{o}C). As the volume for each mobile phase fraction was larger than the equipment operation volume, solvent recovery was carried out as a constant volume diafiltration with feed solution being added to the system at a rate equivalent to the permeation. Diafiltration was continued until the full volume had been added, after which the remaining retentate was concentrated down until the solubility level was reached. To ensure consistent membrane performance a new disc was used for solvent recovery from each fraction. Similar to the solvent swap each membrane disc was pre-conditioned through permeate re-circulation until a stable flux was reached prior to starting the solvent recovery. The flux was measured every 30 minutes during the pre-conditioning and for every 0.05 L permeate passed during the solvent recovery. Permeate samples were collected at the start and finish of each recovery run, as well as for the combined permeate. Feed and retentate samples were collected at the start and finish of the recovery from each fraction respectively.

5.2.6 CCC Separation

The solvent system for CCC operation was selected as HEMWat 17.5, based on previous method development (Ignatova, 2010). HEMWat 17.5 corresponds to a stationary phase composition of 42.11% methanol, 38.42% water, 19.35% ethyl acetate and 0.31% heptane, and a mobile phase composition of 67.32% heptane, 30.29% ethyl acetate, 2.16% methanol and 0.24% water (Garrard *et al.*, 2007). Stationary and mobile phases were made up as individually saturated phases, and partitioning tests were carried out measuring K_d values for the fresh and recovered solvent systems used for CCC Runs 2 and 3, as well as a bulk-phase

system of HEMWat 17.5 (Section 5.3.3). For each partitioning test, 1 mg crude material (residue from full evaporation of mother liquor) was dissolved in 0.5 mL stationary and mobile phase respectively. Samples were mixed and allowed to settle prior to analysis of each phase.

Analytical (Mini CCC Run 2 and 3) and preparatory scale (Midi CCC Run 1) CCC operations were carried out using Mini and Midi centrifuges (Dynamic Extraction Ltd.) respectively (Table 5.1). Both the Mini and Midi scale equipment contains a centrifuge using one or more bobbins, acting as the column during CCC operation. Prior to sample injection, the system was pre-conditioned by pumping the mobile phase through the column, gradually displacing stationary phase. The pre-conditioning was continued until no more stationary phase eluted, at which point maximum retention of the stationary phase was assumed. Sample injection was carried out after the equilibration, followed by an immediate start of the fraction collection. Scale-up between the Mini and Midi runs was based on volumetric scaling of all parameters, to enable direct comparison of testing.

Table 5.1. Process parameters used for CCC Mini and Midi scale operation

Parameter	CCC Mini Centrifuge	CCC Midi Centrifuge
Number of bobbins in centrifuge	Single	Double
Column (bobbin) volume (L)	0.020	0.925
Bobbin bore tubing diameter (mm)	0.8	4.0
Centrifuge spin rate (rpm)	2100	1400[a]
Flow rate (mL min^{-1})	1.5	70
Sample volume (L)	0.9	41
Run time (min)	35	35
Number of collected fractions	10	10
Fraction volume (L)	5.25×10^{-3}	2.45×10^{-1}

[a]Selected to maintain a constant gravitational field to the Mini equipment

5.2.7 Analysis

API and impurity concentrations were monitored by HPLC as detailed in Section 3.2.5, with the detector set to a fixed wavelength of 260 nm. Traces of water in the solvent mixture were measured using a volumetric Mitsubishi Karl Fischer moisturemeter CA-100/KF-100 with a sample injection volume of 0.5 mL. Solvent levels of ethyl acetate, heptane, methanol, MiBK and toluene were analysed using a Hewlett Packard HP 6890 Series gas chromatograph (GC) system. The oven temperature was initially held at 240 °C, with the injector temperature set at 200 °C. The sample injection volume was selected to 1.0 µL using a split mode injection of 40:1, with helium used as a carrier gas with the flow rate determined through a pressure ramp passing from 0.2 to 2.1 bar over 6.3 minutes. Separation was enabled using a DB-624-GC column (10 m long, 200 µm diameter, 1.12 µm film thickness) with the column temperature controlled from an initial value of 35 °C (held for 2.0 min), before increasing to 80 °C (held for 1.0 min) at a rate of 50 °C min^{-1}, and finally increasing to 150 °C (held for 1.0 min) at a rate of 210 °C min^{-1}. Sample detection was enabled through a flame ionization detector set at 250 °C, using a make-up flow of 34.0 mL min^{-1} nitrogen, 450.0 mL min^{-1} air and 40.0 mL min^{-1} hydrogen.

5.3 Results and Discussion

5.3.1 Membrane Screening

The solvent recovery as well as a majority of the solvent swap should ideally be carried out at a composition close to the CCC mobile phase (67.32% heptane, 30.29% ethyl acetate, 2.16% methanol and 0.32% water) which was selected as screening solution I. To obtain maximum information prior to membrane selection, the API as well as all impurities present should be included in the screening solution. However, the impurities are not readily available in dry

form, and consequently the API was selected as the sole marker for evaluating membrane performance (Table 5.2). For operation in the CCC mobile phase, API rejections for Duramem™150, Duramem™200, Starmem™122 and Puramem™280, were observed to be below 90% despite membrane MWCOs being significantly lower than the API molecular weight (~650 g mol^{-1}). Deviations from the expected rejection values are most likely a combination of the different solvent used during the membrane screening compared to the MWCO characterisation, as well as a lack of sharp MWCO curves, and highlight shortcomings of the current characterisation method used for membrane performance.

The highest API rejection in the CCC mobile phase was observed for Starmem™240 at a value of 98.5%, in combination with a flux of 48 L m^{-2} h^{-1}. Starmem™240 could potentially be used for recovery of CCC mobile phase through a single or multiple membrane pass. However, for OSN solvent swapping multiple permeate passes are not suitable from a processing perspective. Previous testing has demonstrated that for less than a 100% rejection, losses of API can be observed throughout OSN diafiltrations. The theoretical API loss for a solvent swap using Starmem™240 was calculated based on a mass-balance. Potential losses add up to a significant value of ~8%, indicating that an OSN solvent swap directly into the mobile phase is not ideal. The second largest component of the CCC mobile phase is ethyl acetate, and in an attempt to improve rejection and minimise yield losses, a solvent swap into pure ethyl acetate rather than the full CCC mobile phase composition was suggested. The resulting solution in ethyl acetate can be mixed with additional solvents into the correct mobile phase composition. Though the resulting sample will be more dilute, the process offers an advantage in that more membranes stable in ethyl acetate compared to heptane, are commercially available. Pure ethyl acetate was selected as screening solution II, again using the API as the marker for membrane performance (Table 5.2). The crystallisation mother

liquor was finally included as screening solution III, to evaluate potential changes in membrane performance for different solvents, and to provide approximate rejections for the impurities present (Table 5.2).

In ethyl acetate the highest membrane performance was observed for Starmem™122 having an API rejection of 99.8%, in combination with a flux of 84 L m^{-2} h^{-1}. For operation in the crystallisation mother liquor (82.0% methanol, 15.9% MiBK and 2.1% toluene), the API rejection of Starmem™122 was however reduced to 98.4%, and the highest membrane performance was observed for Duramem™150 with an API rejection of 99.2%. A similar decrease in rejection in the crystallisation mother liquors compared to ethyl acetate was also observed for Starmem™240 and Puramem™280, whereas the rejection remained constant or increased for Duramem™150 and Duramem™200 for operation in the mother liquors. Changes in rejection are again believed to be a result of the changed solvent-membrane combination, though additional factors such as solvent-solute interactions could also be influential. For the majority of the solvent swap, operation will be carried out in solutions composed mainly of ethyl acetate, with only the initial stage being carried out at a composition closer to the crystallisation mother liquor. Based on process requirements, Starmem™122 was hence selected as the most suitable membrane for the solvent swap.

Table 5.2. Summary of membrane performance data from screening in the CCC mobile phase (screening solution I), pure ethyl acetate (screening solution II) and crystallisation mother liquors (screening solution III) (tests were operated in cross-flow at 30 bar pressure and ambient temperature)

Membrane	Screening solution	R_{API} (%)	Flux (L m^{-2} h^{-1})
Duramem™150	I	76.1	0.2
Duramem™200	I	21.7	28
Starmem™122	I	83.1	8
Starmem™240	I	98.5	48
Puramem™280	I	86.7	9
Duramem™150	II	99.1	5
Duramem™200	II	91.6	29
Starmem™122	II	99.8	84
Starmem™240	II	99.5	88
Puramem™280	II	99.6	77
Duramem™150	III	99.2	16
Duramem™200	III	96.5	55
Starmem™122	III	98.4	59
Starmem™240	III	98.9	48
Puramem™280	III	98.2	53

5.3.2 OSN Solvent Swap

The target composition for the solvent swap was set to 99.99% (by volume) ethyl acetate, with traces of the mother liquors solvent (methanol, MiBK and toluene) limited to maximum values of 0.01% (by volume) respectively. The solvent trace target from the mother liquors was set to a very low level to limit potential contamination of the CCC stationary phase. Data indicate that the target composition was reached after addition of 5.9 DV ethyl acetate, which is equivalent to 8 put-and-take cycles (Figure 5.3 and Table 5.3). The measured solvent composition correlated well with the calculated levels, indicating that the assumed solvent rejection of 0% holds true for the given system. No retention of solvents is hence expected and for a well-mixed solution the solvent composition should be maintained over the

membrane (Figure 5.3). Theoretical calculations were further carried out to compare the solvent consumption for an equivalent solvent swap operated in a continuous, rather than a discontinuous put-and-take, diafiltration mode. Mass-balance calculations demonstrate that for continuous operation, passage of an additional 3.5 DV would be required to reach the desired solvent composition.

Screening data indicated that for Starmem™122 the API rejection was lower in the crystallisation mother liquor compared to ethyl acetate. In an attempt to maximise the rejection, ethyl acetate was added to the crystallisation mother liquor prior to start of the first put-and-take cycle. The starting solution was made up of a 0.4 L 50:50% mixture which was concentrated to 0.2 L prior to the start of the solvent swap. For the mixed feed the API rejection was observed to increase from the expected vale of 98.4% observed during the screening, to a value of 99.3% (Table 5.3). The increased rejection strongly indicates that the performance of Stramem™122 is dependent on membrane-solvent-solute interactions, and demonstrates that the overall API loss can be minimised through early addition of ethyl acetate. After the initial cycle the API rejection ranged between 99.7-99.9%, resulting in an overall API loss of 2.3%. Consistent rejection data throughout operation indicates high membrane stability despite the membrane disc being exposed to multiple pressure cycles and overnight storage. Rejection data was further consistent with the membrane screening, indicating repeatable membrane performance.

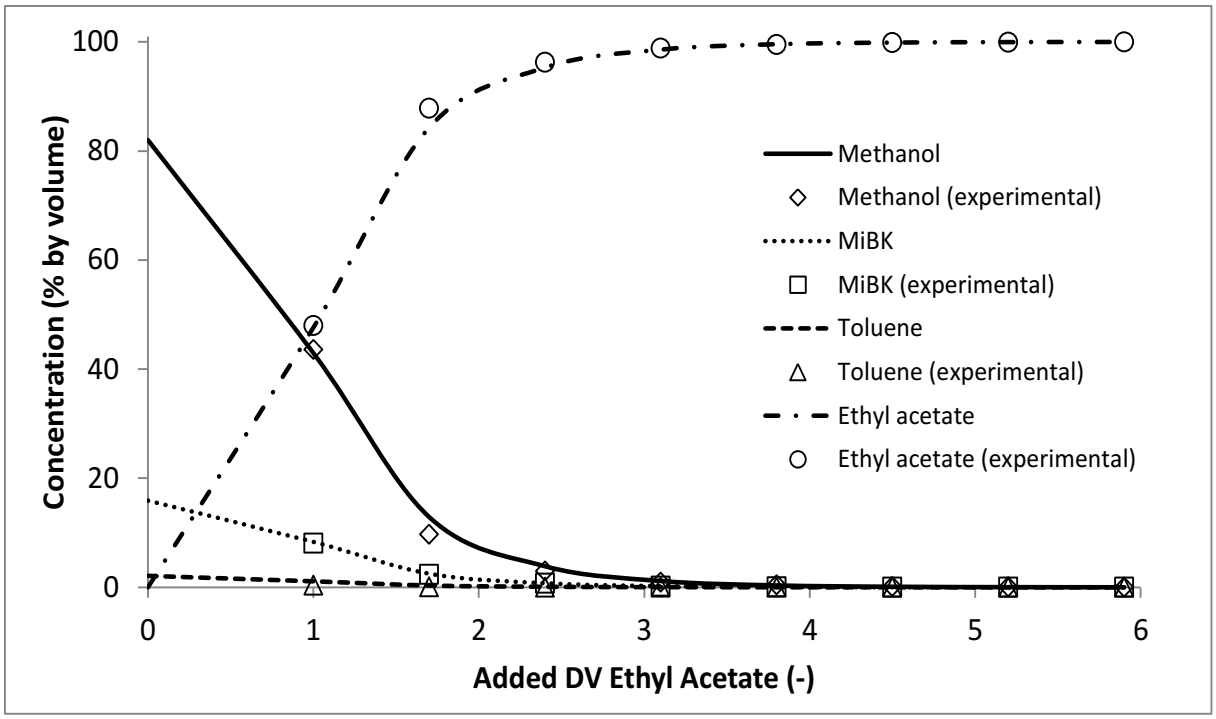

Figure 5.3. Summary of calculated and experimental solvent levels measured throughout put-and-take OSN solvent swap from the crystallisation mother liquor into ethyl acetate (test was operated in dead-end using Starmem™122 at 30 bar pressure and ambient temperature)

Table 5.3. Summary of observed rejections, API losses and solvent compositions calculated throughout OSN solvent swap from the crystallisation mother liquors into ethyl acetate (test was operated in dead-end using Starmem™122 at 30 bar pressure and ambient temperature)

			Solvent composition			
Added DV (-)	**R_{API} (%)**	**API losses (%)**	**Methanol (%[a])**	**MiBK (%[a])**	**Toluene (%[a])**	**Ethyl acetate (%[a])**
1.0	99.3	1.4	43.6	8.1	0.4	48.0
1.7	99.7	1.6	9.7	2.4	0.08	87.8
2.4	99.9	1.7	3.0	0.8	0.01	96.3
3.1	99.9	1.7	0.9	0.2	0.01	98.8
3.8	99.9	1.8	0.4	0.06	0.001	99.5
4.5	99.9	1.8	0.1	0.003	< 0.001	99.9
5.2	99.9	1.8	0.07	< 0.001	< 0.001	99.9
5.9	99.4	2.2	0.01	< 0.001	< 0.001	99.99
Retentate	-	2.3	0.01	< 0.001	< 0.001	99.99

[a]% (by volume)

5.3.3 CCC Separation

For lab-scale CCC operation, solvent phases are commonly made up in bulk by mixing the constituent solvents in ratios, before allowing the system to settle and separating the immiscible fractions for use as stationary and mobile phases respectively. For operation on an industrial scale such bulk-phase preparation is not practical, and stationary and mobile phases are made up as individually saturated phases (Garrard *et al.*, 2007)(Wu *et al.*, 2010). Individually prepared phases were used in this study, and to ensure consistency with bulk-phase solutions, a partitioning test was carried out prior to CCC operation. Partitioning data indicated consistent K_d values of 1.06 for both systems, demonstrating that there was no significant difference resulting from the various methods used for phase preparation. Partitioning data further demonstrated that calculated separation factors for the API and related impurities remained above the desired value of 1.5 for all impurities except two, displaying values of 1.1 and 1.3 respectively. Minor co-elution might occur for impurities having K_d values closer to the API, however previous method development demonstrated that a more suitable solvent system for CCC operation could not be found (Ignatova, 2010).

CCC samples were made up by mixing the retentate from the solvent swap (Section 5.3.2) with fresh solvent into the desired mobile phase composition (67.32% heptane, 30.29% ethyl acetate, 2.16% methanol and 0.24% water). A larger scale CCC run (CCC Run 1) was initially carried out to generate a sufficient volume of mobile phase to enable OSN recovery and recycle into subsequent CCC operation (used in CCC Run 3). CCC Run 1 was operated on a Midi scale, with the stationary phase retention resulting from equilibration of the column measured to 80%. Collected fractions were analysed with HPLC, and data indicated a good separation with early elution of impurities followed by elution of the API during the final 15

min of the CCC run (Figure 5.4). The purity of the API containing fractions ranged between 62.2-100.0%. The lower purities were measured for fractions with low API concentrations, and in absolute values the impurities present were minimal.

Two additional CCC runs were operated on a Mini scale using fresh (CCC Run 2) and recovered solvent (CCC Run 3, Section 5.3.4) respectively as the mobile phase. For both Mini runs the stationary phase retention was measured as 83%, which was similar to the value observed for CCC Run 1. HPLC data, indicated close to identical separation profiles for CCC Run 2 and 3, with the majority of the impurities eluting between 5 and 15 min with only trace amounts visible at higher elution times (Figure 5.4). The API eluted between 20 and 30 min, with fractional purities ranging between 91.6-100.0% for 77.5% and 80.0% of the added API for CCC Run 2 and 3 respectively. All additional API containing fractions ranged in purity between 27.0-85.2%, with the overall API recovery calculated as 99.9% and 101.4% for CCC Run 2 and 3 respectively. Similarly to CCC Run 1, the API fractions with low percentage purity contained a low concentration, and in absolute values the impurities present were minimal. Additionally, though a 90% purity is not sufficient for the final product the API was recovered through crystallisation generally resulting in a purity above 99%. The separation performance observed for CCC Run 1-3 was hence considered sufficient, and initial feasibility for API purification could be considered proven. Additionally, almost identical elution profiles were observed for CCC Runs 2 and 3, with no indication of impurity enrichment in the API containing fractions when recovered solvent was used as the mobile phase for separation. Consistent CCC data confirms OSN as a suitable alternative for recovery and recycling of CCC mobile phase.

Comparing Mini and Midi scale operations, data demonstrate that though the API was eluting over approximately the same time interval, the API peak was broader for CCC Run 1 (Midi run). Minor differences in elution profiles could be a result of small differences in the phase compositions, in combination with differences in mixing occurring for the Mini and Midi scale equipment. However as the API elution intervals, as well as fraction purities, were similar for operation on both Midi and Mini scale, CCC performance was considered consistent.

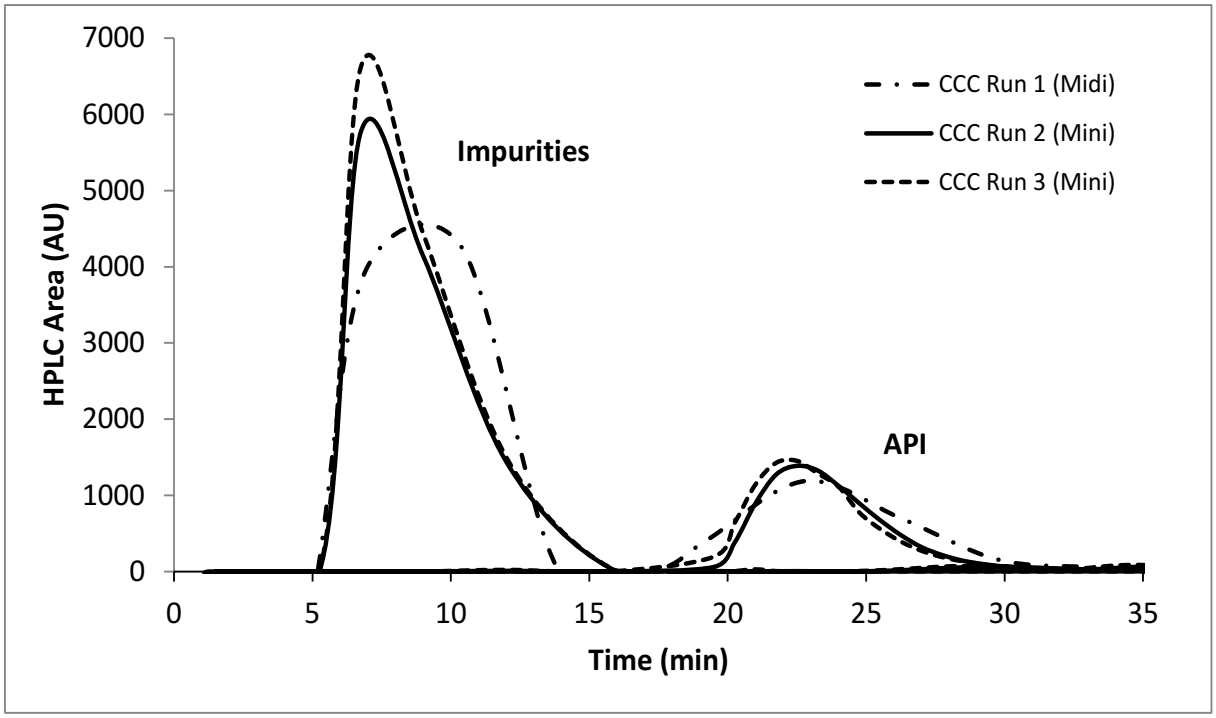

Figure 5.4. Comparison of API and impurity elution during CCC Run 1 (Midi, fresh solvent for mobile phase – material for solvent recovery), Run 2 (Mini, fresh solvent for mobile phase) and Run 3 (Mini, OSN recovered solvent for mobile phase) (test conditions for the Mini and Midi runs were scaled volumetrically and are summarised in Table 5.1)

5.3.4 OSN Solvent Recovery of Mobile Phase

OSN solvent recovery was investigated for the eluted mobile phase collected from CCC Run 1 (Section 5.3.3). Based on solute content and concentration the mobile phase was divided into four fractions, which were investigated individually for solvent recovery (Table 5.4). Separate study of fractions was used to enable recovery of the API, and to minimise the risk of including low molecular weight impurities - which are not easily removed by OSN - into the recovered solvent.

Table 5.4. Summary of solute content, volume of fractions and solute rejections for mobile phase fractions collected for CCC Run 1 (Midi)

Fraction	Solute content	Volume (L)	R_{Solute} (%)	OSN recovery
F0[a]	Low concentration, 2 impurities	0.505	13 – 47	Yes
F1-F2	High concentration, 20 impurities	0.490	0 – 100	No
F3-F5	Low concentration, 7 impurities	0.735	17 – 100	Yes
F6-F10	Intermediate concentration, API only	1.225	98.5	Yes
Total	–	2.955	–	–

[a]Mobile phase used for stationary phase equilibration (collected from column after CCC separation)

A solvent specification was selected, stating that the recovered mobile phase must be within 0.5% (by volume) of the desired solvent composition and contain no more than 1% (by area GC) total of impurities. GC data indicate that for fractions F0 and F3-F5 the overall solute content as well as concentrations were low, and despite rejections ranging between 13-100% solvent recovery could be achieved in a single membrane pass (Table 5.4 and Table 5.5). Fractions F6-F10 contained the API and concentrated material was intended for API recovery through crystallisation. As the rejection of the API was high at 98.5%, solvent recovery could be achieved in a single membrane pass. However, to maximise yield of the recovered API a dual membrane stage was used for solvent recovery, with the retentate from each stage

collected separately. Finally, for fractions F1-F2 the overall impurity content as well as concentration was high, with impurity rejections ranging between 0-100% (Table 5.4). The low rejections, in combination with high starting concentrations, indicate that even if multiple membrane passes were to be used, the recovered solvent would not be within the solvent specification. Fractions F1-F2 were hence considered unsuitable for solvent recovery, and were discarded as waste.

The solvent composition of each recovered fraction was determined using GC and Karl Fisher, prior to combining fractions into the final recovered mobile phase. The composition of the combined solvent was measured as 67.7% heptane, 30.2% ethyl acetate, 1.9% methanol and 0.3% water, hence deviating from the desired composition by a maximum of 0.4% (by volume) for heptane (Table 5.5). Partitioning tests demonstrated consistent K_d values of 1.06 for the API in both the recovered and fresh solvent phases used for CCC Run 2 and 3 respectively, indicating that the minor differences in solvent composition have no significant impact on the solute partitioning. GC analysis further demonstrated that the combined solvent was within the specification, as the impurity trace was limited to 0.46% (by area GC). Implementation of OSN solvent recovery was finally demonstrated through consistent CCC performance, with no indication of impurity build-ups in the API containing fractions, during operation using fresh and recovered mobile phase respectively (Section 5.3.3).

Table 5.5. Solvent composition and impurity content based on GC and Karl Fisher, as well as the volume of solvent recovered from mobile phase fractions collected from CCC Run 1 (OSN solvent recovery was operated in dead-end using Starmem™240 at 30 bar pressure and ambient temperature)

Fraction	Heptane (% v/v[a])	Ethyl acetate (% v/v[a])	Methanol (% v/v[a])	Water (% v/v[a])	Impurities (% a/a[b])	Volume (L)
F0	66.6	30.6	2.2	0.3	0.46	0.435
F3-F5	67.8	29.8	2.1	0.3	0.47	0.660
F6-F10	67.6	30.4	1.7	0.3	0.45	0.890
Combined permeate	67.7	30.2	1.9	0.3	0.46	1.985
Desired composition	67.32	30.29	2.16	0.24		

[a]% volume by GC
[b]% area by GC

5.3.5 Process Comparison

In this chapter, API purification through use of CCC has been demonstrated. However, CCC is known to be a solvent intensive method and in an attempt to minimised the solvent usage CCC was combined with OSN for recovery of mobile phase. Additionally, use of OSN was demonstrated for CCC sample preparation, through enabling a full solvent swap of the process liquors into the CCC mobile phase. Chapters 3 and 4 highlighted high solvent usage as a current limitation of OSN diafiltration, and to evaluate potential benefits of combined OSN and CCC processing a comparison looking at solvent usage for CCC operated on fresh and recovered solvent using OSN prepared samples was carried out (Table 5.6).

As expected calculations indicate that for CCC operation alone, the solvent usage was high at a value of 37.0 L per gram purified API. Assuming that OSN can be used to recover 70% of the mobile phase (recovery level obtained from CCC Run 1), the solvent usage can be reduced to 14.5 L per gram purified API through combined use of CCC and OSN. Combination with OSN was hence demonstrated to reduce the solvent consumption by 62%,

potentially making CCC more financially viable. However, the solvent usage for CCC remained high even when OSN recovery of mobile phase was used, and further developments to reduce the solvent usage are crucial for CCC to gain a more widespread use for industrial applications.

Including the OSN solvent swap, the solvent usage for CCC was calculated as 16.0 and 38.6 L solvent per gram purified API for operation with and without OSN recovery of mobile phase respectively. As the solvent intensity of CCC was high, the percentage increase for inclusion of the OSN solvent swap was limited to 4-10%. However, the solvent usage required for the solvent swap only, was equal to 1.5 L per gram purified API, again highlighting the high solvent intensity of OSN diafiltration. High solvent usage is likely to limit industrial application of OSN solvent swaps, though benefits can be seen in that swaps can be enabled for the difficult case of going from a higher (MiBK, 118 ^{o}C) to a lower boiling point (ethyl acetate, 77 ^{o}C) solvent.

Table 5.6. Summary of calculated solvent usage for CCC operated on fresh and recovered solvent, using samples prepared with OSN and evaporation respectively

Process	Solvent exchange	Solvent recovery[a] (%)	Solvent consumption (L g^{-1} API)
CCC Run 2	Not included	0	37.0
CCC Run 2	Included	0	38.6
CCC Run 3	Not included	70[b]	14.5
CCC Run 3	Included	70[b]	16.0

[a]Solvent recovery was limited to the mobile phase
[b]Equivalent to recovery level obtained in CCC Run 1

5.4 Conclusion

Work presented in this study demonstrated that CCC separations can be made more mass efficient when coupled with OSN technology. An OSN solvent swap was initially used for generation of CCC samples with a suitable composition, as demonstrated through use in successful CCC operation. Although OSN diafiltration was again highlighted as a solvent intensive method, use of OSN solvent swaps can offer potential benefits, compared to thermal techniques, in enabling processing for azeotropic mixtures and for the difficult case of swapping from a higher to a lower boiling point solvent. Additionally, OSN processing avoids potential thermal degradation of the API, and may provide benefits with regards to improved energy efficiency.

Further improvement to the CCC process was addressed through OSN solvent recovery and recycling of mobile phase. Recovered solvent was successfully used for CCC separation, demonstrating consistent performance compared to operations carried out using fresh solvent. OSN implementation for solvent recovery was hence demonstrated, with calculations indicating that even when a relatively solvent intensive OSN solvent swap was used for sample preparation, an overall 56% reduction in solvent usage for CCC could be achieved.

Chapter 6: OSN as an Alternative to Distillation for Solvent Recovery from Crystallisation Mother Liquors

6.1 Introduction

In 2007 the American Chemical Society (ACS), collected mass efficiency data from seven major pharmaceutical companies in a bench-mark study investigating the typical materials and quantities used during development and manufacture of APIs. Data indicated that for production of 1 kg of commercially available API, a median value of 45 kg of material was used (ACS, 2011)(Henderson *et al.*, 2007). Approximately 50% of that material was organic solvents, and for a yearly API production between 10-1000 tonnes, millions of tonnes of solvent are hence being used and disposed of every year (Sheldon, 2007)(ACS, 2011)(Henderson *et al.*, 2007).

The solvent usage of a process can be reduced through solvent recovery, which can offer benefits with regards to: reduced purchase, storage and waste costs; increased compliance with environmental legislation and reduced emission of greenhouse gases. Solvent use has further been reported to account for approximately 60% of the energy used during API production, indicating that solvent recovery could be of interest for improving energy efficiency (Jiménez-González *et al.*, 2005). Despite such advantages, GSK reported that in 2007 less than 50% of the solvents used were recovered, and the majority of waste was still disposed through on-site incineration (Constable *et al.*, 2007). The decision to burn rather than recover solvent was partly based on economic considerations. Additionally, the pharmaceutical industry is highly regulated and any changes to a process will have to be recorded and approved. Amendments to regulatory files is a time-consuming process, and can delay or even hinder the use of a potential solvent recovery step (Stewart Slater *et al.*,

2010)(Walker, 2008). Recent introduction of stricter environmental legislation in combination with increased pressure from regulatory agencies, are making solvent recovery a more competitive alternative to incineration. Consequently, study and development of more efficient solvent recovery techniques is gaining an increased interest in the pharmaceutical industry (Stewart Slater *et al.*, 2010).

A commonly used unit operation in API purification is crystallisation (Genck *et al.*, 2008). Crystallisations are used to isolate solid material from solutions. During operation the process liquors are cooled, or evaporated, to form a supersaturated solution, where the product is dissolved at a higher concentration than is typically observed within the given solvent system. Alternatively, anti-solvent operation can be used where another solvent, in which the product is less soluble, is added to the system. This has the effect of lowering the solubility of the product and initiate subsequent crystallisation. Seed crystals of the desired product can also be added to aid crystallisation. The seed crystals provide a nucleation surface for the product in solution to initiate growth of crystals which gradually precipitate out of solution. The seed crystals can further control the shape and size of the crystals formed (Coulson *et al.*, 2002b). Whilst crystallisations are an effective means to isolate and purify the API, operation can generate large volumes of solute rich waste (mother liquors), containing the impurities removed during operation as well as dissolved API up to the solubility limit. Mother liquors are generally discarded as waste; however further processing could improve process mass efficiency through recovery of organic solvent, as well as offer a potential route for recovery of valuable API.

Solvent recovery is conventionally achieved through distillation which separates components in liquid mixtures based on difference in volatility. In the simplest set-up separation is

achieved through evaporation, where the liquid mixture is heated in order to vaporise components in the liquid. The resultant vapour will be enriched in the more volatile component of the mixture, with the vapour composition being dependent on an equilibrium formed between the vapour and the liquid phase. The vaporised components are recovered in a condenser and collected in a separate receiver. Gradual removal of the more volatile components from the original liquid mixture causes the equilibrium in both the liquid and vapour phase to change over time, gradually resulting in an increase in the proportion of less volatile material in the vapour phase. As the vapour composition is dependent on this equilibrium, achieving a full separation of solvents through evaporation only can be difficult. If a higher degree of separation is desired, distillation columns containing multiple stages for vaporisation and condensation can instead be used. However, this approach results in a higher complexity and cost of operation (Coulson *et al.*, 2002c)(Coulson *et al.*, 2002d). Whilst distillation can be used to generate high purity solvent it is thermally driven and generally requires a high energy-input (Seader *et al.*, 2008). A low energy alternative for solvent recovery is hence highly desirable.

OSN has been suggested as a potential alternative for solvent recovery, with advantages highlighted in the non-thermal processing resulting in potentially improved energy efficiency compared to distillation (White *et al.*, 2006)(Geens *et al.*, 2007)(Vandezande *et al.*, 2008). However, despite low energy usage often being mentioned as a major advantage of OSN, limited data has been presented in literature to support this statement for operation in organic solvents. One comparative study looking at energy requirements for methanol recovery with OSN and distillation respectively was presented by Geens *et al.* in 2007. Their study indicated that the energy requirement was 200 times lower for OSN compared to distillation. However, the study by Geens *et al*. (2007) was based on a low concentration model system and

implementation of OSN solvent recovery in more concentrated, multi-component systems remain untested. OSN solvent recovery has further been demonstrated for lube oil dewaxing (White, 2006), though no data was presented demonstrating purification to the low levels required in the pharmaceutical industry.

In this chapter OSN was investigated as an alternative to distillation, for solvent recovery from crystallisation mother liquors. Two separate streams made up of industrial methylated spirit (IMS) (ethanol containing 3-5% methanol) containing ~6.0 g L^{-1} API 1 (~350 g mol^{-1}) and 18 different impurities; and iso-propyl acetate (IPAc) containing ~2.0 g L^{-1} API 2 (~650 g mol^{-1}), more than 40 different impurities and traces of methanol, water and iso-propyl alcohol (IPA) were tested respectively. Selected feed solutions were made up of different solvent types, containing APIs of significantly varying sizes, and aimed to illustrate OSN implementation for a range of process streams. Recovered solvent was intended for recycling into subsequent crystallisations as detailed in Figure 6.1. In addition to investigate OSN solvent recovery, an energy comparison was carried out for OSN and distillation respectively.

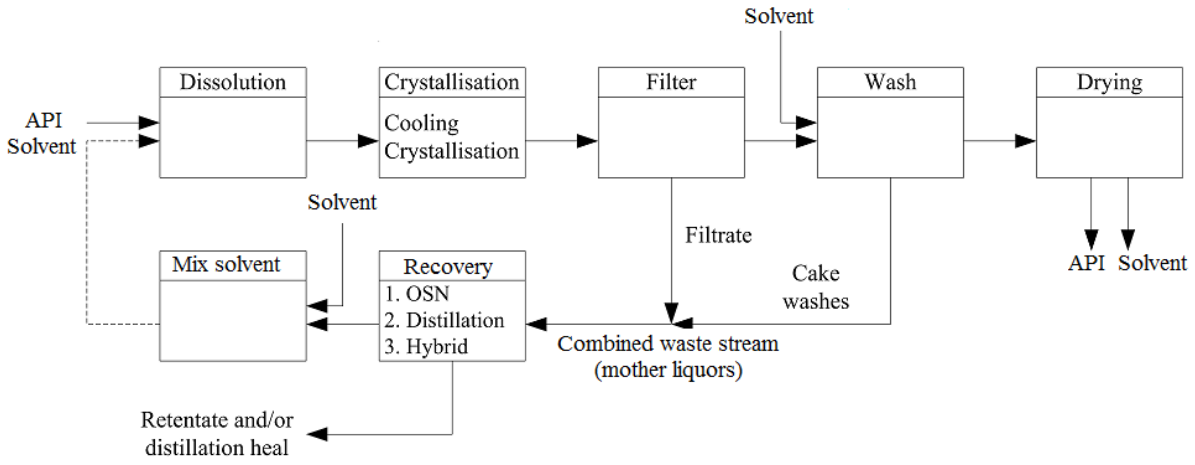

Figure 6.1. Process flow diagram of API crystallisation with solvent recovery and recycle

6.2 Materials and Methods

6.2.1 Feed Solutions

Lab-scale solvent recovery testing was carried out using two different crystallisation mother liquors as feed solutions. Individual process streams were made up of IMS containing ~6.0 g L^{-1} API 1 (~350 g mol^{-1}) and 18 different impurities; and IPAc containing ~2.0 g L^{-1} API 2 (~650 g mol^{-1}), more than 40 different impurities and traces of methanol, water and IPA.

Study of the IPAc process stream (API 2) was further extended to test recycling of recovered solvent into subsequent crystallisations, as well as solvent recovery on a pilot-scale. Intermediate grade API 2 used for crystallisations had been collected from an intermediate stage during API production. Material was made up of API 2 containing traces of the different impurities removed in the mother liquor used for OSN solvent recovery.

6.2.2 Membrane Washing

Prior to addition of the feed solution all membranes were washed by permeation of 40 L pure solvent per m^2 membrane area (*i.e.* 0.2 L for 5.4×10^{-3} m^2 flat sheet discs used in dead-end and cross-flow system, and 4.4 L for 0.11 m^2 spiral wound module). The process solvent (HPLC grade IMS or IPAc) was used for washing, with operation carried out at 30 bar pressure and ambient temperature (25-30 ^{o}C). After washing the filtration system was de-pressurised and the content switched for the feed solution.

6.2.3 Membrane Screening

Membrane screening was carried out in a cross-flow system (Evonik MET), connecting either two or three filtration cells (individual area 5.4×10^{-3} m^2) in series. Based on manufacturer

recommendations and MWCO values, Duramem™150 and Duramem™200 were selected for screening in the IMS process stream (API 1), and Starmem™122, Starmem™240 and Puramem™280 were selected for testing in the IPAc process stream (API 2). For each test the screening solution was added to the system and re-circulated at 30 bar for 3 hours, after which the first set of permeate samples were collected. The pressure was further increased to 60 bar and re-circulation was repeated for an additional 3 hours before a second set of permeate samples were collected. Feed and retentate samples were taken at the start and finish of each screening test, and the flux was measured every 30 minutes throughout operation.

6.2.4 Solvent Recovery

Lab-scale solvent recoveries were carried out in a dead-end filtration cell (Evonik MET). After membrane washing 0.15 L feed solution was added to the system and pre-conditioning was carried out through re-circulation of the permeate for 2 hours at the desired operating pressure. Solvent recovery was then conducted as a concentration, through removal of permeate to an 80% recovery level using Duramem™150 operated at 60 bar (IMS process steam), or Starmem™122 and Puramem™280 operated at 30 and 60 bar respectively (IPAc process stream). Feed and retentate samples were collected at the start and finish of each test, and permeate samples were taken from the combined solvent recovered. The flux was measured every 30 minutes during the pre-conditioning, and after collection of 0, 0.05 and 0.10 L permeate during the concentration.

Pilot-scale solvent recovery was carried out for the IPAc process stream (API 2) only, using a Bench-Top Module Testing Unit (Evonik MET). Based on lab-scale testing and manufacturer recommendations, Puramem™280 (spiral wound module 1.8’’×12’’ equivalent to 0.11 m^2

membrane area) operated at 60 bar was selected for pilot-scale testing. As far as possible, pilot-scale operation was kept consistent with lab-scale test conditions to facilitate comparison. After completion of the membrane washing 2.0 L feed solution was added to the system which was pre-conditioned through permeate re-circulation for 3 hours at 60 bar. An additional 2.0 L feed was then added to the system and the solvent recovery initiated. Recovered solvent was collected in 2.0 L fractions, and the volume level in the feed tank was kept close to a constant level through addition of 1.0 L feed solution for each 1.0 L permeate removed. In total 18 L feed was processed with 14 L (equivalent to the maximum recovery level of 80%) collected as recovered solvent. Feed and retentate samples were taken at the start and finish of the experiment, and permeate samples were collected from each 2.0 L fraction combined solvent recovered. The flux was measured every 30 minutes during the pre-conditioning and after each permeate fraction collected.

6.2.5 Solvent Recycling and Crystallisation

Solvent recycling into API crystallisations was carried out for API 2 in the IPAc process stream only. Operation was conducted as a cooling crystallisation, with the API recovered through filtration, cake washing and drying (Figure 6.1, Section 6.1). Filtrate and solvent from cake washes were combined into mother liquors, used as feed solution for OSN solvent recovery and recycling.

In total four crystallisations were carried out using fresh solvent (batch 1), or OSN recovered solvent from the previous crystallisation cycle (batches 2-4). OSN processing for all solvent recovery cycles was carried out using Puramem™280 operated at 60 bar.

6.2.6 Analysis

API and impurity concentrations in the feed, retentate and permeate samples were monitored by HPLC as detailed in Section 3.2.5. Isolated API from crystallisations were dissolved and analysed through a 45 minute gradient HPLC method using an Agilent 1200 Series HPLC system. No details regarding the HPLC method can be disclosed to ensure confidentiality of the API structure and properties.

Solvent levels of IMS (ethanol and methanol), IPAc, methanol and IPA were measured by GC as detailed in Section 5.2.7. Traces of water in the recovered solvent was analysed by a volumetric Mitsubishi Karl Fischer moisturemeter CA-100/KF-100 using a 0.5 mL sample.

6.3 Results and Discussion

6.3.1 Membrane Screening

The ideal membrane for solvent recovery should fully retain all solutes present in the feed solution, while allowing solvent to pass through the membrane unhindered. Membrane screenings were carried out for process streams in IMS and IPAc respectively. Screenings were conducted at an intermediate and maximum pressure to investigate potential influences of pressure, and membrane performance was characterised with regards to API rejection and permeate flux (Table 6.1).

For operation in the IMS process stream API 1 rejections above 99% were observed for Duramem™150 during operation at both 30 and 60 bar. The most suitable membrane performance was observed for Duramem™150 at 60 bar, demonstrating a 99.4% rejection of API 1 in combination with a flux of 10 L m^{-2} h^{-1}. During screening in the IPAc process

stream, high API 2 rejections above 99% were measured for all membranes tested. The highest membrane performance was observed for Starmem™122 having a > 99.9% rejection of API 2 during operation at both 30 and 60 bar. Limited improvement in membrane performance, was observed for operation at a higher pressure, and consequently Starmem™122 operated at 30 bar was selected for further study. Suitable performance was also observed for Puramem™280 operated at 60 bar. Puramem™280 can currently be supplied with the documentation required for pharmaceutical manufacturing, and to facilitate potential scale-up both Starmem™122 and Puramem™280 were selected for lab-scale solvent recovery testing.

Table 6.1. Summary of API 1 and API 2 rejections and fluxes measured during membrane screening in IMS and IPAc process streams (tests were operated in cross-flow at 30 or 60 bar pressure and ambient temperature)

Membrane	Feed solution	Pressure (bar)	R_{API} (%)	Flux (L m^{-2} h^{-1})
Duramem™150	IMS (API 1)	30	99.2	7
Duramem™150	IMS (API 1)	60	99.4	10
Duramem™200	IMS (API 1)	30	95.6	31
Duramem™200	IMS (API 1)	60	97.0	41
Starmem™122	IPAc (API 2)	30	> 99.9	36
Starmem™122	IPAc (API 2)	60	> 99.9	40
Starmem™240	IPAc (API 2)	30	99.7	60
Starmem™240	IPAc (API 2)	60	99.8	65
Puramem™280	IPAc (API 2)	30	99.6	45
Puramem™280	IPAc (API 2)	60	99.8	54

6.3.2 Solvent Recovery

Selected solvent specifications for the IMS process stream (API 1), state that the composition of the recovered solvent must contain a minimum of 95% (by volume) ethanol, and no more than 5% (by volume) methanol and 0.5% water respectively. Additionally impurity traces

should be kept to a low value ideally close to zero. GC analysis demonstrate that when Duramem™150 operated at 60 bar was used for lab-scale OSN solvent recovery, the composition of the collected permeate was equal to 95.7% (by volume) ethanol; 3.9% (by volume) methanol; and 0.4% (by volume) water (Table 6.2), which was within the stated target composition. Comparison with the original feed solution further showed that only minor changes in the solvent composition occurred over the membrane, indicating that for a well-mixed solution no significant solvent rejection was observed. As ethanol and methanol cannot be detected by HPLC, no quantification of the solutes present in the permeate could be carried out. However, graphical illustration indicated that OSN removed the majority of the solutes present in the feed solution with only minor traces being observed in the recovered permeate (Figure 6.2). Closer study of HPLC data further demonstrated that the majority of the solutes present in the permeate was API 1 (Table 6.2), which was not expected to be a concern as the recovered solvent was intended for recycling into subsequent crystallisations.

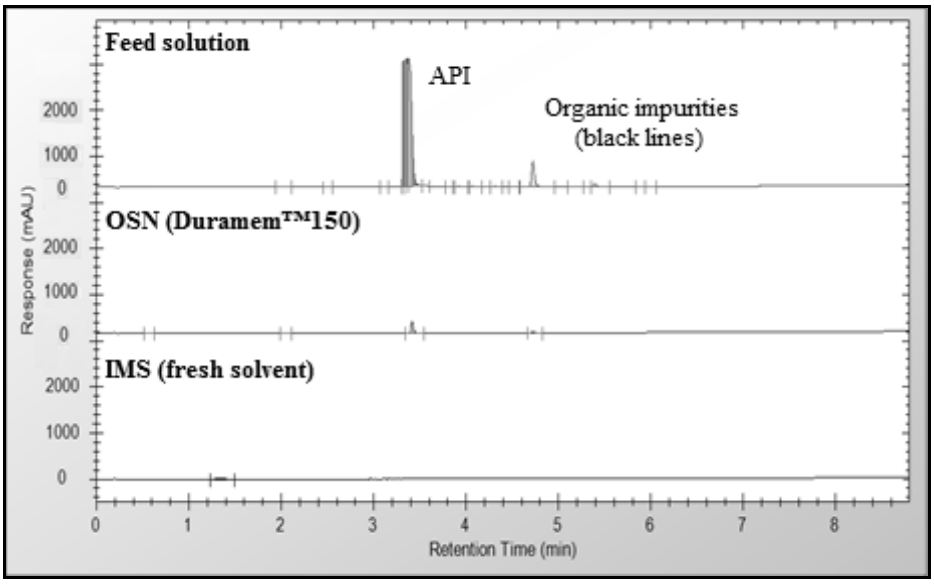

Figure 6.2. HPLC chromatograms of feed solution, OSN recovered solvent (dead-end filtration at 60 bar pressure and ambient temperature) and fresh IMS (IMS process stream)

Table 6.2. API 1 rejection, solvent composition and solute content based on GC, Karl Fischer and HPLC for the feed solution and OSN recovered solvent from the IMS process stream (dead-end filtration at 60 bar pressure and ambient temperature)

Recovery Process	R_{API} (%)	Ethanol (% v/v)	Methanol (% v/v)	Water (%v/v)	API 1 (% HPLC)	Impurities (% HPLC)
Target composition	–	> 95	< 5	< 0.5	–	–
Feed solution (IMS)	–	95.9	3.7	0.4	–	–
Lab-scale (Duramem™150)	99.1	95.7	3.9	0.4	92.3	7.7

For the IPAc process stream (API 2) the selected solvent specification state that the recovered solvent must contain a minimum of 99% (by area GC) IPAc and no more than 0.87% (by weight) water. This specification was developed for solvent recovered through distillation, where only volatile components need to be considered, making GC a suitable method of analysis. However, as OSN separation is based primarily on steric differences, non-volatile components might also be present in the permeate. IPAc can be detected with HPLC which was used as an additional control of the OSN generated solvent, with the solvent specification extended to state that the recovered solvent must contain a minimum of 99% (by area GC and HPLC respectively) IPAc.

Lab-scale solvent recovery testing for the IPAc process stream (API 2) was carried out using Starmem™122 and Puramem™280 operated at 30 and 60 bar respectively. The purity of the OSN recovered solvent was compared to the distillate, with data indicating that both processes removed the majority of the API and impurities present in the mother liquor, with only trace amounts remaining in the recovered solvent (Figure 6.3 and Table 6.3). OSN recovered solvent from both Starmem™122 and Puramem™280 contained more than 99% (by area HPLC) IPAc, and was hence within the stated specification for HPLC. GC and Karl Fischer data further demonstrated that traces of methanol, IPA and water were consistent, and

within specification, for the distillate and OSN samples respectively, with the level of IPAc being above 99% (by area GC) for all samples (Table 6.4). Recovered solvent from both the distillation and OSN was hence within the stated solvent specification.

For the IPAc process stream (API 2) OSN solvent recovery was repeated at a pilot-scale to investigate consistency of membrane performance during scale-up. Puramem™280 was selected for operation based on suitable performance observed on a lab-scale (Figure 6.3), and as membrane can be supplied with documentation required for pharmaceutical manufacturing. Throughout pilot-scale operation the flux was observed to decrease from 66 to 32 L m^{-2} h^{-1}, which was within the expected range based on lab-scale testing. The observed decrease in flux was likely a result of increased concentration effects occurring throughout operation. The rejection of API 2, and the measured solvent composition, remained constant throughout operation and average values were calculated and used for comparison (Table 6.3 and Table 6.4). HPLC data indicate that the rejection of API 2 was 99.3% for the spiral-wound module, which was lower compared to value of 99.8% observed for flat sheet Puramem™280 membranes used on a lab-scale. For lab-scale operation the membrane discs used are inspected individually, and selectively cut to minimise the number of defects present. However, for pilot-scale operation membranes are pre-packed into modules and equivalent membrane selection is not possible. The membrane module could hence contain a larger number of defects per membrane area, potentially explaining the observed variation in membrane performance.

As a result of the decreased rejection a lower purity of the recovered IPAc solvent was measured for the pilot-scale, compared to the lab-scale run. The recovered solvent was still within specification for GC, but the purity with HPLC was 98.8% (by area HPLC) hence failing the specification on this criterion (Table 6.3 and Table 6.4). More detailed examination of the HPLC data demonstrated that 0.6% (by area HPLC) of the solutes present was API 2, and as the recovered solvent was intended for recycling into subsequent crystallisations, the API present in the solvent was not considered a concern. Excluding the API, the impurities present in the recovered solvent was limited to 0.6% (by area HPLC) and the recovered solvent was considered to be within specification.

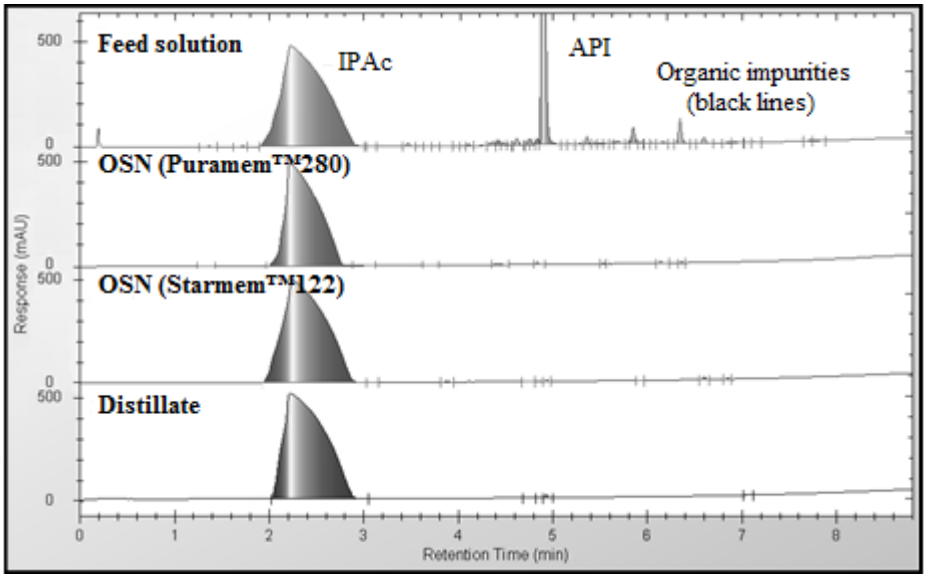

Figure 6.3. HPLC chromatograms of feed solution and recovered solvent from lab-scale OSN processing (dead-end filtration at 30 or 60 bar pressure and ambient temperature) and distillation (IPAc process stream)

Table 6.3. API 2 rejection, solvent composition and impurity content based on HPLC data for distillate and OSN permeate recovered from the IPAc process stream (lab-scale dead-end filtration at 30 or 60 bar pressure and ambient temperature, and pilot-scale operation using spiral-wound module operated at 60 bar pressure and ambient temperature)

Recovery Process	R_{API} (%)	IPAc (% HPLC)	Impurities (% HPLC)	API 2 (% HPLC)
Distillate (IPAc)	–	99.9	0.1	< 0.1
Lab-scale (Starmem™122)	99.9	99.7	0.3	< 0.1
Lab-scale (Puramem™280)	99.8	99.7	0.3	< 0.1
Pilot-scale[a] (Puramem™280)	99.3	98.8	0.6	0.6

[a]Based on average for 7×2.0 L fractions collected

Table 6.4. Solvent composition and impurity content based on GC and Karl Fischer analysis of distillate and OSN permeate recovered from IPAc process stream (API 2)

Recovery Process	IPAc (% GC)	Impurities (% GC)	Methanol (% GC)	IPA (% GC)	Water (% weight)
Distillate (IPAc)	99.9	< 0.1	0.03	0.005	0.18
Lab-scale (Starmem™122)	99.9	< 0.1	0.05	0.003	0.17
Lab-scale (Puramem™280)	99.9	< 0.1	0.04	0.002	0.14
Pilot-scale[a] (Puramem™280)	99.8	0.2	0.03	0.005	0.15

[a]Based on average for 7×2.0 L fractions collected

6.3.3 Solvent Recycling and Crystallisation (API 2 in IPAc process stream)

HPLC and GC data indicate that the OSN recovered solvent for the IPAc process stream was within specification. A slight increase in the level of organic impurities was however observed in the permeate compared to the distillate (Table 6.3). As the recovered solvent was intended for recycling into subsequent crystallisations, which in itself is a purification process, the increased impurity trace was not expected to be a concern. However, to fully investigate whether the purity of the OSN recovered IPAc was sufficient, crystallisation and solvent recycling was carried out for four subsequent crystallisation batches of API 2. The initial API batch was crystallised using fresh IPAc and was carried out as a reference, as well

as to generate material for OSN operation. OSN was then used to recover solvent (IPAc) from the collected mother liquor and solvent was recycled into the second crystallisation batch. Crystallisation and OSN solvent recovery was continued until four individual batches of API 2 had been completed. Solvent recycling should ideally be carried out on a pilot-scale however sufficient material was not available, limiting study to lab-scale operation. Additionally, as a result of limited material availability of API 1 solvent recycling and crystallisation was only carried out for API 2.

Selected specification for API 2, state that the crystallised material can contain maximum levels of 0.3% and 0.15% (by area HPLC) of impurities A and B respectively, while maintaining the total impurity trace below 1.0% (by area HPLC). HPLC data demonstrated that isolated API from all batches was within the stated specification, with yields remaining within the expected range (Table 6.5). Minor variations were observed in the impurity levels between batches, however there was no indication of a build-up of impurities resulting from the solvent recycling.

Table 6.5. Yield and impurity levels measured for crystallised API 2 from batches 1-4

Batch	Impurity A (% HPLC)	Impurity B (% HPLC)	Impurity total (% HPLC)	Within specification (-)	Yield[a] (%)
1 (Fresh solvent)	0.06	0.05	0.21	Yes	86.5
2 (1st OSN recycle)	0.08	0.05	0.49	Yes	87.3
3 (2nd OSN recycle)	0.03	0.06	0.33	Yes	87.6
4 (3rd OSN recycle)	0.03	0.04	0.27	Yes	87.5

[a]Expected value between 84-90% (based on % weight and represent the recovered API mass after removal of impurities and API losses during crystallisation, filtration and washing)

Recovered IPAc from each cycle was analysed with regards to the API 2 rejection and the solvent purity. HPLC, GC and Karl Fischer data indicate that the solvent composition and purity was similar for all three recovery cycles (Table 6.6 and Table 6.7). Consistent flux and

rejection data was further observed during the first and second solvent recovery stage, while a lower rejection (98.9% *cf.* 99.8%) and a higher flux was observed for the third recovery run. Fresh membrane discs were used for each solvent recovery test, and the decreased rejection in combination with the increased flux, could indicate damage to the membrane disc used, or a leak around the membrane seal. As the overall impurity concentration for the solvent recovered from the third cycle was consistent with solvent from the first and second run (only API 2 content was observed to be higher), the solvent was deemed of sufficient quality for recycling into subsequent crystallisations.

Table 6.6. Rejection of API 2, flux and solvent composition for OSN recovered solvent (test operated in dead-end using Puramem™280 at 60 bar pressure and ambient temperature) recycled into crystallisation batches 2-4 based on HPLC analysis (IPAc process stream)

Recovery Process	R_{API} (%)	Flux (L m^{-2} h^{-1})	IPAc (% HPLC)	Impurities (% HPLC)	API 2 (% HPLC)
OSN from batch 1	99.8	29–36	99.7	0.3	> 0.1
OSN from batch 2	99.8	28–38	99.4	0.3	0.3
OSN from batch 3	98.9	39–48	98.8	0.3	0.9

Table 6.7. Solvent composition of OSN recovered IPAc (test operated in dead-end using Puramem™280 at 60 bar pressure and ambient temperature) used for recycling into crystallisation batches 2-4 based on GC and Karl Fischer analysis (IPAc process stream)

Recovery Process	IPAc (% GC)	Impurities (% GC)	Methanol (% GC)	IPA (% GC)	Water (% weight)
OSN from batch 1	99.8	0.2	0.03	0.004	0.22
OSN from batch 2	99.8	0.2	0.06	0.003	0.22
OSN from batch 3	99.8	0.1	0.06	0.003	0.23

6.3.4 Energy Evaluation and Process Comparison

OSN is commonly mentioned as a more energy-efficient alternative to distillation, however little data has been presented in literature to support this statement for processing in organic solvents. As part of this solvent recovery study an energy evaluation was carried out based on batch distillation and a pump pressurised pilot-scale OSN system. The IPAc process stream (API 2) was selected as a model system for calculations.

Energy consumption for batch distillation was calculated based on evaporation from a vessel attached to an overhead condenser. The overall power consumption was calculated through summation of individual contributions required to heat the liquid to the boiling point, vaporise the solvent and re-condense in the overhead condenser. An ideal system was assumed for calculations, however for a non-ideal system heat losses to the surroundings should further be included resulting in the true power consumption most likely being higher compared to the calculated value. The power consumption was calculated according to Equation 6.1, where Q is the required power, F_M is the molar flow, Δc is the heat capacity at constant pressure, ΔT is the temperature difference between the feed and the boiling point and ΔH_{Vap} is the latent heat of vaporisation (Geens *et al.*, 2007).

$$Q_{Distillation} = Q_{Heating} + Q_{Vaporisation} + Q_{Condensation}$$
$$Q_{Heating} = F_M \Delta c \Delta T \qquad \text{Equation 6.1}$$
$$Q_{vaporisation} = Q_{Condensation} = F_M \Delta H_{Vap}$$

Based on the IPAc process stream, a 90% recovery level and an overall processing time of 2 hours was assumed for distillation solvent recovery from a 100 L batch. Assuming an ideal system with no heat losses to the surroundings, and a constant heat of vaporisation, the total power required for processing was calculated according to Equation 6.1 with F_M = 0.11 mol s^{-}

[1], Δc = 199.4 J mol^{-1} K^{-1}, ΔT = 64 K and ΔH_{Vap} = 37.2 kJ mol^{-1} giving a value of $Q_{\text{Distillation}}$ = 9.3 kW or 66.8 MJ for a 2.0 hour operating time (Haynes, 2012).

OSN on the other hand is a non-thermal technique, and the majority of power required for operation is consumed by a pump generating the required back-pressure to the system. An OSN system operated in a feed-and-bleed configuration was assumed for calculations, and the energy required for processing was calculated according to Equation 6.2, where F is the pump flow rate of the feed (*f*) and feed-and-bleed re-circulation (*fb*), η is the pump efficiency, and ΔP is the trans-membrane pressure (*TM*) and the pressure drop over the membrane module (*D*) respectively (Mulder, 1996f)(Geens *et al.*, 2007).

$$Q_{OSN} = \frac{F_f \Delta P_{TM}}{\eta} + \frac{F_{fb} \Delta P_D}{\eta} \qquad \text{Equation 6.2}$$

Using OSN for solvent recovery, the maximum recovery level is limited based on solubility and require that the concentration of all solutes remain above the solubility limit to prevent solutes from crashing out and damaging the membrane module. For the IPAc process stream, the maximum volume recovery was limited to 80%. To maintain equivalent processing time to the distillation, a membrane area of 1.0 m^2 was assumed for calculations, which combined with an average flux of 45 L m^{-2} h^{-1} equals a processing time of 1.8 hours for recovery of 80% from a 100 L batch. Based on the processing time, F_f was calculated as 56 L h^{-1} and F_{fb} was selected to 278 L h^{-1} (5×F_f). ΔP_D was assumed as 0.5 bar and η as 0.3, resulting in a total energy requirement of Q_{OSN} = 0.3 kW or 2.1 MJ for a 1.8 h operating time.

Based on equivalent processing times energy-calculations demonstrated that even when ideal conditions were assumed for the distillation, the overall energy consumption was significantly lower for OSN compared to distillation. However, for the solvent recovery studied in this chapter the maximum amount of solvent recovered by OSN was limited to 80%, whereas the distillation could be continued to a higher level of 90% recovery of the original volume. To enable comparison of data, the energy consumed by OSN and distillation respectively was expressed per unit of solvent recovered (Curzons *et al.*, 2001). Calculations indicate that the overall energy requirement was 25 times lower for OSN, at a value of 0.03 MJ per L recovered solvent, compared to 0.74 MJ per L recovered solvent for the distillation (Table 6.8). The volume of solvent recovered by OSN was however lower compared to distillation, resulting in a larger amount of waste remaining after recovery processing. In order to reach equivalent volume recovery of 90%, a combined approach was investigated using OSN to recover the initial 80% of the original solution added, and distillation to recover an additional 10% up to 90% total. The energy-consumption for combined processing was calculated as 0.08 MJ per L recovered solvent, *i.e.* a value which was still 9 times lower compared to distillation alone.

Table 6.8. Process evaluation summarising key results relating to energy efficiency

Parameter	No recovery	OSN	Distillation	Combination
Amount of solvent recovered (%)	0	80	90	90
Total energy required (MJ)	N/A	2.1	66.8	9.6
Energy required per L recovered solvent (MJ L^{-1})	N/A	0.03	0.74	0.08

Mentioned recovery levels of 80 and 90% for OSN and distillation respectively, refer to processing of the waste stream only. To fully evaluate the impact of the waste minimisation on process mass efficiency, the full crystallisation process including solvent recovery stages

must be considered. The E factor – defined as the total mass waste of a process divided by the mass of product produced – is a commonly used metric for mass efficiency (Sheldon, 2007). For an assumed crystallisation batch, generating a 100 L waste stream, the E factor was calculated to respective values of 9.7 when no solvent recovery was used, 4.8 for OSN processing with an 80% recovery, and 4.2 for distillation (or combined processing) with a 90% recovery (Table 6.9). Comparison of E factor values indicate that despite the difference in recovery levels achieved with OSN and distillation, the improvement in mass efficiency for the full process was similar, at 51% and 57% respectively, compared to when no solvent recovery was used.

As indicated by the higher E factor, variations in the recovery level for OSN and distillation will result in a higher quantity of waste remaining after OSN processing. Residual waste is disposed through incineration, and energy required for waste disposal should be included in the energy-evaluation. The energy for incineration can be calculated as the sum of the energy required to heat the waste to the boiling point, vaporise the waste stream and to heat enough air to ensure a sufficient supply of oxygen for full combustion. The energy released during combustion of the waste, must further be subtracted from the energy consumed to obtain the energy required or released during incineration.

Energy for incineration was calculated based on a 100 L batch, assuming recovery levels of 0%, 80% and 90%, for no solvent recovery, OSN and distillation respectively. To facilitate calculations the density (ρ = 0.87 g mL^{-1}), molecular weight (MW = 102.13 g mol^{-1}), boiling point (T_{bp} = 88.6 ^{o}C or 362 K), heat capacity (Δc = 199.4 J K^{-1} mol^{-1}), heat of vaporisation (ΔH_{Vap} = 32930 J mol^{-1}) and heat of combustion (ΔH_c^o = 2878000 J mol^{-1}) for the waste

liquor, were assumed equal to values for pure IPAc (Haynes, 2012). The mols of waste, was calculated based on the density and the molecular weight. Values were then used to calculate the energy required for heating and vaporising the waste, as well as the energy released during combustion, according to Equation 6.3, Equation 6.4 and Equation 6.5 (Table 6.9), assuming that the waste solution was initially at room temperature (T_{start} = 25 ^{o}C or 298 K).

$$E_{Heating} = n\Delta T\Delta c \qquad \text{Equation 6.3}$$

$$E_{Vap} = n\Delta H_{vap} \qquad \text{Equation 6.4}$$

$$E_{Combustion} = n\Delta H_{c}^{o} \qquad \text{Equation 6.5}$$

The molar quantity of oxygen required to enable full combustion, was calculated through balancing the combustion reaction. Assuming a 20% oxygen content in air, and a 75% burning efficiency of the incinerator, the required molar quantity of air could further be determined. EU directive 2000/76/EC states that non-chlorinated solvents must be incinerated at a minimum temperature of 850 ^{o}C, and the energy required to heat the air to that desired temperature (Table 6.9) was calculated based on Equation 6.3 assuming that the air was initially at room temperature, and using an average value of the heat capacity for air at 25 ^{o}C and 850 ^{o}C (Δc_{Air} = 1.074 J K^{-1} mol^{-1}) (EUR-Lex, 2000)(Haynes, 2012).

The energy required for heating the air, as well as heating and vaporising the waste stream, was combined with the energy released during combustion to determine the energy for incineration. Calculations indicate that the energy released during combustion of waste was significantly higher compared to the energy consumed (Table 6.9). Assuming that 75% of the energy released during incineration can be recovered for steam production, calculations indicate that 17.4 MJ of energy was released for each L IPAc waste incinerated.

Calculated net release of energy during incineration of IPAc waste indicates that from an energy-perspective, the most efficient alternative would be incineration of the full waste stream, with no application of solvent recovery. However, lack of waste minimisation result in a higher E factor for the process, as well as an increased cost for use of fresh solvent, and cannot be considered as a sustainable alternative. Additionally, if the solvent used for processing is a less efficient fuel, the energy released during incineration would be smaller or even negative. Incineration would then no longer be the most energy-efficient alternative.

Finally important to note is that though the energy required to manufacture the membranes is likely to be relatively low, the process generates waste water, which require an energy input for disposal and treatment. Currently membrane replacement is recommended after an interval of several years, and so the relative increase in energy consumption resulting from manufacturing of the membranes is likely to average out to a low value. For detailed studies of OSN energy efficiency the energy consumed for membrane manufacturing should however be included in calculations.

Table 6.9. Summary of key results with regards to mass efficiency and waste incineration

Parameter	No recovery	OSN	Distillation	Combination
Amount of solvent recovered (%)	0	80	90	90
E factor (-)	9.7	4.8	4.2	4.2
Number of mol waste (mol)	848	170	85	85
Energy required to heat waste (MJ)	10.8	2.2	1.1	1.1
Energy required to vaporise waste (MJ)	27.9	5.6	2.8	2.8
Energy required to heat air (MJ)	87.6	17.5	8.8	8.8
Energy released from combustion (MJ)	2440.9	488.2	244.1	244.1
Energy released from incineration (MJ)[a]	1736.0	347.2	173.6	173.6

[a]Assuming recovery of 75% of energy released during incineration

In addition to improvements in energy efficiency and waste reduction, capital investment and operating costs, as well as the calculated pay-back period for membrane equipment are important to consider. The process streams studied in this chapter are currently under development, and no details regarding costing or calculated savings can be published due to project confidentiality. However, it is important to note that equipment for distillation is readily available in most batch pharmaceutical plants, meaning that a strong business case would be needed to justify the initial investment cost required for OSN operation. Additionally, the membrane used for OSN is a consumable product, and though consistent performance and stability has been observed during long-term operation (Sereewatthanawut *et al.*, 2010), modules will have to be replaced on a regular basis. Module replacement will result in an increased investment, as well as maintenance cost, and must be considered when evaluating potential benefits to OSN application.

6.4 Conclusion

The work presented in this chapter demonstrates that OSN can be used to recovery high purity solvents from two different, concentrated, multi-component process mother-liquors. Energy-calculations further indicate that for the IPAc process stream studied, the required energy per L recovered solvent was 25 times lower when OSN was used compared to distillation. Calculations confirm the low energy-consumption of OSN, highlighting the technique as a promising alternative to distillation.

The maximum recovery level of OSN operation is limited by solubility of all solutes present in the process stream, resulting in the recovery level of OSN being potentially lower compared to distillation. Equivalent volume recovery can be obtained through combined use

of OSN and distillation, and for the IPAc process stream studied in this chapter the energy-requirement for combined processing was still 9 times lower compared to distillation alone.

In addition to being an energy-efficient alternative, OSN is a non-thermal technique and can offer benefits in situations where distillation is unsuitable. OSN separation is based mainly on steric differences, rather than volatilities, and can hence be used in situations where azeotrope formation is a problem, or when the desired feed composition is challenging to maintain with distillation (*e.g.* for solvent mixtures such as IMS). Additionally, the risk of yield losses occurring due to API degradation, or impurity generation resulting from unwanted side-reactions occurring in the concentrate, is much lower for non-thermal OSN operation compared to distillation, and OSN could offer a potential route for recovery of a second API crop from the waste stream.

Chapter 7: Predictions and Modelling of Membrane Performance in OSN

7.1 Introduction

Modelling of solvent and solute transport across a membrane, can be a useful tool to gain increased understanding of membrane separation processes. Accurate predictions of the rejection and flux could also minimise the extensive screening work required for membrane selection, hence greatly facilitating OSN application. A good predictive model should provide a quantitative method based on physical parameters. Additionally, some general assumptions regarding the system are often made to limit the complexity of the calculations, as well as broaden the model application range. The most suitable model should be simple enough to use, while still maintaining accurate predictions.

In the pharmaceutical industry, application of a transport model predicting membrane performance could potentially be used in process development, optimisation and scale-up. Predicting membrane performance is primarily of interest for solute rejection, as APIs are commonly expensive and have a limited availability during development. However, OSN application studies (Chapters 3, 4 and 5) demonstrate that even minor variations in rejection can result in a significant solute loss over the membrane. To enable direct membrane selection through use of transport models, rejection predictions must hence maintain a very high accuracy. For a lower accuracy prediction, modelling of solute transport would only provide a rough guideline for membrane selection, and though useful as an initial tool, a membrane screening must still be conducted. Conversely, flux values are directly related to the membrane area and though a high flux is desirable, it is not always required to enable OSN application in a pharmaceutical manufacturing environment. Flux predictions having a lower

accuracy could hence still be used for direct membrane selection. However, accurate flux data can easily be measured through a single low cost experiment, using fresh solvent or the intended feed solution, and any suggested model must maintain a low experimental burden to motivate model application.

Extensive work relating to modelling of membrane performance has been presented in the literature. Initial predictions were based on black-box models of irreversible thermodynamics, with little consideration given to the membrane structure or transport mechanism (Kedem and Katchalsky, 1958)(Spiegler and Kedem, 1966). Application of black-box models demonstrated some success (Perry and Linder, 1989)(Schrig and Widmer, 1992), however use was limited to simple systems and more detailed models accounting for the membrane structure and mode of transport were soon desired. Currently, two main model groups have been developed, assuming solution-diffusion (dense membranes) or pore-flow (porous membranes) transport respectively (Figure 7.1).

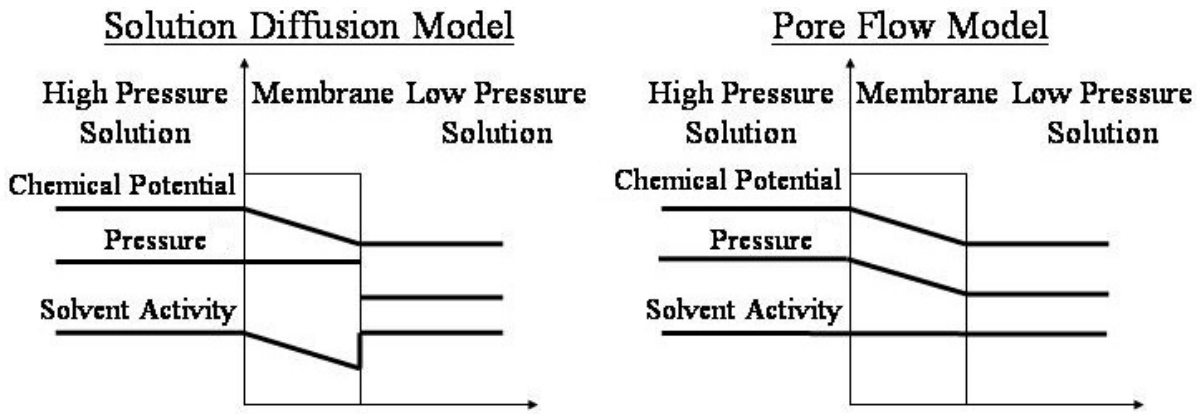

Figure 7.1. Graphic illustration comparing solution-diffusion and pore-flow models (Wijmans and Baker, 1995)

The solution-diffusion model assumes a homogeneous dense membrane structure, where solvents and solutes dissolve in the top-layer before being transported through the membrane through un-coupled diffusion. The concentration gradient over the membrane acts as the driving force, and separation is enabled based on differences in the dissolving power and rate of diffusion and permeability of the solvent and solutes (Wijmans and Baker, 1995). The pore-flow model, assumes a looser membrane structure with cylindrical pores evenly distributed throughout the membrane. Separation is based primarily on steric exclusion, with pressure-driven convective flow acting as the mode of transport through the membrane. The most fundamental pore-flow model available is the Maxwell-Stefan equation which predicts transport of solutes through pores, based on friction coefficients. However, friction coefficients are difficult to determine with high accuracy, and the Nernst-Planck equation is more commonly used as a simplified version for predicting solute transport (Bowen *et al.*, 1996)(Straatsma *et al.*, 2002). For solvent transport the Hagen-Poiseuille equation, relating the flux to the pressure driving force, has been suggested in literature as a suitable basis for flux predictions in NF membranes (Mulder, 1996e)(Bowen and Welfoot, 2002) (Robinson *et al.*, 2004)(Bowen and Welfoot, 2005)(Dijkstra *et al.*, 2006). However, the Hagen-Poiseuille equation was originally developed for application in looser UF membranes, and for NF application the increased drag forces resulting from transport through narrow pores must be considered. Additional parameters such as interactions with the membrane, molecular shape and system charge have also been demonstrated as influential for solvent and solute transport, and have been included during developments of the original pore-flow models (Matsuura and Sourirajan, 1981)(Deen, 1987)(Donnan, 1995).

Both the solution-diffusion and pore-flow models were initially developed for application in aqueous systems. The possibility to apply existing models to OSN has since been investigated experimentally (Silva *et al.*, 2005)(Geens *et al.*, 2006b), with studies demonstrating that solvent interactions have a significant influence on the membrane performance and should hence be included during modelling. Some of the more important factors influencing transport in OSN have been identified as the viscosity (a measure of solvent diffusivity); the molar volume (a measure of steric influences); the membrane surface tension (a measure of solvent-membrane interactions); and polarity effects (a measure of solvent-membrane interactions) (Machado *et al.*, 2000)(Bhanushali *et al.*, 2001)(Geens *et al.*, 2006a)(Darvishmanesh *et al.*, 2009). Based on inclusion of these mentioned parameters, a number of models aimed at predicting fluxes during OSN operation have been developed (Machado *et al.*, 2000)(Bhanushali *et al.*, 2001)(Geens *et al.*, 2006a)(Darvishmanesh *et al.*, 2009). Developed models have demonstrated accurate flux predictions for the solvent-membrane combinations used for model development, however prediction becomes more difficult for solvent mixtures or when models are applied to solvent-membrane combinations outside the original scope. A potential explanation for variations in model performance could be that the nanostructure of OSN membranes approaches the resolution limit of currently available characterisation techniques (*e g.* SEM and TEM). Despite extensive research, conclusive data confirming the membrane structure is still lacking and assumptions made during model development cannot be confirmed. Additionally, interactions between the membrane and organic solvents are believed to cause structural changes, resulting in the structure observed in a dry environment possibly changing during operation. Lack of conclusive data confirming the OSN membrane structures, in combination with less consistent performance being observed for OSN compared to aqueous membrane operation, potentially make the developed models less reliable. Inclusion of additional parameters to account for solvent influences further requires

more extensive characterisation work prior to model implementation. As a result current models for predicting OSN performance are lacking, highlighting model development as a desired area of research.

This chapter investigates the predictive power and experimental work required for application of a currently available OSN model, with the aim of highlighting desirable model developments for facilitating application in the pharmaceutical industry. A study was carried out investigating the performance of a recently developed model for the prediction of solvent permeation through OSN membranes (Darvishmanesh *et al.*, 2009). This model was selected for study, as it is based on a semi-empirical approach and has been developed to account for both diffusive and viscous flow through incorporation of the viscosity, surface tension and polarity. Semi-empirical model development is considered as a favourable approach due to the difficulties in describing the true membrane structure. Additionally, data presented by Darvishmanesh *et al.* (2009) indicate accurate permeability predictions for a wide range of solvents from various classes when using two different polymeric OSN membranes (SolSep 030505 and MPF-50). The accuracy and scope of the model suggested by Darvishmanesh *et al.* (2009) was investigated through extended application of the model to two additional OSN membranes (Starmem™122 and Duramem™200) not studied during model development.

The study presented in this chapter was limited to modelling of solvent fluxes, as accurate predictions of pure solvent fluxes is an important step to facilitate the development of a model capable of the more difficult task of predicting rejections.

7.2 Theory and Data

7.2.1 General Model for Prediction of OSN Solvent Permeation

The model selected for study is based on a semi-empirical approach for the prediction of solvent permeation through OSN membranes. The model assumes a parallel matrix of defined pores, separated by the membrane polymer (Figure 7.2), with transport occurring through a combination of viscous convective flow (through pores) and solution-diffusion (through the membrane matrix) (Darvishmanesh *et al.*, 2009).

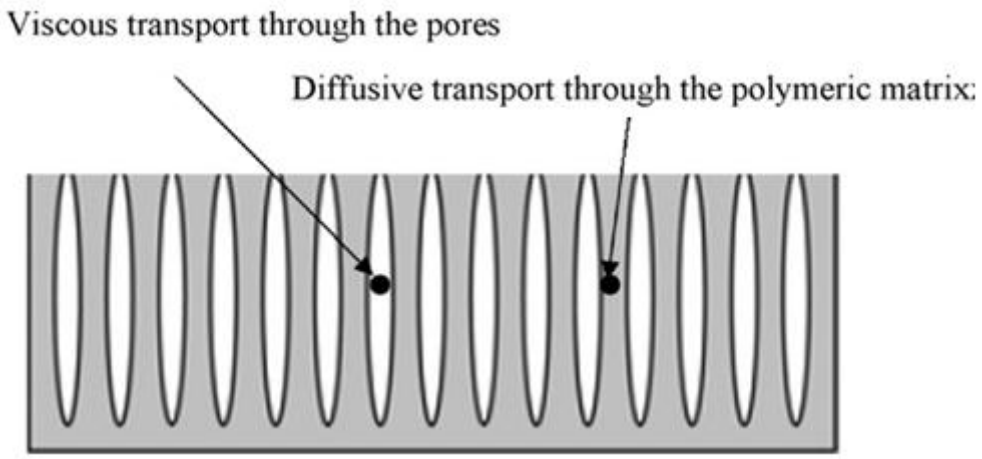

Figure 7.2. Assumed membrane structure and transport mechanism for suggested general model for prediction of solvent permeation (Darvishmanesh *et al.*, 2009)

This model was developed based on the solution-diffusion with imperfection (SDI) model. The SDI model partly accounts for solvent influences by including a viscosity dependence, assuming an inverse proportionality to the permeability (Mason and Lonsdale, 1990). Darvishmanesh *et al.* (2009) further modified the model to account for additional solvent influences, through inclusion of surface tensions and dielectric constants. To maintain mathematical integrity of the model both surface tensions and dielectric constants were

included as ratios, adjusted to account for the membrane being hydrophobic or hydrophilic respectively. For surface tensions the ratio was calculated between the membrane and the solvent, whereas for the dielectric constants water and hexane were selected as a comparative basis for hydrophilic and hydrophobic membranes respectively. Authors assume that solvent transport is occurring mainly through diffusion, and hence only included the dielectric effects in the diffusive part of the model (Darvishmanesh *et al*., 2009).

The suggested general model for prediction of solvent permeation is presented in Equation 7.1 where J is the solvent flux, a_0 and b_0 are the specific diffusivity and permeability values determined empirically based on experimental data, α is the ratio of the dielectric constants (ε) calculated according to Equation 7.2, β is the ratio of the surface tensions (γ) calculated according to Equation 7.3, μ is the viscosity, ΔP is the pressure and $\Delta\Pi$ is the osmotic pressure (assumed as zero for pure solvents) (Darvishmanesh *et al.*, 2009).

$$J = \frac{a_0 \alpha}{\mu^{1-\beta}}\left(\Delta P - \Delta\Pi\right) + \frac{b_0}{\mu^{1-\beta}}\Delta P \qquad \text{Equation 7.1}$$

$$\alpha_{Hydrophilic} = \frac{\varepsilon_{Solvent}}{\varepsilon_{Water}} \text{ or } \alpha_{Hydrophobic} = \frac{\varepsilon_{Hexane}}{\varepsilon_{Solvent}} \qquad \text{Equation 7.2}$$

$$\beta_{Hydrophilic} = \frac{\gamma_{Solvent}}{\gamma_{Membrane}} \text{ or } \beta_{Hydrophobic} = \frac{\gamma_{Membrane}}{\gamma_{Solvent}} \qquad \text{Equation 7.3}$$

The general model for the prediction of solvent permeation suggested by Darvishmanesh *et al.* (2009) offers a potential benefit compared to the previously developed OSN models (Table 7.1) in that transport through both solution-diffusion and pore-flow is accounted for. Additionally, the influence of the membrane and solvent surface tension are included as a ratio, rather than a differential, hence eliminating the risk of predicting an infinite flux when

the surface tension values are similar. In addition to the surface tensions Darvishmanesh *et al.* (2009) also include the dielectric constants as a ratio. However, for solvents displaying a ratio of one, where the solvent parameters are similar to the membrane or selected reference solvent, the model would be reduced to depend on a smaller number of variables. Additionally, no steric influence was included in the model, potentially limiting the accuracy of predictions for larger molecules. Finally, the viscosity, which is believed to be an influential variable in predicting solvent permeability, is included as an inverse dependence in-line with existing OSN models (Table 7.1). The viscosity figure is based on the bulk value however the value inside the membrane is likely to be higher due to increased drag forces. This has the potential to result in an over-prediction of the overall permeability (Bowen and Welfoot, 2002).

Table 7.1. Summary of previously developed OSN models for prediction of solvent permeation where ΔP is the pressure difference, J is the flux, λ is a solvent-membrane specific parameter, γ is the surface tension, f is a solvent independent parameters used to characterise the membrane NF (*1*) and UF (*2*) sub-layers, μ is the viscosity, V_m is the molar volume, Φ is a sorption value used as a measure of membrane-solvent interaction and n is a constant

Model	Model Limitations
$J \propto \frac{\Delta P}{\lambda\left[\left(\gamma_{membrane}-\gamma_{solvent}\right)+f_1\mu\right]+f_2\mu}$ [a]	Assumes transport through pore-flow only $\Delta\gamma$ could be zero predicting an infinite J
$J \propto \left(\frac{V_M}{\mu}\right)\left(\frac{1}{\phi^n\gamma_{solvent}}\right)$ [b]	Assumes transport through solution-diffusion only J decrease for an increased solvent-membrane affinity J increase for an increased solvent size (V_m) Sorption value (ϕ) is difficult to measure
$J \propto \left(\frac{V_M}{\mu\left(\gamma_{membrane}-\gamma_{solvent}\right)}\right)$ [c]	$\Delta\gamma$ could be zero predicting an infinite J J increase for an increased solvent size (V_m)

[a]Machado *et al.*, 2000

[b]Bhanushali *et al.*, 2001

[c]Geens *et al.*, 2006a

7.2.2 Investigation of General Model for Prediction of Solvent Permeation

Darvishmanesh *et al.* (2009) presented model predictions for solvent permeation through two polymeric OSN membranes (SolSep 030505 and MPF-50) and one ceramic membrane (HITK 275). As polymeric membranes are the primary focus of this thesis, data presented for SolSep 030505 and MPF-50 were selected for further study.

For SolSep 030505 model predictions were based on permeation of a homologous series of six primary alcohols, whereas model application for MPF-50 was based on permeation of seven organic solvents from different classes. Graphic illustration of presented data indicated that the model provided similar predictions of the permeability compared to experimental values (Figure 7.3), and the error variance was reported to be within 0.5-5.0%. Prior to model application specific diffusivity and permeability values (a_0 and b_0) were determined using an error minimisation between the experimentally measured and modelled flux values.

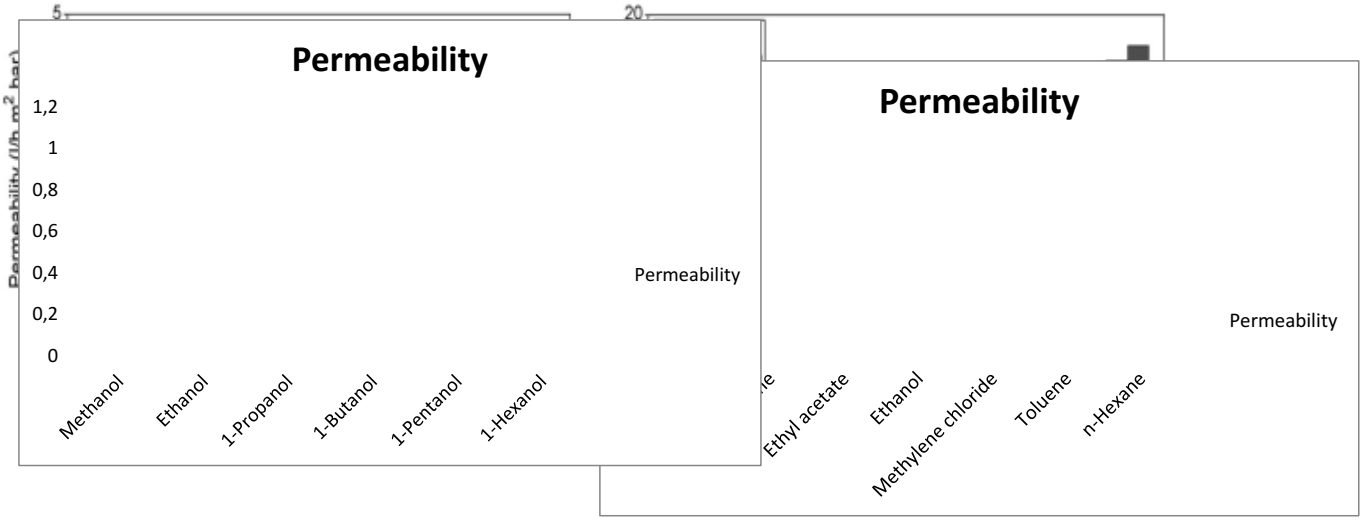

Figure 7.3. Summary of experimental and modelled solvent permeability values presented by Darvishmanesh *et al.*, 2009 for six primary alcohols through SolSep 030505 (*left*) and seven solvents from various classes for MPF-50 (*right*) using suggested general model for prediction of solvent permeation

It is important to note that during model development Darvishmanesh *et al.* (2009) used experimental flux data for all solvent tested to determine a_0 and b_0, and no prediction of solvent fluxes was hence demonstrated for the presented model. If flux measurements for multiple solvents have to be used to enable model application, the experimental burden of the model becomes high compared to direct flux measurements, as modelling also requires the membrane surface tension to be determined. The experimental work required for model application could be minimised, if the characterisation data needed (*i.e.* flux values for a range of solvents and membrane surface tension) could be obtained from literature. To facilitating model application it is hence highly desirable that additional data, based on standardised characterisation techniques, is supplied by membrane manufacturers.

Darvishmanesh *et al.* (2009) presented experimental and modelled data as permeability values (L m^{-2} h^{-1} bar^{-1}), and though this is a relevant measure of membrane performance, the absolute flux value (L m^{-2} h^{-1}) is more commonly discussed during industrial OSN implementation. Absolute flux values were calculated based on the presented permeability and an operating pressure of 10 bar, before re-evaluating the deviations between the modelled and experimental data. For SolSep 030505, where solvents from the same family were used to determine a_0 and b_0, the modelled fluxes differed from the experimental values by 1-7 L m^{-2} h^{-1}, corresponding to a relative deviation of 4-24% (Table 7.2). Comparison of experimental and modelled data hence indicate that though the difference in absolute flux appears low, the percentage deviation for a low flux solvent could still be significant. Equivalent comparison of absolute flux values were carried out for MPF-50, where seven solvents from different classes were used to determine a_0 and b_0. Similar to SolSep 030505, some differences in the absolute flux, ranging between 4-22 L m^{-2} h^{-1}, were observed for MPF-50 (Table 7.2). Variations between the experimental and modelled fluxes corresponded to percentage deviations between 7-51%,

again highlighting that though the difference in absolute flux appear small, the relative difference can be significant and care must be taken before relying on the modelled values. Additionally, larger deviations in the modelled flux were observed when solvents from different families were used to determine a_0 and b_0, indicating a lack of consistency in model predictions for various solvents.

Table 7.2. Absolute values of experimental and modelled solvent fluxes of SolSep 030505 and MPF-50 operated at 10 bar presented by Darvishmanesh *et al.*, 2009

Solvent	Membrane	Experimental Flux ($L\ m^{-2}\ h^{-1}$)	Model Flux[a] ($L\ m^{-2}\ h^{-1}$)	Flux Deviation (%)
Methanol	SolSep 030505	45	43	4
Ethanol	SolSep 030505	29	36	-24[b]
1-Propanol	SolSep 030505	26	25	4
1-Butanol	SolSep 030505	22	19	14
1-Pentanol	SolSep 030505	19	15	21
1-Hexanol	SolSep 030505	17	13	24
Methanol	MPF-50	25	30	-20[b]
Acetone	MPF-50	62	50	19
Ethyl acetate	MPF-50	55	60	-9[b]
Ethanol	MPF-50	10	15	-50[b]
Methylene chloride	MPF-50	54	50	7
Toluene	MPF-50	43	65	-51[b]
n-Hexane	MPF-50	182	170	7

[a]Based on data in Figure 7.3 (Figure 4 and Figure 5 in Darvishmanesh *et al.*, 2009)
[b]Modelled flux is higher compared to experimental value (negative deviation)

7.3 Materials and Methods

7.3.1 Membrane and Solvent Selection

Commercially available membranes Starmem™122 (not cross-linked) and Duramem™200 (cross-linked) were selected for testing. Both membranes have a MWCO of approximately 200 g mol^{-1}, hence representing some of the tightest OSN membranes currently available.

Solvents selected for modelling were based on previous testing of MPF-50, which included methanol, ethyl acetate, toluene, acetone, ethanol, methylene chloride and n-hexane (Darvishmanesh *et al.*, 2009). Use of chlorinated solvents and n-hexane is however not recommended for the Duramem™ series, and acetonitrile, IPA, and MEK were instead included for testing. All solvents used were of HPLC grade.

7.3.2 Contact Angle Measurements and Membrane Surface Tension

Contact angle measurements were carried out for Starmem™122 and Duramem™200 using methanol, ethyl acetate, toluene and water. Testing was conducted using a sessile drop goniometer with circle drop fitting, and ten repeat samples were performed for each solvent-membrane combination. The surface tension of each membrane was automatically calculated during the measurements, using a pre-set computer model based on the Owen-Wendt-Kaelble-Rabel equation (Kwok and Neumann, 1999)(DataPhysics Instruments GmbH, 2012). Membrane surface tensions were calculated using contact angle measurements for water and methanol only, as well as a combination of all solvents tested.

Membrane samples used for contact angle measurements were prepared by permeation of 0.2 L methanol in a dead-end filtration cell at 30 bar pressure and ambient temperature (25-30 ^{o}C). Membranes were then removed from the filtration cell and dried in an oven at 40 ^{o}C for 24 h prior to contact angle analysis. Flushing of membrane discs was carried out to remove preservatives added by the membrane manufacturer.

7.3.3 Membrane Pre-conditioning and Pure Solvent Flux Measurements

Pure solvent fluxes were measured in a dead-end filtration system (Evonik MET Ltd.) operated at 30 bar pressure and ambient temperature (25-28 ^{o}C). Membrane discs were washed by permeation of 0.2 L methanol at the desired operating pressure, prior to pre-conditioning through permeate re-circulation for 1.0 hour, or until a stable flux was reached. To monitor progress towards equilibrium, the flux was measured every 20 minutes throughout the pre-conditioning. When a stable flux was reached, the system was depressurised, drained and rinsed with the next solvent selected for testing, prior to addition of 0.2 L solvent. The system was then re-pressurised to 30 bar and the initial 20 mL permeate was removed as waste, before repeating the pre-conditioning. Solvents tested were divided into two groups with fluxes measured using the same membrane disc during one day of operation (Membrane disc 1: methanol, ethyl acetate, toluene, ethanol and Membrane disc 2: acetone, acetonitrile, IPA, MEK). To ensure consistent performance of the membrane disc, control measurements of the pure methanol flux were periodically carried out between flux measurements for the additional solvents tested. Measured methanol fluxes were further used to normalise the fluxes measured for all additional solvents tested.

7.3.4 Flux Predictions Using General Model for Solvent Permeation

The general model for prediction of solvent permeation (Equation 7.1) was solved using an Excel spread-sheet. Required values for the solvent viscosities, surface tensions and dielectric constants were collected from literature (Table 7.3), whereas the membrane surface tension was determined experimentally based on contact angles (Section 7.4.1). The pressure was set to the operating pressure and the osmotic pressure was assumed negligible as pure solvents were used for testing. Values of the specific diffusivity and permeability (a_0 and b_0) were

determined based on a least square-error minimisation, between the experimentally measured and predicted solvent fluxes respectively. Excel add-in Solver was used for error-minimisation, using default conditions for calculations.

Table 7.3. Summary of viscosities, surface tensions and dielectric constants for the pure solvents selected for testing (Darvishmanesh *et al.*, 2009)(Haynes, 2012)

Solvent	Viscosity (mPa s)	Surface tension (mN m^{-1})	Dielectric constant (-)
Methanol	0.54	22.12	33.0
Ethyl acetate	0.42	23.24	6.0
Toluene	0.55	27.92	2.4
Acetone	0.34	23.30	20.7
Acetonitrile	0.34	28.66	35.7
Ethanol	1.08	21.99	24.9
IPA	2.04	20.93	20.2
MEK	0.39	23.96	18.2

7.4 Results and Discussion

7.4.1 Contact Angle Measurements and Membrane Surface Tension

Prior to application of the general model for prediction of solvent permeation discussed in this chapter, the membrane surface tension must be determined. The surface tension cannot be measured directly, and was calculated based on contact angle measurements using the Owen-Wendt-Kaelble-Rabel equation (Kwok and Neumann, 1999)(DataPhysics Instruments GmbH, 2012). The equation contains two unknown parameters (dispersive and polar component), and contact angles from a minimum of two solvents are hence required for determination of the surface tension. As the surface tension of a given membrane is constant, any two solvents can be used for calculations, provided that accurate contact angles can be obtained for the selected solvents. Additionally, data for more than two solvents can be included to further increase the accuracy of the calculation.

The resolution limit for accurate contact angle measurements is set to 10^{o}, in combination with a standard deviation below 5^{o}. To maintain consistency of testing, three organic solvents commonly used for OSN operation (methanol, ethyl acetate and toluene) were selected for testing. Additionally, as the selected membranes are known to be hydrophobic, water measurements were included to obtain data well spread in the measurable interval. Measured contact angles indicate that all organic solvents tested had a high affinity for the membrane, resulting in low average contact angles between 6.9-12.2^{o} for Starmem™122 and 6.4-10.8^{o} for Duramem™200 (Table 7.4). Measured contact angles for the organic solvents were hence close to the resolution limit, and though the standard deviation remained within the allowed interval for all solvent-membrane combinations tested, measurements of ethyl acetate with Starmem™122, and toluene with Starmem™122 and Duramem™200, failed specification as the measured contact angle was below the resolution limit. Contact angles for water, were high at 77.5^{o} and 72.9^{o} for Starmem™122 and Duramem™200 respectively, while maintaining the standard deviation below 5^{o} (Table 7.4). Contact angles for water were hence within specification, and could be combined with data for organic solvents to calculate the membrane surface tension.

As contact angles measured for ethyl acetate (Starmem™122) and toluene (Starmem™122 and Duramem™200) failed specification, surface tension calculations were limited to combinations of data for water and methanol only, as well as a combination of all solvents tested. Calculations of the surface tension demonstrated similar values when water and methanol only were used compared to a combination of data from all solvents tested (26.8 ± 1.6 *cf.* 27.6 ± 0.8 for Starmem™122 and 30.5 ± 1.1 *cf.* 29.9 ± 0.3 for Duramem™200), and values based on all four solvents was used for further model application (Table 7.4). Calculations additionally demonstrated that the surface tensions of Starmem™122 and

Duramem™200 were similar in value, which is expected as the membranes are made of a similar primary material (polyimide). The slightly higher surface tension observed for Duramem™200 could further be a result of the materials added during cross-linking of the membrane.

Table 7.4. Average contact angles and standard deviations measured for Starmem™122 and Duramem™200, using methanol, ethyl acetate, toluene and water, as well as calculated surface tensions for a combination of water-methanol and all solvents tested respectively

Parameter	Starmem™122	Duramem™200
Contact angle (methanol)	12.2 ± 3.9	10.5 ± 2.9
Contact angle (ethyl acetate)	6.9 ± 1.8	10.8 ± 4.0
Contact angle (toluene)	8.9 ± 2.4	6.4 ± 1.8
Contact angle (water)	77.5 ± 4.8	72.9 ± 2.7
Surface tension (methanol-water)	26.8 ± 1.6	30.5 ± 1.1
Surface tension (all solvents)	27.6 ± 0.8	29.9 ± 0.3

7.4.2 Pure Solvent Flux Measurements

In addition to the membrane surface tension, a range of solvent fluxes must be measured prior to model application to enable parameter fitting of a_0 and b_0 values. To investigate the application span of the model, solvents from different families were selected for parameter fitting and model application. When possible, selected solvents were kept consistent with previous testing by Darvishmanesh *et al.* (2009) (Section 7.3.1), however the pressure was increased to 30 bar to reflect the more common operating pressures used for Starmem™122 and Duramem™200. As expected the measured solvent fluxes were observed to vary significantly for the different solvents-membrane combinations tested, ranging between 26-194 L m^{-2} h^{-1} for Starmem™122 and 5-164 L m^{-2} h^{-1} for Duramem™200. Significant differences in fluxes for the same solvent, was further observed for the two membranes respectively (Table 7.5).

Table 7.5. Pure solvent fluxes measured for Starmem™122 and Duramem™200 (test was operated in cross-flow at 30 bar pressure and ambient temperature), and used to determine a_0 and b_0 as well as for model application and comparison

Solvent	Flux Starmem™122 (L m^{-2} h^{-1})	Flux Duramem™200 (L m^{-2} h^{-1})
Methanol	194	86
Ethyl acetate	122	38
Toluene	45	5
Acetone	191	164
Acetonitrile	177	98
Ethanol	84	50
IPA	26	12
MEK	148	53

7.4.3 Permeability Predictions for Starmem™122 and Duramem™200

Determined surface tension data and measured solvent fluxes, were used for application of the general model for prediction of solvent permeation, to Starmem™122 and Duramem™200. Model application was initially carried out using all solvents tested for determination of a_0 and b_0 to mimic protocol used by Darvishmanesh *et al.* (2009), and investigate the accuracy of model predictions for a larger range of commercially available membranes.

Comparison of experimental and modelled data for Starmem™122 operated at 30 bar, using all solvents tested to determine a_0 and b_0, indicated a reasonable prediction of the permeability with deviations ranging between 0.1-0.6 L m^{-2} h^{-1} bar^{-1} for all solvents except methanol with a deviation of 1.7 L m^{-2} h^{-1} bar^{-1}, and MEK with a deviation of 1.0 L m^{-2} h^{-1} bar^{-1} (Figure 7.4). MEK was not one of the solvents included during development of the model, which could potentially explain the high deviation observed. However, MEK values of viscosity, surface tension and dielectric constant (polarity) are within a similar range to the other solvents tested and no direct explanation for the higher deviation can be found. Methanol has a high

dielectric constant (33.0 *cf.* 2.4-24.9) compared to the other solvent included for study, which could potentially explain the poor model prediction. However, the dielectric constant of acetonitrile is higher compared to methanol (35.7 *cf.* 33.0). Despite this a good model prediction is obtained for acetonitrile indicating that the dielectric constant alone is not sufficient to explain the high model deviation observed for methanol. In general the observed variations between the experimental and modelled permeability were within the same range as data presented for SolSep 030505 and MPF-50, indicating consistent model performance for Starmem™122.

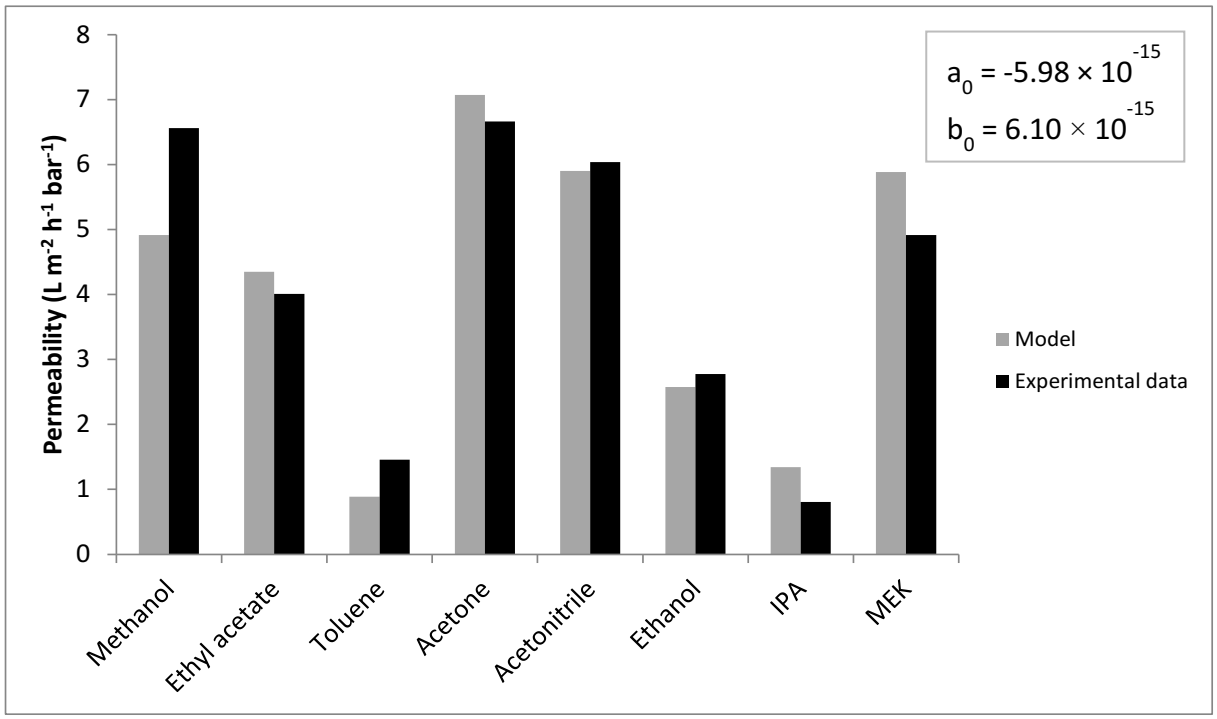

Figure 7.4. Experimental and modelled values of pure solvent permeability through Starmem™122 operated in cross-flow at 30 bar pressure and ambient temperature, using a_0 and b_0 values based on all solvents tested

In addition to the permeability, absolute flux values were compared to investigate the influence of pressure on the suggested model. Modelled flux values for the solvents tested were observed to deviate from the experimental values by 4-49 L m^{-2} h^{-1}, corresponding to a relative difference of 2-65% (Table 7.6). Observed differences were larger compared to data presented by Darvishmanesh *et al.* (2009), which could potentially be a result of the higher pressure (30 bar *cf.* 10 bar) used for flux measurements in this study. The applied model assumes linear scaling between the pressure and the flux, and though this assumption has been observed to hold true for a range of solvent-membrane combinations, the increase in flux is commonly observed to plateau at higher pressures (Section 2.4.1). If the suggested model is applied to a solvent-membrane combination demonstrating such behaviour, the assumption of linear scaling will not hold true, hence resulting in an over-prediction of the flux.

Data presented for Starmem™122 indicate that sufficient flux predictions were obtained for ethyl acetate; acetone; acetonitrile; and ethanol; whereas the relative deviation between the experimental and modelled fluxes for all additional solvents tested were large, ranging between 25-65% (Table 7.6). Significant variations in the accuracy of model predictions for various solvents - even when all solvents tested were used to determine a_0 and b_0 - indicate an inconsistency in the model performance and care must be taken before relying on modelled values.

Table 7.6. Experimental and modelled solvent fluxes with calculated deviations for Starmem™122 operated in cross-flow at 30 bar pressure and ambient temperature, using all solvents tested to determine a_0 and b_0

Solvent	Experimental Flux ($L\ m^{-2}\ h^{-1}$)	Model Flux ($L\ m^{-2}\ h^{-1}$)	Flux Deviation (%)
Methanol	194	145	25
Ethyl acetate	122	132	-8[a]
Toluene	45	28	38
Acetone	191	203	-6[a]
Acetonitrile	177	173	2
Ethanol	84	78	7
IPA	26	43	-65[a]
MEK	148	177	-20[a]

[a]Modelled flux is higher compared to experimental value (negative deviation)

Model application was repeated for Duramem™200 operated at 30 bar, using all solvents tested to determine a_0 and b_0. Similar to Stramem™122, permeability values were close to the experimental data with deviations ranging between 0-0.6 L m^{-2} h^{-1} bar^{-1} for all solvents tested except acetonitrile and MEK with respective deviations of 2.6 and 1.1 L m^{-2} h^{-1} bar^{-1} (Figure 7.5). Consistent with testing of Starmem™122, deviations observed for MEK and acetonitrile could potentially be explained with MEK not being included during model development and the high dielectric constant of acetonitrile. Such explanations are however not sufficient to explain the large deviations in permeability observed for acetonitrile and MEK, highlighting a lack of model consistency. This raises an important concern regarding the model suitability to describe and predict solvent permeation for any given membrane-solvent combination. Reasonable predictions were however observed for the majority of the solvents tested indicating that the suggested model has some potential in predicting solvent permeation.

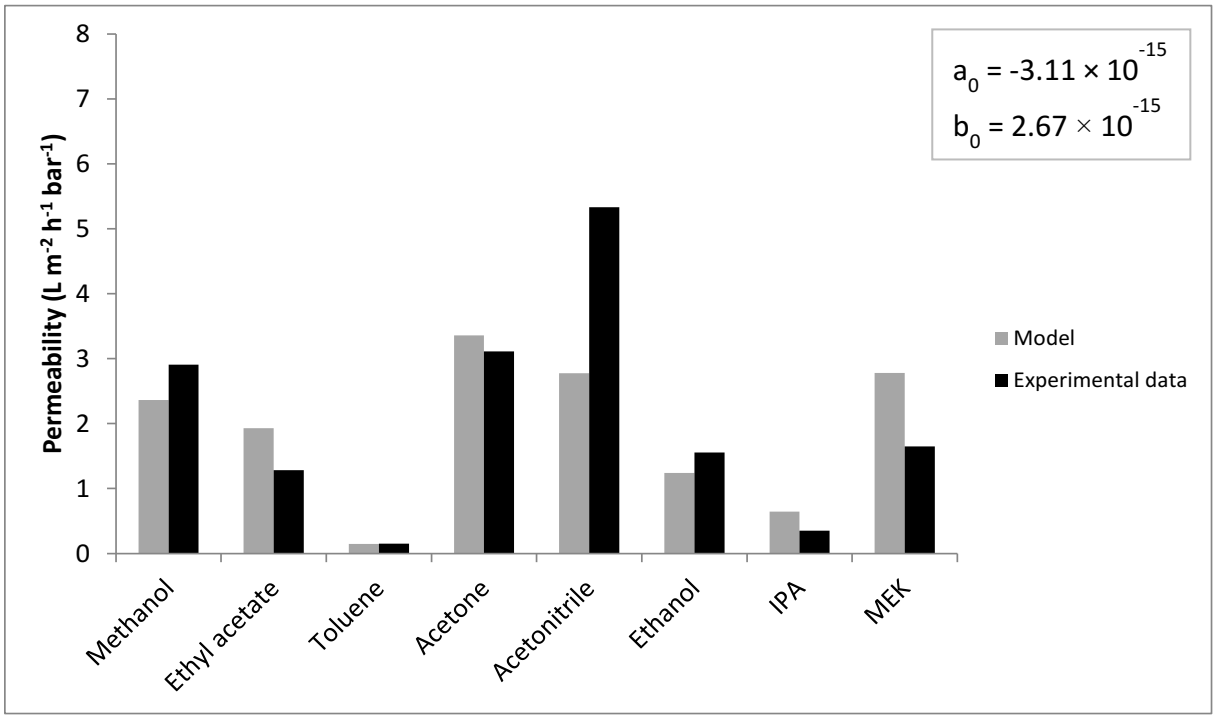

Figure 7.5. Experimental and modelled values of pure solvent permeability through Duramem™200 operated in cross-flow at 30 bar pressure and ambient temperature, using a_0 and b_0 values based on all solvents tested

In addition to permeability values, the fluxes obtained for Duramem™200 operated at 30 bar were studied. Data indicate that experimental and modelled fluxes differ by 0-79 L m^{-2} h^{-1}, corresponding to a relative deviation of 0-83% (Table 7.7). Significant variations observed between the experimental and modelled fluxes for Duramem™200 are consistent with observations made for Starmem™122. Observed differences in flux are again believed to be partly a result of the increased pressure used during operation of Duramem™200. Though accurate predictions of the solvent permeation were observed for some solvents using both Starmem™122 and Duramem™200, observed deviations for additional solvents tested were significant, and model predictions lacked consistency indicating that the predictive power of the model is not sufficient for direct application in membrane selection. The suggested model

could however still offer benefits in predicting general trends in flux variations based on differences in viscosity, surface tension and polarity.

Table 7.7. Experimental and modelled solvent fluxes with calculated deviations for Duramem™200 operated in cross-flow at 30 bar pressure and ambient temperature, using all solvents tested to determine a_0 and b_0

Solvent	Experimental Flux ($L\ m^{-2}\ h^{-1}$)	Model Flux ($L\ m^{-2}\ h^{-1}$)	Flux Deviation (%)
Methanol	86	70	19
Ethyl acetate	38	57	-50[a]
Toluene	5	5	0
Acetone	98	106	-8[a]
Acetonitrile	164	85	48
Ethanol	50	40	20
IPA	12	22	-83[a]
MEK	53	89	-68[a]

[a]Modelled flux is higher compared to experimental value (negative deviation)

7.4.4 Application of General Model for Prediction of Solvent Permeation Based on Parameter Fitting from a Limited Number of Solvents

In addition to model implementation using all solvents tested to determine a_0 and b_0, predictions of solvent permeation was attempted through use of three solvents only (methanol, ethyl acetate and toluene) to determine a_0 and b_0. If a_0 and b_0 values - obtained from a limited number of solvents - could be used to accurately predict fluxes of additional solvents, the suggested model could be used as a general platform for flux predictions while maintaining characterisation work to a minimum. The aim of this test was hence to investigate the true predictive power of the suggested model for prediction of solvent permeation.

To minimise the experimental work required prior to modelling, it is desirable to use data presented by the manufacturer, or in literature, to enable model application. Methanol, ethyl

acetate and toluene were hence selected for use as solvents have been studied extensively for OSN application. Predictions of solvent permeation were initially carried out for Starmem™122 operated at 30 bar. Data indicated that when three solvents only were used to determine a_0 and b_0, the modelled permeability differed from the experimental values by 0.4-1.8 L m^{-2} h^{-1} bar^{-1} (Figure 7.6). Observed deviations were in a similar range compared to when all solvents tested were used to determine a_0 and b_0, however differences for individual solvents were generally higher, indicating a larger inaccuracy of predictions when fewer solvents were used for characterisation.

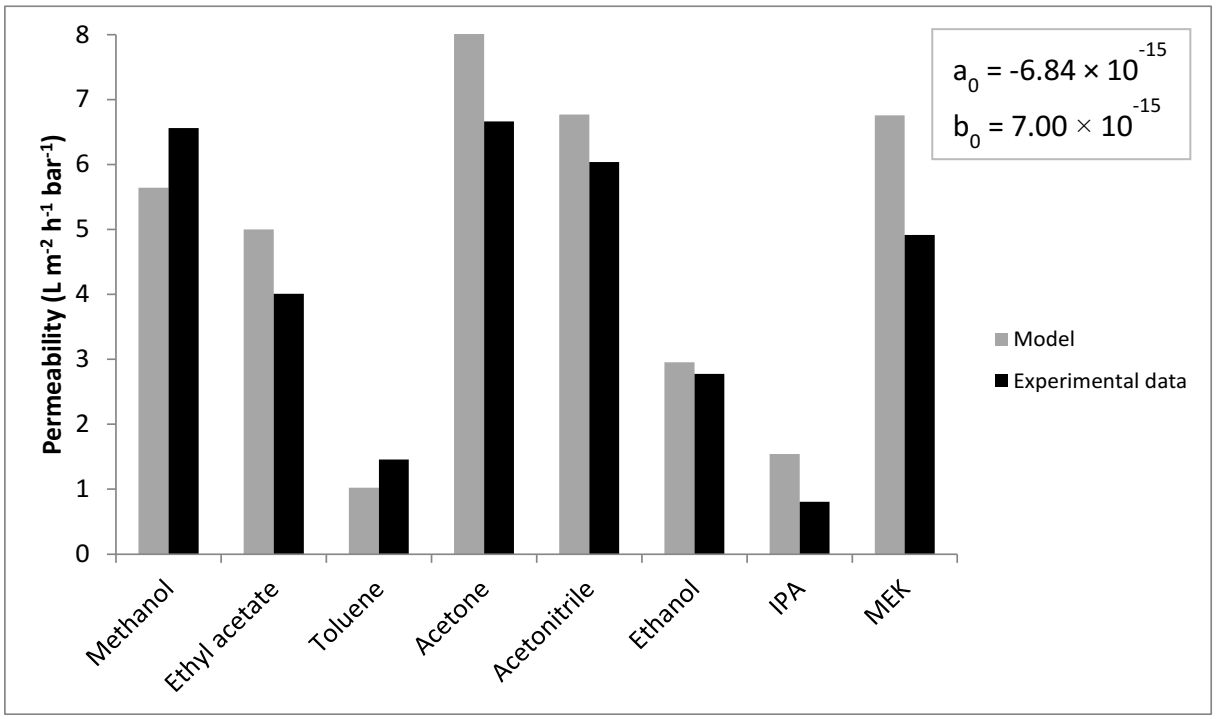

Figure 7.6. Experimental and modelled values of pure solvent permeability through Starmem™122 operated in cross-flow at 30 bar pressure and ambient temperature, using a_0 and b_0 values based on methanol, ethyl acetate and toluene only

In addition to permeability, the experimental and modelled flux values for Starmem™122 were compared for data predicted using three solvents only to determine a_0 and b_0.

Comparison demonstrated that the modelled fluxes differed from the experimental values by 5-56 L m^{-2} h^{-1}, corresponding to a relative deviation of 6-88% (Table 7.8). Though reasonable flux predictions were made for ethanol and acetonitrile, the model was not consistent for all solvents tested, and could not be considered reliable. The predictive power of the suggested model was hence concluded as insufficient for prediction of fluxes for the membrane-solvent combinations studied in this chapter.

Table 7.8. Experimental and modelled solvent fluxes with calculated deviations for Starmem™122 operated in cross-flow at 30 bar pressure and ambient temperature, using methanol, ethyl acetate and toluene to determine a_0 and b_0

Solvent	Experimental Flux (L m^{-2} h^{-1})	Model Flux (L m^{-2} h^{-1})	Flux Deviation (%)
Methanol	194	166	14
Ethyl acetate	122	152	-25[a]
Toluene	45	32	29
Acetone	191	233	-22[a]
Acetonitrile	177	198	-12[a]
Ethanol	84	89	-6[a]
IPA	26	49	-88[a]
MEK	148	204	-38[a]

[a]Modelled flux is higher compared to experimental value (negative deviation)

Additional testing was carried out using various solvent combinations to determine a_0 and b_0, with subsequent prediction of solvent permeation for additional solvents. Though sufficient predictions were always observed for some of the solvents included for testing, modelled data was not consistent and no general improvement in the predictive power was observed for a given solvent combination. Model predictions were further carried out for Duramem™200 operated at 30 bar, using methanol, ethyl acetate and toluene only to determine a_0 and b_0. However, error minimisation resulted in similar values compared to when all solvents were used for parameter characterisation, and as significant relative flux deviations were observed

for Duramem™200, the model predictive power was considered insufficient and model application limited to descriptions of trends only.

7.4.5 Comparison of Solvent Permeability Predictions

To evaluate the performance of the suggested model for prediction of solvent permeation a comparison of observed deviations between the modelled and experimental permeabilities was carried out. Comparison was based on the minimum and maximum deviation observed by Darvishmanesh *et al.* (2009) during model development (SolSep 030505 and MPF-50), during application to additional OSN membranes investigated in this chapter (Starmem™122 and Duramem™200) and during investigation of model performance based on three solvents only for parameter fitting (Starmem™122 (three solvents)) (Figure 7.7). Comparison of model performance indicate that the most accurate predictions were obtained for SolSep 030505 with the minimum and maximum deviation ranging between 0.1 and 0.7 L m^{-2} h^{-1} bar^{-1}. Model application for SolSep 030505 was based on parameter fitting using only solvents from the same class (alcohols), and the consistency of the solvents used for testing could potentially explain the higher accuracy observed. For MPF-50, Starmem™122 and Duramem™200 similar deviations ranging between 1.5-2.6 L m^{-2} h^{-1} bar^{-1} were observed indicating consistent performance when the model was extended to additional OSN membranes. However, for MPF-50, Starmem™122 and Duramem™200 the observed deviations between the modelled and experimental data were relatively large indicating that the overall predictive performance of the suggested model may be limited. Finally comparing the deviations between modelled and experimental data for Starmem™122 when three solvents and all solvents were used for parameter fitting respectively, similar overall deviations were observed indicating consistent model performance. Further study of the data

does however demonstrate that when three solvents only were used for parameter fitting larger individual deviations were observed for the various solvents tested, indicating a decreased accuracy of model predictions when less solvents were used for parameter fitting.

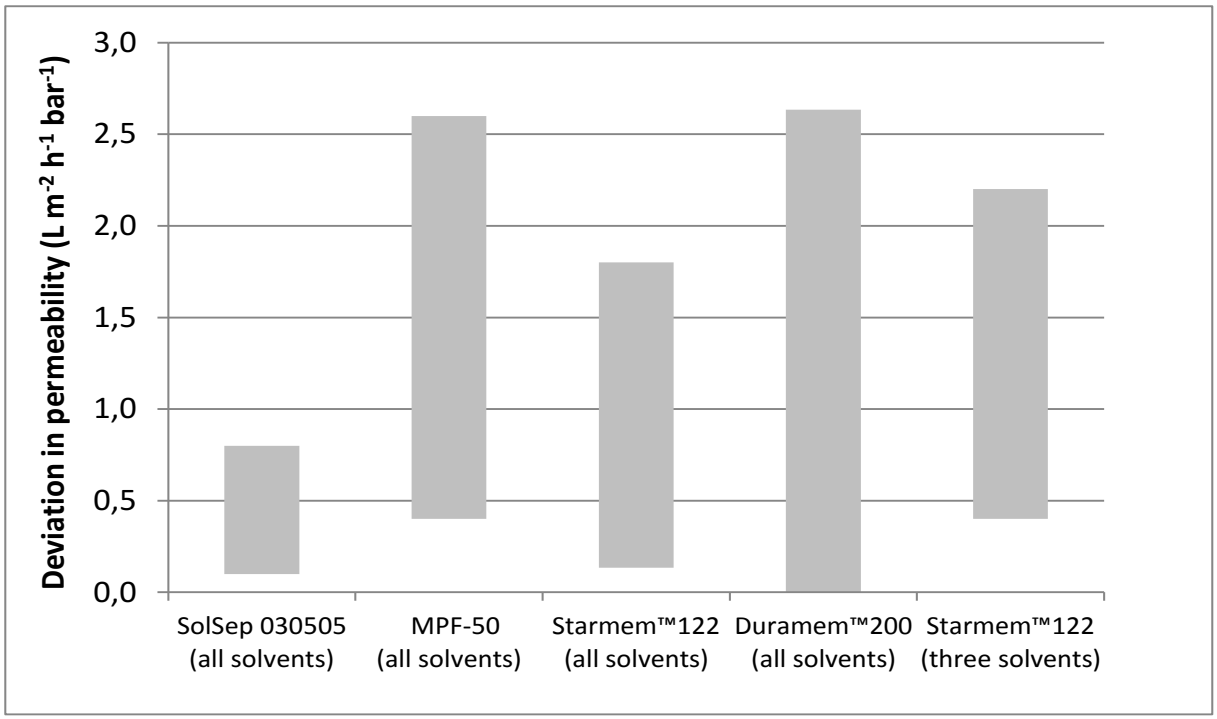

Figure 7.7. Lowest and highest deviation observed between the predicted and experimental permeability data obtained during model development (SolSep 030505 and MPF-50), for testing of model using additional OSN membranes (Starmem™122 and Duramem™200) and for model application based on three solvents only for parameter fitting

7.5 Conclusion and Recommendations for OSN Modelling

Data presented in this chapter demonstrate that though reasonable predictions of solvent permeability were presented by Darvishmanesh *et al.* (2009), significant relative deviations between the experimental and modelled values were observed when permeabilities were translated into absolute flux values. Additionally, when the suggested model was extended to

application in tighter OSN membranes (Starmem™122 and Duramem™200) operated at a higher pressure (30 bar), high deviations were again observed, indicating that the model predictive power was not sufficient for the membrane-solvent systems studied. The suggested model could still offer benefits in predicting general trends for permeation of various solvents based on viscosity, surface tension and polarity, however care must be taken before relying on modelled values and all data should be validated experimentally.

Darvishmanesh *et al.* (2009) used all solvents tested to determine the specific diffusivity and permeability values (a_0 and b_0). Prior to model application the fluxes of all solvents tested - as well as the surface tension of the membrane - hence had to be measured, resulting in a high experimental burden for the suggested model. Additionally, as all solvents tested were used to determine a_0 and b_0, no true predictions of the solvent permeations were really made. Despite this, significant model deviations were observed indicating that the predictive power of the model is limited.

Experimental work required prior to model application is simple to perform, but can be material- and time-consuming depending on the number of solvents selected for testing. Additionally, the pure solvent flux can easily be measured in a single, low-cost experiment, and if more extensive work is required to enable model application, benefits to modelling become limited. To make modelling more accessible, ideally no or little experimental work should be required prior to model application. A potential solution to minimise the experimental burden could be to base models on manufacturer supplied parameters. It is hence highly desirable that additional data (*e.g.* solvent fluxes, membrane surface tension and MWCO curves) based on consistent characterisation techniques, should be supplied by the membrane manufacturers.

Model limitations with regards to insufficient predictive power and extensive characterisation work required, strongly indicate that further developments in OSN modelling are desirable if modelling is to be used as a direct tool for membrane selection. For application in the pharmaceutical industry a simple model requiring little or no experimental work is highly desirable to facilitate direct model application. Additionally, as the solvent flux can easily be measured, and the processing time adjusted by varying the membrane area, the primary focus in model development should be placed on prediction of the solute rejection. Obtaining accurate models for flux predictions is however also important as development may increase the understanding of how OSN membranes work, hence providing a valuable foundation for accurate rejection modelling.

Chapter 8: Overall Conclusions and Final Remarks

As a result of recent developments and commercialisation of additional OSN membranes, the potential application area of OSN is growing. The pharmaceutical industry is often discussed as a suitable area for OSN implementation, and the central theme of this thesis is to investigate OSN applications in pharmaceutical processing. Focus is placed primarily on investigating the possibility of using OSN for a range of operations including API purification, solvent swapping and solvent recovery. Additionally, potential benefits and limitations to OSN compared to alternative unit operations including chromatography, adsorbents, distillation and LLE are evaluated. In the final section of this thesis, modelling of OSN membrane performance is discussed. The modelling section aims to investigate prediction performance of currently available OSN models, as well as to provide recommendations and a basis for future development of models suited for industrial application.

Objective 1: Investigate application of OSN in pharmaceutical processes including API purification, solvent swapping and solvent recovery

GSK case studies presented in this thesis demonstrate that OSN can successfully be used in API purification (Chapters 3 and 4), solvent swapping (Chapter 5) and solvent recovery and recycle (Chapters 5 and 6). The range of potential OSN applications is further demonstrated through case studies being operated in various organic solvents including THF, ethyl acetate, methanol, MiBK, heptane, IMS and IPAc, using solutes of different sizes and properties.

A promising application area for OSN was identified in solvent swapping. OSN can be used to enable solvent swaps between any miscible solvents, independent of the individual solvent

boiling points and potential azeotrope formation. The solvent composition was demonstrated as maintained over the membrane indicating a potential to use OSN for solvent swaps for both single solvents as well as solvent mixture.

Based on case studies some general conclusions and recommendations regarding OSN application can be made. Firstly, during OSN operation a high rejection of the desired component is required to minimise solute losses over the membrane. Data presented in this thesis demonstrates that even for a seemingly high rejection (> 98%) solute losses can add up to significant values (Chapter 3 and 4). Availability of OSN membranes capable of close to the ideal rejection of 100% are hence of outmost importance for industrial OSN application, and should be a main focus of research within membrane development and commercialisation.

Flux is an important measure of OSN membrane performance. However, the volumetric flow rate is directly related to the membrane area, and the overall OSN processing time can hence be adjusted by increasing the membrane surface used. A high flux is still desirable to minimise membrane requirements, and the resulting investment and maintenance cost. High flux is however not required to enable OSN application and though important, flux should not be the primary focus during membrane development for pharmaceutical applications.

Objective 2: Provide process comparisons for OSN and unit operations currently in use

In addition to demonstrating that OSN can be used for applications in the pharmaceutical industry, a process comparison with unit operations currently in place was carried out to investigate potential benefits and limitations to OSN application. Such studies demonstrate that OSN can offer significant advantages with regard to improved energy efficiency

compared to distillation (Chapter 6) and in enabling processing in situations where current unit operations are unsuitable to use (*e.g.* in solvent swaps from a higher to a lower boiling point solvent, Chapter 5). Additionally, OSN can be operated at room temperature and is hence ideal for use with temperature sensitive material, and in minimising product degradation and side-reactions occurring in the feed stream during processing.

OSN could additionally be a promising alternative for use in API purification, especially for separation of solutes having a large difference in molecular weight (> 500 g mol^{-1}). If a membrane with a high API rejection can be identified, OSN could offer benefits with regards to reduced yield losses (Chapter 3 and 4). However, use of OSN in API purification is highly depending on the membranes available for testing. As the range of commercially available membranes is currently limited, potential benefits to OSN application have to be evaluated on a case by case basis.

Additionally, when operated in a diafiltration mode OSN can be a relatively solvent intensive technique (Chapter 3, 4 and 5). This high solvent usage is likely to stifle OSN application, and should be addressed to facilitate a more wide-spread laboratory and industrial use. A potential route to minimise the solvent requirement, could be through development of membranes with sharper MWCO curves. Such developments would also offer additional benefits in enabling separation of molecules having similar molecular sizes. Another alternative for minimising OSN solvent intensity could be combination with a solvent recovery and recycle system. Solvent recycle was successfully demonstrated in this thesis by combining OSN with an adsorbent loop (Chapter 4), and has previously been studied by Sereewatthanawut *et al.* (2010) through use of multiple OSN stages. Further study of suitable alternatives for solvent recovery and recycle should additionally be investigated to facilitate future OSN applications.

Objective 3: Evaluate the use of modelling for prediction of OSN performance

Various models have been suggested for prediction of membrane performance in OSN systems. When models are applied to the membrane-solvent-solute systems used during development, reasonable predictions of flux and rejection can be obtained. However, when model application is extended to other membranes, solutes, solvents or solvent mixtures larger deviations in the model are commonly observed. Significant variation in model predictions indicates that current models are not sufficiently accurate to enable direct membrane selection. Available models can still offer benefits in predicting trends for membrane performance, however inconsistencies highlight that further model developments are highly desirable.

In this thesis a model based on a semi-empirical approach was selected for study. Currently the structure of OSN membranes cannot be conclusively determined due to limitations in available characterisation techniques. Additionally, the structure, material and properties of commercially available OSN membranes vary significantly between manufacturers, indicating that several variables might have to be included in order to develop a model providing high accuracy predictions. As transport through OSN membranes is not fully understood, the potential for model development based on a first principles approach is currently limited. A semi-empirical model might hence be more suitable for initial model developments and may offer benefits in limiting the computational complexity of the developed model. Additionally, development of a semi-empirical model providing accurate predictions could help increase the understanding of the mechanism behind solvent and solute transport through OSN membranes.

Many of the models currently available for prediction of OSN performance require significant experimental work prior to model application. Both the flux and rejection can easily be measured in single experiments, and if more extensive work is required to enable model application benefits to modelling become limited. For application in the pharmaceutical industry a simple model requiring little or no experimental work is highly desirable as a tool for membrane selection. To facilitate model developments more extensive data, based on consistent characterisation techniques, should hence be supplied by membrane manufacturers.

In this thesis only models developed for predicting flux has been studied. Developing accurate flux models could be a useful method for gaining additional understanding of transport through OSN membranes. However, as fluxes can easily be measured and the processing time adjusted by varying the membrane area, the primary focus in model development should be placed on predicting solute rejection.

The Future of OSN and Membrane Technology in the Pharmaceutical Industry

In summary, the work presented in this thesis demonstrates that the most promising application areas for OSN, using currently commercially available membranes, can be found in separation of molecules having a large difference in molecular weight (approximately > 500 g mol^{-1}) and for applications where traditional unit operations are unsuitable (*e.g.* for processing of temperature sensitive material and certain solvent swaps). OSN may also be of interest to groups specialising in large scale chromatographic separations, where the use of OSN can significantly improve process mass efficiency. This approach is particularly suited for applications involving high molecular weight products. In addition to nanofiltration, similar applications of membrane technology can also be extended across the filtration

spectrum and may offer process improvements within the growing areas of production of high molecular weight compounds such as proteins and oligonucleotides.

To further extend the application range of OSN, developments and commercialisation of additional membranes is highly desirable. From an industrial perspective, focus should then be placed on developing membranes capable of a 100% rejection for molecules covering a large range of molecular weights, as well as developing membranes with sharp MWCO curves to enable separation of molecules of similar size. To facilitate industrial OSN application the high solvent burden of diafiltration operations should also be addressed through either membrane or process developments.

Finally important to mention is that although many promising OSN applications have been demonstrated on a lab-scale, attempts to encourage capital expenditure for plant installations of membrane equipment have had limited success to date. To facilitate large-scale implementation of OSN more direct interactions between the membrane manufacturers and plant based end users is hence advisable. A potential area of application with great promise for large-scale OSN operation can be found in solvent recovery and recycle. Process streams of interest include not only crystallisation mother liquors, but also wash liquors from filter dryers where waste streams are commonly made up of only one solvent containing traces of the final API. Availability of various size membrane modules with consistent performance is crucial for this novel technique to gain a wide-spread use in regulated environments such as the pharmaceutical industry. Further developments to ensure consistency of modules used for large-scale OSN operation is hence highly recommended as a future area of research.

References

1. Aerts, S., Weyten, H., Buekenhoudt, A., Gevers, L. E. M., Vankelecom, I. F. J., Jacobs, P. A., Recycling of homogeneous Co-Jacobsen catalyst through solvent-resistant nanofiltration, *Chemical Communications*, 6 (2004) 710-711
2. American Chemical Society (2011) *ACI GCI Pharmaceutical Roundtable* [Online]. Available from: http://chemistry.org/greenchemistryinstitute/pharma_roundtable.html [Accessed 05 Aug 2012]
3. Baker, R. W. (2004a) Ch 1 Overview of Membrane Science and Technology. In: Baker, R. W. (ed.) *Membrane Technology and Applications*. 2nd Edition, Chichester, Wiley & Sons Ltd., pp. 1-14
4. Baker, R. W. (2004b) Ch 3 Membranes and Modules. In: Baker, R. W. (ed.) *Membrane Technology and Applications*. 2nd Edition, Chichester, Wiley & Sons Ltd., pp. 89-160
5. Baker, R. W. (2004b) Ch 6 Ultrafiltration. In: Baker, R. W. (ed.) *Membrane Technology and Applications*. 2nd Edition, Chichester, Wiley & Sons Ltd., pp. 237-272
6. Bhanushali, D., Bhattacharyya, D., Advances in Solvent-Resistant Nanofiltration Membranes, *Annals of the New York Academy of Science*, 984 (2003) 159-177
7. Bhanushali, D., Kloos, S., Bhattacharyya, D., Solute transport in solvent-resistant nanofiltration membranes for non-aqueous systems: experimental results and the role of solute–solvent coupling, *Journal of Membrane Science*, 208 (2002) 343-359
8. Bhanushali, D., Kloos, S., Kurth C., Bhattacharyya, D., Performance of solvent-resistant membranes for non-aqueous systems: solvent permeation results and modeling, *Journal of Membrane Science*, 189 (2001) 1-21
9. Bhattacharya, S., Hwang, S.-T., Concentration polarization, separation factor, and Peclet number in membrane processes, *Journal of Membrane Science*, 132 (1997) 73-90
10. Borsig GmbH (2012) *GMT INNOVATIVE MEMBRAENS AND MODULES* [Online]. Available from: http://www.gmtmem.com/en/products/membranes [Accessed 10 Jul 2012]
11. Borsig Membrane Technology (2011a) MEMBRANES FOR ORGANOPHILIC NANOFILTRATION solvent stable type GMT-oNF-1, Borsig GmbH., Gladbeck, Germany
12. Borsig Membrane Technology (2011b) MEMBRANES FOR ORGANOPHILIC NANOFILTRATION solvent stable type GMT-oNF-2, Borsig GmbH., Gladbeck, Germany
13. Bowen, R. W., Mukhtar, H., Characterisation and prediction of separation performance of nanofiltration membranes, *Journal of Membrane Science*, 112 (1996) 263-274
14. Bowen, R. W., Welfoot, J. S. (2005) Ch 6 Modelling the performance of nanofiltration membranes. In: Schäfer, A. I., Fane, A. G., Waite, T. D. (eds.) *Nanofiltration Principles and Applications*. 1st Edition, Oxford, Elsevier Ltd., pp. 120-146
15. Bowen, W. R:, Welfoot, J. S., Modeling the performance of membrane nanofiltration – critical assessment and model development, *Chemical Engineering Science*, 57 (2002) 1121-1137
16. Constable, D. J. C., Jimenez-Gonzalez, C., Henderson, R. K., Perspective on Solvent Use in the Pharmaceutical Industry, *Organic Process Research & Development*, 11 (2007) 133-137
17. Coulson J. M., Richardson, J. F., Harker, J. H., Backhurst, J. R., (2002a) Ch 17 Adsorption. In: *Coulson and Richardson's Chemical Engineering Volume 2 – Particle Technology and Separation Processes*, 5th Edition, Oxford, Butterworth-Heinemann, pp. 970-1052

18. Coulson J. M., Richardson, J. F., Harker, J. H., Backhurst, J. R., (2002b) Ch 15 Crystallisation. In: *Coulson and Richardson's Chemical Engineering Volume 2 – Particle Technology and Separation Processes*, 5th Edition, Oxford, Butterworth-Heinemann, pp. 827-900
19. Coulson J. M., Richardson, J. F., Harker, J. H., Backhurst, J. R., (2002c) Ch 11 Distillation. In: *Coulson and Richardson's Chemical Engineering Volume 2 – Particle Technology and Separation Processes*, 5th Edition, Oxford, Butterworth-Heinemann, pp. 542-580
20. Coulson J. M., Richardson, J. F., Harker, J. H., Backhurst, J. R., (2002d) Ch 14 Evaporation. In: *Coulson and Richardson's Chemical Engineering Volume 2 – Particle Technology and Separation Processes*, 5th Edition, Oxford, Butterworth-Heinemann, pp. 771-826
21. Cuperus, I. F. P., Recovery of Organic Solvents and Valuable Components by Membrane Separation, *Chemie Ingenieur Technik*, 77 (2005) 1000-1001
22. Curzons, A. D., Constable, D. J., Mortimer, D. N., Cunningham, V. L., So you think your process is green, how do you know? – Using principles of sustainability to determine what is green – a corporate perspective, *Green Chemistry*, 3 (2001) 1-6
23. Darnoko, D., Cheryan, M., Carotenoids from red Palm Methyl Esters by Nanofiltration, *Journal of the American Oil Chemist's Society*, 83 (2006) 365-370
24. Darvishmanesh, S., Buekenhoudt, A., Degrève, J., Van der Bruggen, B., General model for prediction of solvent permeation through organic and inorganic solvent resistant nanofiltration membranes, *Journal of Membrane Science*, 334 (2009) 43-49
25. DataPhysics Instruments GmbH (2012) *Interfacial Chemistry Introduction into Methods of Measuring and Analyzing Contact Angles for the Determination of Surface Free Energies of Solids* [Online]. Available from: http://www.dpc.kt.dtu.dk/upload/centre/dpc/documents/instrumentation/dataphysics-measuring%20cas.pdf [Accessed 22 Aug 2012]
26. Datta, A., Ebert, K., Plenio, H., Nanofiltration for homogeneous catalysis separation: soluble polymer supported palladium catalysts for Heck, Sonogashira and Suzuki coupling of aryl halides, *Organometallics*, 22 (2003) 4685-4691
27. de Smet, K., Aerts, S., Ceulemans, E., Vankelecom, I. F. J., Jacobs, P. A., Nanofiltration-coupled catalysis to combine the advantages of homogeneous and heterogeneous catalysis, *Chemical Community*, 7 (2001) 597-598
28. Deen, W. M., Hindered Transport of Large Molecules in Liquid-Filled Pores, *AIChE Journal*, 33 (1987) 1409-1425
29. Dijkstra, M. F. J., Bach, S., Ebert, K., A transport model for organophilic nanofiltration, *Journal of Membrane Science*, 286 (2006) 60-68
30. Donnan, F. G., Theory of membrane equilibria and membrane potentials in the presence of non-dialysing electrolytes. A contribution to physical-chemical physiology, *Journal of Membrane Science*, 100 (1995) 45-55
31. Du, Q., Jerz, G., Waibel, R., Winterhalter, P., Isolation of dammarane saponins from *Panax notoginseng* by high-speed counter-current chromatography, *Journal of Chromatography A*, 1008 (2003) 173-180
32. EUR-Lex (2000) *Directive 2000/76/EC of the European Parliament and of the Council of 4 December 2000 on the incineration of waste* [Online]. Available from: http://eur-lex.europa.eu/LexUriServ/LexUriServ.do?uri=CELEX:32000L0076:EN:NOT [Accessed 09 Aug 2012]

33. European Medicines Agency. (2007) *Guidelines on the Limits of Genotoxin Impurities* [Online]. Available from: http://www.ema.europa.eu/docs/en_GB/document_library/Scientific_guideline/2009/09/WC500002903.pdf [Accessed 08 May 2012]
34. Evonik MET Ltd. (2011a) Organic Solvent Nanofiltration Membranes StarMem™, Evonik MET Ltd., Wembley, United Kingdom
35. Evonik MET Ltd. (2011b) DuraMem® Membrane Flat Sheet Instructions for Use, Evonik MET Ltd., Wembley, United Kingdom
36. Evonik MET Ltd. (2011c) PuraMem® Membrane Flat Sheet Instructions for Use, Evonik MET Ltd., Wembley, United Kingdom
37. Evonik MET Ltd. (2011d) PuraMem®S Membrane Series Brochure, Evonik MET Ltd., Wembley
38. Fane, A. G. (2005) Ch 4 Module design and operation. In: Schäfer, A. I., Fane, A. G., Waite, T. D. (eds.) *Nanofiltration Principles and Applications*, 1st Edition, Oxford, Elsevier Ltd., pp. 67-88
39. Ferreira, F. C., Macedo, H., Cocchini, U., Livingston, A. G., Development of a Liquid-Phase Process for Recycling Resolving Agents within Diastereomeric Resolutions, *Organic Process Research & Development*, 10 (2006) 784-793
40. Food and Drug Administration (2009) *Food and Drug Administration Amendments Act (FDAAA) of 2007* [Online]. Available from: http://www.fda.gov/RegulatoryInformation/Legislation/FederalFoodDrugandCosmeticActFDCAct/SignificantAmendmentstotheFDCAct/FoodandDrugAdministrationAmendmentsActof2007/default.htm [Accessed 24 Jul 2012]
41. Food and Drug Administration. (2011) *Legislation* [Online]. Available from: http://www.fda.gov/RegulatoryInformation/Legislation/default.htm [Accessed 24 Jul 2012]
42. Garrard, I. J., Janaway, L., Fisher, D., Minimising Solvent usage in High Speed, High Loading, and High resolution Isocratic Dynamic Extraction, *Journal of Chromatography & Related Technologies*, 30 (2007) 151-163
43. Geens, J., Boussu, K., Vandecasteele, C., Van der Bruggen, B., Modelling of solute transport in non-aqueous nanofiltration, *Journal of Membrane Science*, 281 (2006b) 139-148
44. Geens, J., De Witte, B., van der Bruggen, B., Removal of API's (Active Pharmaceutical Ingredients) from Organic Solvents by Nanofiltration, *Separation Science and Technology*, 42 (2007) 2435-2449
45. Geens, J., Hillen, A., Bettens, B., Van der Bruggen, B., Vandecasteele, C., Solute transport in non-aqueous nanofiltration: effect of membrane material, *Journal of Chemical Technology and Biotechnology*, 80 (2005b) 1371-1377
46. Geens, J., Peeters, K., Van der Bruggen, B., Vandecasteele, C., Polymeric nanofiltration of binary water-alcohol mixtures: Influence of feed composition and membrane properties on permeability and rejection, *Journal of Membrane Science*, 255 (2005a) 255-264
47. Geens, J., Van der Bruggen, B., Vandecasteele, C., Transport model for solvent permeation through nanofiltration membranes, *Separation and Purification Technology*, 48 (2006a) 255-263
48. Genck, W. J., Dickey, D. S., Baczek, F. A., Bedell, D. C., Brown, K., Chen, W., Ellis, D. E., Harriott, P., Laros, T. J., Li, W., McGillicuddy, J. K., McNulty, T. P., Oldshue, J. Y., Schoenbrunn, F., Smith, J. C., Taylor, D. C., Wells, D. R., Wisdom, T. W. (2008) Ch 18 Liquid-Solid Operations and Equipment. In: Perry R. H., Green, D. W. (eds.)

Perry's Chemical Engineers' Handbook, 8th Edition, New York, McGraw-Hill, pp.18.39-18.58
49. Gevers, L. E. M., Meyen, G., De Smet, K., Van De Velde, P., Du Prez, F., Vankelecom, I. F. J., Jacobs, P. A., Physico-chemical interpretation of the SRNF transport mechanism for solute through dense silicon membranes, *Journal of Membrane Science*, 274 (2006) 173-182
50. Ghazali, N. F., Ferreira, F. C., White, A. J. P., Livingston, A. G., Enantiomere separation by enantioselective inclusion complexation-organic solvent nanofiltration, *Tetrahedron: Asymmetry*, 17 (2006) 1846-1852
51. Gibbins, E., D'Antonio, M., Nair, D., White, L. S., Freitas dos Santos, L. M., Vankelecom, I. F. J., Livingston, A. G., Observations on solvent flux and solute rejection across solvent resistant nanofiltration membranes, *Desalination*, 147 (2002) 307-313
52. Gould, R. M., White, L. S., Wildemuth, C. R., Membrane Separation in Solvent Lube Dewaxing, *Environmental Progress*, 20 (2001) 12-16
53. Guzlek, H., Baptista, I. I. R., Wood, P. L., Livingston, A., A novel approach to modeling counter-current chromatography, *Journal of Chromatography A*, 1217 (2010) 6230-6240
54. Han, S., Wong, H.-T., Livingston, A. G., Application of Organic Solvent Nanofiltration to Separation of Ionic Liquids and Products from Ionic Liquid Mediated Reactions, *Chemical Engineering Research and Design*, 83 (2005) 309-316
55. Haynes, W. M. (2012) In: Haynes, W. M. (ed.) *CRC handbook of Chemistry and Physics*, Internet Version, Taylor and Francis
56. Henderson, R. K., Kindervater, J., Manley, J. B. (2007) *Lessons learned through measuring green chemical performance – The pharmaceutical experience* [Online]. Available from: http://portal.acs.org/portal/PublicWebSite/greenchemistry/industriainnovation/roundtable/CTP_005585 [Accessed 06 Aug 2012]
57. Ignatova, S., Brunel University (2010) *API Recovery from Pharmaceutical Waste Streams by High Performance Counter-current Chromatography (HPCCC) and Intermittent Counter-current Extraction (ICcE)* [Online] Available from: http://www.dynamicextractions.com/projects/wp-content/uploads/2011/07/Prep-2011-Ignatova-July-2011-Final.pdf [Accessed 31 Jul 2012]
58. Inopor GmbH (2012) Membranes [Online]. Available from: http://www.inopor.com/en/membranes_e.html [Accessed 06 Jun 2012]
59. Ito, Y. J., Golden rules and pitfalls in selecting optimum conditions for high-speed counter-current chromatography, *Journal of Chromatography A*, 1065 (2005) 145-168
60. Jiménez-González, C., Curzons, A. D., Constable, D. J. C., Cunningham, V. L., Expanding GSK's Solvent Selection Guide – application of life cycle assessment to enhance solvent selections, *Clean Technologies and Environmental Policy*, 7 (2005) 42-50
61. Jimenez Solomon, M. F., Bhole, Y., Livingston, A. G., High flux membranes for organic solvent nanofiltration (OSN) – Interfacial polymerization with solvent activation, *Journal of Membrane Science*, 423-424 (2012) 371-382
62. Kedem, O., Katchalsky, A., Thermodynamic analysis of the permeability of biological membranes to non-electrolytes, *Biochimica et Biophysica Acta*, 27 (1958) 229-246
63. Kong, Y., Shi, D., Yu, H., Wang, Y., Yang, J., Zhang, Y., Separation performance of polyimide nanofiltration membranes, *Desalination*, 191 (2006) 254-261

64. Koros, W. J., Ma, Y. H., Shimidzu, T., Terminology for membranes and membrane processes (IUPAC recommendations 1996), *Journal of Membrane Science*, 120 (1996) 149-159
65. Kühnert, J.-T., Fraunhofer-Institut für Keramische Technologien und Systeme (IKTS), E-mail communication, September 2012
66. Kwok, D. Y., Neumann, A. W., Contact angle measurement and contact angle interpretation, *Advances in Colloid and Interface Science*, 81 (1999) 167-249
67. Lee, C., Helmy, R., Strulson, C., Plewa, J., Kolodziej, E., Antonucci, V., Mao, B., Welch, C. J., Ge, Z., Al-Sayah, M. A., Removal of Electrophilic Potential Genotoxic Impurities Using Nucleophilic Reactive Resins, *Organic Process Research & Development*, 14 (2010), 1021-1026
68. LeVan, M. D., Carta, G., (2008) Section 16 Adsorption and Ion Exchange. In: Perry, R. H., and Green, D. W. (eds.) *Perry's Chemical Engineers' Handbook*, 8th Edition, New York, McGraw-Hill
69. Li, X. Monsuur, F., Denoulet, B., Dobrak, A., Vandezande, P., Vankelecom, I. F. J., Evaporative Light Scattering Detector: Towards a General Molecular Weight Cutoff Characterization of Nanofiltration Membranes, *Analytical Chemistry*, 81 (2009) 1801-1809
70. Lin, J. C.-T., Livingston, A. G., Nanofiltration membrane cascade for continuous solvent exchange, *Chemical Engineering Science*, 62 (2007) 2728-2736
71. Lin, L., Rhee, K. C., Koseoglu, S. S., Bench-scale membrane degumming of crude vegetable oil: Process optimization, *Journal of Membrane Science*, 134 (1997) 101-108
72. Linder, C., Nemas, M., Perry, M., Katraro, R. (1993) *Silicon derived solvent stable membranes*, US Patent 5,265,734 (Patent)
73. Linder, C., Perry, M., Nemas, M., Tikva, P., Monosson, N., Katraro, R., Lezion, R. (1991) *Solvent stable membranes*, US Patent 5,039,421 (Patent)
74. Livingston, A. G., Boam, A. T., Meniconi, A., Lim, F.-W., Makowski, M. (2011) *Pilot Plant Development of Molecular Separations by Organic Solvent Nanofiltration* [Online]. Available from: https://aiche.confex.com/aiche/2011/webprogram/Paper227382.html [Accessed 09 Jul 2012]
75. Livingston, A. G., Peeva, L., Han, S., Nair, D., Luthra, S. S., White, L. S., Freitas dos Santos, L. M., Membrane Separation in Green Chemical Processing – Solvent Nanofiltration Liquid Phase Organic Synthesis Reactions, *Annals of the New York Academy of Science*, 984 (2003) 123-141
76. Livingston, A. Nasso, M., Molecular separation: the new frontier in liquid filtration, *The Chemical Engineer*, Apr (2009) 34-36
77. Loeb, S., Sourirajan, S., Sea Water Demineralization by Means of an Osmotic Membrane, *Advances in Chemical Series*, 38 (1962) 117
78. Luthra, S. S., Yang, X., Freitas dos Santos, L. M., White, L. S., Livingston, A. G., Homogeneous phase transfer catalyst recovery and re-use using solvent resistant membranes, *Journal of Membrane Science*, 201 (2002) 65-75
79. Machado, D. R., Hasson, D., Semiat, R., Effect of solvent properties on permeate flow through Nanofiltration membranes. Part I: investigation of parameters affecting solvent flux, *Journal of Membrane Science*, 163 (1999) 93-102

80. Machado, D. R., Hasson, D., Semiat, R., Effect of solvent properties on permeate flow through nanofiltration membranes Part II Transport model, *Journal of Membrane Science*, 166 (2000) 63-69
81. Mason, E. A., Lonsdale, H. K., Statistical-Mechanical Theory of Membrane Transport, *Journal of Membrane Science*, 51 (1990) 1-81
82. Matsuura, T., Sourirajan, S., Reverse Osmosis Transport through Capillary Pores under the Influence of Surface forces *Industrial Engineering Chemical Process Design and Development*, 20 (1981) 273-282
83. Mulder, M. (1996a) Ch I Introduction. In: Mulder, M. (ed.) *Basic Principles of Membrane Technology*. 2nd Edition, Dordrecht, Kluwer Academic Publisher, pp. 1-21
84. Mulder, M. (1996b) Ch II Materials and material properties. In: Mulder, M. (ed.) *Basic Principles of Membrane Technology*. 2nd Edition, Dordrecht, Kluwer Academic Publisher, pp. 22-70
85. Mulder, M. (1996c) Ch III Preparation of synthetic membranes. In: Mulder, M. (ed.) *Basic Principles of Membrane Technology*. 2nd Edition, Dordrecht, Kluwer Academic Publisher, pp. 71-156
86. Mulder, M. (1996d) Ch VI Membrane processes. In: Mulder, M. (ed.) *Basic Principles of Membrane Technology*. 2nd Edition, Dordrecht, Kluwer Academic Publisher, pp. 280-415
87. Mulder, M. (1996e) Ch V Transport in membranes. In: Mulder, M. (ed.) *Basic Principles of Membrane Technology*. 2nd Edition, Dordrecht, Kluwer Academic Publisher, pp. 210-279
88. Mulder, M. (1996f) Ch VII Polarisation phenomena and membrane fouling. In: Mulder, M. (ed.) *Basic Principles of Membrane Technology*. 2nd Edition, Dordrecht, Kluwer Academic Publisher, pp. 416-464
89. Mulder, M. (1996g) Ch VIII Module and process design. In: Mulder, M. (ed.) *Basic Principles of Membrane Technology*. 2nd Edition, Dordrecht, Kluwer Academic Publisher, pp. 465-523
90. Mulder, M. H. V., van Voorthuizen, E. M., Peeters, J. M. M. (2005) Ch 5 Membrane characterization. In: Schäfer, A. I., Fane, A. G., Waite, T. D. (eds.) *Nanofiltration Principles and Applications*, 1st Edition, Oxford, Elsevier Ltd., pp. 89-117
91. Nair, D., Scarpello, J. T., Vankelecom, I. F. J., Freitas dos Santos, L. M., White, L. S., Kloetzing, R. J., Welton, T., Livingston, A. G., Increased catalytic productivity for nanofiltration-coupled Heck reactions using highly stable catalyst systems, *Green Chemistry*, 4 (2002) 319-324
92. Nair, D., Wong, H.-T., Han, S., Vankelecom, I. F. J., White, L. S., Livingston, A. G., Boam, A. T., Extending Ru-BINAP catalyst Life and Separating Products from Catalyst Using Membrane Recycle, *Organic Process Research & Development*, 13 (2009) 863-869
93. Nghiem, L. D., Schäfer, A. I. (2005) Ch 20 Trace contaminant removal with nanofiltration. In: Schäfer, A. I., Fane, A. G., Waite, T. D. (eds.) *Nanofiltration Principles and Applications*, 1st Edition, Oxford, Elsevier Ltd., pp. 479-520
94. Nunes, S. P., Peinemann, K.-V. (2006) Part I.3 Membrane Preparation. In: Nunes, S. P., Peinemann, K.-V. (eds.) *Membrane technology in the Chemical Industry*, 2nd Edition, Weinheim, Wiley-VCH Verlag GmbH &Co., pp. 9-14
95. Oatley, D. L. (2003) *CHARACTERISATION AND PREDICTION OF MEMBRANE SEPARATION PERFORMANCE – AN INDUSTRIAL ASSESSMENT*. PhD Thesis. University of Wales Swansea.

96. Othman, R., Mohammad, A. W., Ismail, M., Salimon, J., Application of polymeric solvent resistant nanofiltration membranes for biodiesel production, *Journal of Membrane Science*, 348 (2010) 287-297
97. Peeva, L. G., Gibbins, E., Luthra, S. S., White, L. S., Stateva, R. P., Livingston, A. G., Effect of concentration polarization and osmotic pressure on flux in organic solvent nanofiltration, *Journal of Membrane Science*, 236 (2004) 121-136
98. Perry, M., Linder, C., Intermediate RO-UF membranes for concentration and desalting of low molecular weight organic solutes, *Desalination*, 71 (1980) 233-245
99. Pink, C. J., Wong, H., Ferreira, F. C., Livingston, A. G., Organic Solvent Nanofiltration and Adsorbents; A Hybrid Approach to Achieve Ultra Low Palladium Contamination of Post Coupling Reaction Products, *Organic Process Research & Development*, 12 (2008) 589-595
100. Priske, M., Wiese, K.-D., Drews, A., Kraume, M., Baumgarten, G., Reaction integrated separation of homogenous catalysts in the hydroformulation of higher olefins by means of organophilic nanofiltration, *Journal of Membrane Science*, 360 (2010) 77-83
101. Raman, L. P., Cheryan M, Rajagopalan N. Solvent Recovery and Partial Deacidification of Vegetable Oils by Membrane Technology, *Fett/Lipid*, 98 (1996) 10-14
102. Raman, L. P., Cheryan, M., Rajagopalan, N., Consider Nanofiltration for membrane separations, *Chemical Engineering Progress*, 90 (1994) 68-74
103. Raman, N. V. V. S. S., Prasad, A. V. S. S., Ratnakar Reddy, K., Strategies for the identification, control and determination of genotoxic impurities in drug substances: A pharmaceutical industry perspective, *Journal of Pharmaceutical and Biomedical Analysis*, 55 (2011) 662-667
104. Reddy Maddula, S., Kharkar, M., Manudhane, K., Kale, S., Bhori, A., Lali, A., Dubey, P. K., Janardana Sarma, K. R., Bhattacharya, A., Bandichhor, R., Preparative Chromatography technique in the Removal of Isostructural Genotoxic Impurity Rizatriptan: Use of Physicochemical Descriptors of Solute and Adsorbent, *Organic Process Research & Development*, 13 (2009) 683-689
105. Reddy, K. K., Kawakatsu, T., Snape, J. B., Nakajima, M., Membrane Concentration and Separation of L-Aspartic Acid and L-Phenylalanine Derivatives in Organic Solvents, *Separation Science and Technology*, 31 (1996) 1161-1178
106. Robinson, D. I., Control of Genotoxic Impurities in Active Pharmaceutical Ingredients: A Review and Perspective, *Organic Process Research & Development*, 14 (2010) 946-959
107. Robinson, J. P., Tarleton, E. S., Millington, C. R., Nijmeijer, A., Solvent flux through dense polymeric nanofiltration membranes, *Journal of Membrane Science*, 230 (2004) 29-37
108. Scarpello, J. T., Nair, D., Freitas dos Santos, L. M., White, L. S., Livingston, A. G., The separation of homogeneous organometallic catalysts using solvent resistant nanofiltration, *Journal of Membrane Science*, 203 (2002) 71-85
109. Schäfer, A. I., Andritsos, N., Karabelas, A. J., Hoek, E. M. V., Schneider, R., Nyström, M. (2005) Ch 8 Foluing in nanofiltration. In: Schäfer, A. I., Fane, A. G., Waite, T. D. (eds.) *Nanofiltration Principles and Applications*, 1st Edition, Oxford, Elsevier Ltd., pp. 479-520
110. Schirg, P., Widmer, F., Characterisation of nanofiltration membranes for the separation of aqueous dye-salt solutions, *Desalination*, 89 (1992) 89-107
111. Schülé, A., Ates, C., Palacio, M., Stofferis, J., Delatinne, J.-P., Martin, B., Lloyd, S., Monitoring and Control of Genotoxic Impurity Acetamide in the Synthesis of Zaurategrast Sulfate, *Organic Process Research & Development*, 14 (2010) 1008-1014

112. Seader, J. D., Siirola, J. J., Barnicki, S. D. (2008) Ch 13 Distillation. In: Perry, R. H., Green, D. W. (eds.) *Perry's Chemical Engineers' Handbook*, 8th Edition, New York, McGraw-Hill, pp. 13.4-13.6
113. See Toh, Y. H., Lim, F. W., Livingston, A. G., Polymeric membranes for nanofiltration in polar aprotic solvents, *Journal of Membrane Science*, 301 (2007b) 3-10
114. See Toh, Y. H., Loh, X.X., Li, K., Bismarck, A., Livingston, A. G., In search of a standard method for the characterisation of organic solvent nanofiltration membranes, *Journal of Membrane Science*, 291 (2007a) 120-125
115. See-Toh, Y., Silva, M., Livingston, A., Controlling molecular weight cut-off curves for highly solvent stable organic solvent nanofiltration (OSN) membranes, *Journal of Membrane Science*, 324 (2008) 220-232
116. Sereewatthanawut, I., Baptista, I. I. R., Boam, A. T., Hodgson, A., Livingston, A. G., Nanofiltration process for the nutritional enrichment and refining of rice bran oil, *Journal of Food Engineering*, 102 (2011) 16-24
117. Sereewatthanawut, I., Lim, F. W., Bhole, Y. S., Ormerod, D., Horvath, A., Boam, A., Livingston, A. G., Demonstration of Molecular Purification in Polar Aprotic Solvents by Organic Solvent Nanofiltration, *Organic Process Research & Development*, 14 (2010) 600-611
118. Sheldon, R. A., The E Factor: fifteen years on, *Green Chemistry*, 9 (2007) 1273-1283
119. Sheth, J. P., Qin, Y., Sirkar, K. S., Baltzis, B. C., Nanofiltration-based diafiltration for solvent exchange in pharmaceutical manufacturing, *Journal of Membrane Science*, 211 (2003) 251-261
120. Shi, D., Kong, Y., Yu, J., Wang, Y., Yang, J., Separation performance of polyimide nanofiltration membranes for concentrating spiramycin extract, *Desalination*, 191 (2006) 309-317
121. Silva, P., Han, S., Livingston, A. G., Solvent transport in organic solvent nanofiltration, *Journal of Membrane Science*, 262 (2005) 49-59
122. Silva, P., Livingston, A. G., Effect of concentration polarisation in organic solvent nanofiltration – flat sheet and spiral wound systems, *Desalination*, 199 (2006b) 248-250
123. Silva, P., Livingston, A. G., Effect of solute concentration and mass transfer limitations on transport in organic solvent nanofiltration – partially rejection solute, *Journal of Membrane Science*, 280 (2006a) 889-898
124. Silva, P., Peeva, L. G., Livingston, A. G:, Organic solvent nanofiltration (OSN) with spiral-wound membrane elements – Highly rejected solute system, *Journal of Membrane Science*, 349 (2010) 167-174
125. So, S., Peeva, L. G., Tate, E. W., Leatherbarrow, R. J., Livingston, A. G., Organic Solvent Nanofiltration, *Organic Process Research & Development*, 14 (2010) 1313-1325
126. SolSep BV. (2008) Info on all membrane types SolSep BV. Membrane Processing in Organic Solvents, SolSep BV., Apeldoorn, the Netherlands
127. Sourirajan, S., Separation of hydrocarbon liquids by flow under pressure through porous membranes, *Nature*, 203 (1964) 1348-1349
128. Spiegler, K. S., Kedem, O., Thermodynamics of hyperfiltration (reverse osmosis): criteria for efficient membranes, *Desalination*, 1 (1966) 311-326
129. Stamatialis, D. F., Stafie, N., Buadu, K., Hempenius, M., Wessling, M., Observation on the permeation of solvent resistant nanofiltration membranes, *Journal of Membrane Science* 279 (2006) 424-433
130. Stewart Slater, C., Savelski, M. J., Carole, W. A., Constable, D. J., C. (2010) Ch3 Solvent Use and Waste Issues. In: Dunn, P. J., Wells, A. S., Williams, M. T. (eds.)

Green Chemistry in the Pharmaceutical Industry, 1st Edition, Weinheim, Wiley-VCH Verlag GmBH & Co., pp. 49-82
131. Straatsma, J., Bargeman, G., van der Horst, H. C., Wesselingh, J. A., Can nanofiltration be fully predicted by a model?, *Journal of Membrane Science*, 198 (2002) 273-284
132. Székely, G., Bandarra, J., Heggie, W., Sellergren, B., Ferreira, F. C., Organic solvent nanofiltration: A platform for removal of genotoxins from active pharmaceutical ingredients, *Journal of Membrane Science*, 381 (2011) 21-33
133. Székely, G., Bandarra, J., Heggie, W., Sellergren, B., Ferreira, F. C., A hybrid approach to reach stringent low genotoxic impurity contents in active pharmaceutical ingredients: Combining molecularly imprinted polymers and organic solvent nanofiltration for removal of 1,3-diisopropylurea, *Separation and Purification Technology*, 86 (2012a) 79-87
134. Székely, G., Fritz, E., Bandarra, J., Heggie, W., Sellergren, B., Removal of potentially genotoxic acetamide and arylsulfonate impurities from crude drugs by molecular imprinting, *Journal of Chromatography A*, 1240 (2012b) 52-58
135. The Food and Drug Administration. (2008) *Guidance for Industry Genotoxic and Carcinogenic Impurities in Drug Substances and Products: Recommended Approaches* [Online]. Available from: http://www.fda.gov/downloads/Drugs/GuidanceComplianceRegulatoryInformation/Guidances/ucm079235.pdf [Accessed 08 May 2012]
136. Tsuru, T., Miyawaki, M., Kondo, H., Yochioka, T., Asaeda, M., Inorganic membranes for nanofiltration of nonaqueous solutions, *Separation and Purification Technology*, 32 (2003) 105-109
137. Tsuru, T., Nano/subnano-tuning of porous ceramic membranes for molecular separation, *Journal of Sol-Gel Science and Technology*, 46 (2008) 349-361
138. Van der Bruggen, B., Geens, J., Vandecasteele, C., Fluxes and rejection for nanofiltration with solvent stable polymeric membranes in water, ethanol and n-hexane, *Chemical Engineering Science*, 57 (2002a) 2511-2518
139. Van der Bruggen, B., Geens, J., Vandecasteele, C., Influence of Organic Solvents on the Performance of Polymeric Nanofiltration Membranes, *Separation Science and Technology*, 37 (2002b) 783-797
140. Van der Bruggen, B., Schaep, J., Wilms, D., Vandecasteele, C., Influence of molecular size, polarity and charge on the retention of organic molecules by nanofiltration, *Journal of Membrane Science*, 156 (1999) 29-41
141. Van Doorslaer, C., Glas, D., Peeters, A., Cano Odena, A., Vankelecom, I., Binnemans, K., Mertens, P., De Vos, D., Product recovery from ionic liquids by solvent-resistant nanofiltration: application to ozonation of acetals and methyl oleate, *Green Chemistry*, 12 (2010) 1726-1733
142. Vandezande, P., Gevers, L. E. M., Vankelecom, I. F. J., Solvent resistant nanofiltration: separating on a molecular level, *Chemical Society Review*, 37 (2008) 365-405
143. Vankelecom, I. F. J., De Smet, K., Gevers, L. E. M., Livingston, A., Nair, D., Aerts, S., Kuypers, S., Jacobs, P. A., Physico-chemical interpretation of the SRNF transport mechanism for solvents through dense silicon membranes, *Journal of Membrane Science*, 231 (2994) 99-108
144. Vasapollo, G., Del Sole, R., Mergola, L., Lazzio, M. R., Scardino, A., Scorrano, S., Mele, G., Molecularly Imprinted Polymers: Present and Future Prospective, *International Journal of Molecular Science*, 12 (2011) 5908-5945

145. Waite, T. D. (2005) Ch 7 Chemical speciation effects in nanofiltration separation. In: Schäfer, A. I., Fane, A. G., Waite, T. D. (eds.) *Nanofiltration Principles and Applications*, 1st Edition, Oxford, Elsevier Ltd., pp. 148-168
146. Walker, D. (2008) Ch 8 Chemical Engineering. In: Walker, D. (eds.) *The Management of Chemical Process Development in the Pharmaceutical Industry*, 1st Edition, the United States, Wiley-Interscience John Wiley & Sons, pp 165-202
147. Wenten, I. G., Recent developments in membrane science and its industrial applications, *Journal of Science and Technology*, 24 (2002) 1009-1024
148. White, L. S. (2001) *Polyimide membrane for hyperfiltration recovery of aromatic solvents*, US Patent 6,180,008 B1 (Patent)
149. White, L. S., Development of large-scale applications in organic solvent nanofiltration and pervaporation for chemical and refining processes, *Journal of Membrane Science*, 286 (2006) 26-35
150. White, L. S., Nitsch, A. R., Solvent recovery from oil filtrates with a polyimide membrane, *Journal of Membrane Science*, 179 (2000) 267-274
151. White, L. S., Wang, I.-F., Minhas, B. S. (1993) *Polyimide membranes for separation of solvents from lube oil*, US Patent 5,264,166 (Patent)
152. White, L. S., Wildemuth, C. R., Aromatics Enrichment in Refinery Streams Using Hyperfiltration, *Industrial Engineering Chemical Research*, 45 (2006) 9136-9143
153. Whu, J. A., Baltzis, B. C., Sirkar, K. K., Nanofiltration studies of larger organic microsolutes in methanol solutions, *Journal of Membrane Science*, 170 (2000) 159-172
154. Wijmans, J. G., Baker, R. W., The solution-diffusion model: a review, *Journal of Membrane Science*, 107 (1995) 1-21
155. Wong, H., Pink, C. J., Ferreira, F. C., Livingston, A. G., Recovery and reuse of ionic liquids and palladium catalyst for Suzuki reactions using organic solvent nanofiltration, *Green Chemistry*, 8 (2006) 373-379
156. Wu, D., Jiang, X., Wu, S., Direct purification of tanshinones from *Salvia miltiorrhiza* Bunge by high-speed counter-current chromatography without presaturation of the two-phase solvent mixture, *Journal of Separation Science*, 33 (2010) 67-73
157. Yang, X. J., Livingston, A. G., Freitas dos Santos, L., Experimental observations of nanofiltration with organic solvents, *Journal of Membrane Science*, 190 (2001) 45-55
158. Yaroshchuk, A. E., Rejection mechanisms of NF membranes, *Membrane Technology*, 100 (1998) 9-12
159. Zhao, Y. Yuan, Q., A comparison of Nanofiltration with aqueous and organic solvents, *Journal of Membrane Science*, 279 (2006a) 453-458
160. Zhao, Y., Yuan, Q., Effect of membrane pretreatment on performance of solvent resistant nanofiltration membranes in methanol solutions, *Journal of Membrane Science*, 280 (2006b) 195-201
161. Zwijnenberg, H. J., Krosse, A. M., Ebert, K., Peinemann, K.-V., Cuperus, F. P., Acetone-Stable Nanofiltration Membranes in Deacidifying Vegetable Oil, *Journal of the American Oil Chemist's Society*, 76 (1999) 83-87